

AD-A056 232

MECHANICAL TECHNOLOGY INC LATHAM N Y

A NUMERICAL SOLUTION FOR A GENERALIZED ELLIPTICAL CONTACT OF LA--ETC(U)

MAY 78 J A MCCORMICK

N00014-72-C-0083

NL

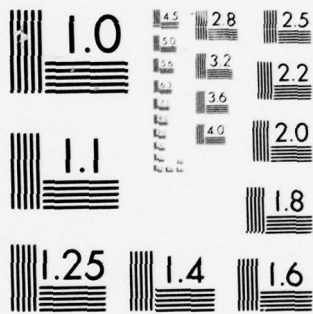
UNCLASSIFIED

MTI-78TR52

1 OF 2

AD  
A056232





MICROCOPY RESOLUTION TEST CHART  
NATIONAL BUREAU OF STANDARDS-1963-A



AD NO. \_\_\_\_\_

DC FILE COPY

AD A 056232

LEVEL

II

③

MT  
MT  
MT  
MT  
MT

APPROVED FOR PUBLIC RELEASE  
DISTRIBUTION UNLIMITED

DDC  
JUL 14 1978  
E

78 07 06 034

Mechanical Technology Incorporated

Research and Development Division



**Mechanical Technology Incorporated**  
**Research and Development Division**  
**968 Albany-Shaker Road**  
**Latham, New York 12110**  
**(518) 785-2211**

AD No. \_\_\_\_\_  
DDC FILE COPY AD A056232

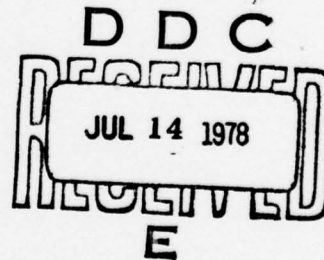
MTI 78TR52

A NUMERICAL SOLUTION FOR A  
GENERALIZED ELLIPTICAL CONTACT  
OF LAYERED ELASTIC SOLIDS

Prepared By:  
J.A. McCormick

Prepared For:  
Office of Naval Research  
Arlington, Virginia 22217

May 1978



DISTRIBUTION STATEMENT A

Approved for public release;  
Distribution Unlimited

MECHANICAL TECHNOLOGY INCORPORATED  
968 Albany-Shaker Road  
Latham, New York 12110

78 07 06 034



Unclassified

SECURITY CLASSIFICATION OF THIS PAGE (When Data Entered)

REPORT DOCUMENTATION PAGE		READ INSTRUCTIONS BEFORE COMPLETING FORM
1. REPORT NUMBER MTI-78TR52 ✓	2. GOVT ACCESSION NO.	3. RECIPIENT'S CATALOG NUMBER
4. TITLE (and Subtitle) A Numerical Solution for a Generalized Elliptical Contact of Layered Elastic Solids .	5. TYPE OF REPORT & PERIOD COVERED Final Report. 1978	6. PERFORMING ORG. REPORT NUMBER
7. AUTHOR(s) John A. McCormick	8. CONTRACT OR GRANT NUMBER(s) N00014-72-C-0083 ✓	10. PROGRAM ELEMENT, PROJECT, TASK AREA & WORK UNIT NUMBERS
9. PERFORMING ORGANIZATION NAME AND ADDRESS Mechanical Technology Incorporated 968 Albany-Shaker Rd. Latham, New York 12110	11. REPORT DATE May 1978	13. NUMBER OF PAGES 140 12 153p.
11. CONTROLLING OFFICE NAME AND ADDRESS Office of Naval Research Arlington, Virginia 22217	15. SECURITY CLASS. (of this report) Unclassified	15a. DECLASSIFICATION/DOWNGRADING SCHEDULE
14. MONITORING AGENCY NAME & ADDRESS (if different from Controlling Office)		
16. DISTRIBUTION STATEMENT (of this Report)  Distribution of this document is unlimited.		
17. DISTRIBUTION STATEMENT (of the abstract entered in Block 20, if different from Report)		
18. SUPPLEMENTARY NOTES		
19. KEY WORDS (Continue on reverse side if necessary and identify by block number)  Elastic Contact Layered Elastic Solids Elastomeric Compliant Bearing		
20. ABSTRACT (Continue on reverse side if necessary and identify by block number)		

DD FORM 1 JAN 73 1473

EDITION OF 1 NOV 65 IS OBSOLETE

Unclassified

SECURITY CLASSIFICATION OF THIS PAGE (When Data Entered)

224 550

actt

## CONTENTS

	Page
LIST OF FIGURES . . . . .	vi
ABSTRACT. . . . .	viii
1. INTRODUCTION. . . . .	1
2. SOLUTION FOR SURFACE DISPLACEMENT DUE TO CONCENTRATED NORMAL FORCE. . . . .	6
2.1 Formulation of Boundary Value Problem. . . . .	6
2.2 Formal Solution by Integral Transforms . . . . .	9
3. ANALYTICAL FORMULATION OF INTEGRAL EQUATION FOR CONTACT PROBLEM . . . . .	18
3.1 Surface Displacement Due to Non-Axisymmetric Pressure Distribution. . . . .	18
3.2 Derivation of Integral Equation. . . . .	18
4. NUMERICAL FORMULATION . . . . .	28
4.1 Discretized Integral Equation and Method of Solution . .	28
4.2 Evaluation of Influence Coefficients for Discretized Integral Equation. . . . .	40
4.2.1 Formulation in Terms of Integral Functions. . . .	40
4.2.2 Evaluation of Integral Functions. . . . .	47
4.3 Computer Programs. . . . .	54
5. NUMERICAL RESULTS . . . . .	55
5.1 Test for Numerical Accuracy. . . . .	55
5.2 Numerical Solutions. . . . .	61
6. SUMMARY AND CONCLUSIONS . . . . .	88
REFERENCES. . . . .	91
APPENDIX I - ANALYTICAL EVALUATION OF BASIC INTEGRALS . . . . .	92
APPENDIX II - SURFACE DISPLACEMENT DUE TO AXISYMMETRIC ELLIPSOIDAL PRESSURE DISTRIBUTION . . . . .	97
APPENDIX III - DESCRIPTION OF COMPUTER PROGRAM "HIJPRG" . . . .	99

# LIST OF TABLES

		Page
Table 2-1	Simultaneous Equations in Constants for Hankel Transform Solution . . . . .	14
Table 4-1	Influence Coefficients for Equation 4.9. . . . .	37
Table 5-1	Comparison Between Numerical and Exact Solutions for Hertz Contact. . . . .	57
Table 5-2	Comparison Between Numerical and Exact Solutions for Surface Displacements Due to Axisymmetric Ellipsoidal Pressure Distribution. . . . .	59
Table 5-3	Comparison of Numerical Solutions for Axisymmetric Layered Contact with Results of Chen and Engel [4] . . . .	60

ACCESSION for	
NTIS	White Section <input checked="" type="checkbox"/>
DOC	Dark Section <input type="checkbox"/>
UNANNOUNCED	<input type="checkbox"/>
JUSTIFICATION	
BY	
DISTRIBUTION/AVAILABILITY CODES	
Dist.	AVAIL. and/or SPECIAL
A	

PRECEDING PAGE BLANK-NOT FILMED

## CONTENTS (cont.)

	Page
APPENDIX IV - DESCRIPTION OF COMPUTER PROGRAM "PSOLV". . . . .	102
APPENDIX V - LISTING OF COMPUTER PROGRAM "PSOLV" . . . . .	105
APPENDIX VI - LISTING OF COMPUTER PROGRAM "HIJPRG" . . . . .	129



# LIST OF FIGURES

Figure 2-1	Configuration for Concentrated Force Problem . . . . .	Page 7
Figure 3-1	Typical Contact Pressure Distribution . . . . .	19
Figure 3-2	Contact Between Elliptical Paraboloid and Layered Halfspace. . . . .	20
Figure 4-1	Discretization of Contact Zone . . . . .	29
Figure 4-2	Element of Linear Pressure Variation . . . . .	30
Figure 4-3	Discretized Pressure Distribution. . . . .	31
Figure 4-4	Elemental Region of Integration for Discretized Integral Equation . . . . .	33
Figure 4-5	Classes of $u$ - $v$ Regions of Integration for Hankel Inver- sion Integrals . . . . .	50
Figure 5-1	Axisymmetric Pressure Profiles, Material Combination (i)	62
Figure 5-2	Axisymmetric Pressure Profiles, Material Combination (ii) . . . . .	63
Figure 5-3	Axisymmetric Pressure Profiles, Material Combination (iii). . . . .	64
Figure 5-4	Axisymmetric Pressure Profile Shapes, Material Combina- tion (i) . . . . .	65
Figure 5-5	Axisymmetric Pressure Profile Shapes, Material Combina- tion (ii). . . . .	66
Figure 5-6	Axisymmetric Pressure Profile Shapes, Material Combina- tion (iii) . . . . .	67
Figure 5-7	Major Halfwidth versus Layer Thickness at Fixed Curva- ture Ratio, Material Combination (i) . . . . .	69
Figure 5-8	Major Halfwidth versus Layer Thickness at Fixed Curva- ture Ratio, Material Combination (ii). . . . .	70
Figure 5-9	Major Halfwidth versus Layer Thickness at Fixed Curva- ture Ratio, Material Combination (iii) . . . . .	71
Figure 5-10	Minor Halfwidth versus Layer Thickness at Fixed Curva- ture Ratio, Material Combination (i) . . . . .	72



# LIST OF FIGURES (cont.)

	Page
Figure 5-11 Minor Halfwidth versus Layer Thickness at Fixed Curvature Ratio, Material Combination (ii) . . . . .	73
Figure 5-12 Minor Halfwidth versus Layer Thickness at Fixed Curvature Ratio, Material Combination (iii). . . . .	74
Figure 5-13 Approach versus Layer Thickness at Fixed Curvature Ratio, Material Combination (i). . . . .	75
Figure 5-14 Approach versus Layer Thickness at Fixed Curvature Ratio, Material Combination (ii) . . . . .	76
Figure 5-15 Approach versus Layer Thickness at Fixed Curvature Ratio, Material Combination (iii). . . . .	77
Figure 5-16 Control Pressure versus Layer Thickness at Fixed Curvature Ratio, Material Combination (i). . . . .	78
Figure 5-17 Central Pressure versus Layer Thickness at Fixed Curvature Ratio, Material Combination (ii) . . . . .	79
Figure 5-18 Control Pressure versus Layer Thickness at Fixed Curvature Ratio, Material Combination (iii). . . . .	80
Figure 5-19 Ellipticity Ratio versus Layer Thickness at Fixed Curvature Ratio, Material Combination (i). . . . .	82
Figure 5-20 Ellipticity Ratio versus Layer Thickness at Fixed Curvature Ratio, Material Combination (ii) . . . . .	83
Figure 5-21 Ellipticity Ratio versus Layer Thickness at Fixed Curvature Ratio, Material Combination (iii). . . . .	84
Figure 5-22 Loading of Surface Layer by Edge of Crowned Disc. . . . .	86
Figure I-1 Regions of Integration. . . . .	93

### ACKNOWLEDGMENTS

This report was submitted by the author to the graduate faculty of Rensselaer Polytechnic Institute as a thesis in partial fulfillment of the requirements for the degree of Doctor of Philosophy in Mechanics. Special thanks go out to Dr. Jed Walowit and Professor Frederick F. Ling for their generous technical guidance throughout the duration of the study. The assistance of Miss Tenley James of Mechanical Technology Incorporated in all facets of computer programming and operation was particularly valuable.

The investigation was performed for the office of Naval Research under Contract N00014-72-C-0083, with Mr. Stanley Doroff as project monitor.

# ABSTRACT

A numerical method is developed to compute the pressure distribution and normal approach in a generalized elliptical contact between layered linearly elastic solids. The computed quantities are obtained as an approximate solution to an integral equation formulated for the most general case of Hertz's assumptions, i.e., the frictionless contact between arbitrary surfaces whose undeformed normal separation can be approximated by the separation between an elliptical paraboloid and the tangent plane at its vertex. The numerical method is based on a discretized representation of the unknown pressure distribution. Values of pressure are defined at points on a two-dimensional rectilinear grid and a linear function approximates the pressure distribution between adjacent points. Expression of the integral equation at each grid point yields a system of linear equations in the discrete pressures, with coefficients formed from integrals of the kernel function over right triangular regions between adjacent points. The kernel, given by a Hankel transform inversion, is integrated numerically by Gaussian quadrature.

The method is applied to the contact between a homogeneous solid and a layered solid consisting of an isotropic surface layer of uniform thickness in perfect adhesion to an isotropic substrate. Comparisons with available solutions for the limiting cases of Hertz contact between homogeneous solids and axisymmetric contact of layered solids establish the accuracy of the numerical method. Solutions obtained for three sets of material properties over ranges of the contact zone ellipticity ratio and major halfwidth to layer

thickness ratio are given as plots which show the major and minor halfwidths, approach, and central pressure as functions of layer thickness at fixed load and fixed principle curvature ratio of the parabolic separation. As the layer thickness decreases, the contact zone ellipticity ratio is found to increase for a high-modulus layer bonded to a low-modulus substrate and decrease for a low-modulus layer bonded to a high-modulus substrate.

## NOMENCLATURE

$a$  = major contact zone halfwidth (in.).

$a_o$  = major contact zone halfwidth for axisymmetric Hertz contact, defined in Equation 3.27 (in.).

$b$  = minor contact zone halfwidth (in.).

$d$  = normal approach (in.).

$d_o$  = normal approach for axisymmetric Hertz contact, defined in Equation 3.25 (in.).

$E_1$  = elastic modulus of layer (lb/in.<sup>2</sup>).

$E_2$  = elastic modulus of substrate (lb/in.<sup>2</sup>).

$E_3$  = elastic modulus of homogeneous solid (lb/in.<sup>2</sup>).

$F$  = magnitude of concentrated force (lb).

$g_i$  ( $i = 1, \dots, 6$ ) = constants for Hankel transform solution, defined in Table 2-1.

$G$  = Hankel transform of stress function, defined in Equation 2.6.

$h$  = layer thickness (in.).

$J_o$  = Bessel function of the first kind of order zero.

$J_1$  = Bessel function of the first kind of order one.

$m(i)$  ( $i = 1, \dots, n$ ) = grid point number in  $\eta$  direction locating contact zone boundary.

$n$  = number of grid points along major halfwidth.

$N$  = total number of grid points in contact zone.

$p$  = contact pressure (lb/in.<sup>2</sup>).

$p^o$  = pressure at center of contact (lb/in.<sup>2</sup>).

$p_o^o$  = pressure at center of contact for axisymmetric Hertz contact, defined in Equation 3.26 (lb/in.<sup>2</sup>).

$r$  = radial coordinate (in.).

$R_x$  = major radius of curvature of separation profile (in.).



$R_y$  = minor radius of curvature of separation profile (in.).  
 $u_r$  = radial (tangential) displacement (in.).  
 $u_z$  = axial (normal) displacement (in.).  
 $u_o$  = normal displacement at surface (in.).  
 $\tilde{u}_o$  = dimensionless surface displacement ( $= 2R_x u_o / a^2$ ).  
 $W$  = contact load (lb).  
 $\bar{W}$  = dimensionless contact load, defined in Equation 3.14.  
 $x$  = coordinate parallel to major halfwidth (in.).  
 $X$  = Love's stress function.  
 $\hat{X}$  = modified stress function ( $= X/h^3$ ).  
 $y$  = coordinate parallel to minor halfwidth (in.).  
 $z$  = axial (normal) coordinate  
 $\alpha$  = major halfwidth to layer thickness ratio ( $= a/h$ ).  
 $\beta$  = elastic property ratio between layer and homogeneous solid, defined in Equation 3.6.  
 $\Gamma$  = dimensionless normal approach, defined in Equation 3.9.  
 $\epsilon$  = curvature ratio ( $= R_x / R_y$ ).  
 $\zeta$  = dimensionless coordinate ( $= z/h$ ).  
 $\eta$  = dimensionless coordinate ( $= y/a$ ).  
 $\lambda$  = dimensionless coordinate ( $= r/a$ ).  
 $\nu_1$  = Poisson's ratio of layer.  
 $\nu_2$  = Poisson's ratio of substrate.  
 $\nu_3$  = Poisson's ratio of homogeneous solid.  
 $\xi$  = dimensionless coordinate ( $= x/a$ ).  
 $\rho$  = ellipticity ratio ( $= a/b$ ).  
 $\bar{\rho}$  = dimensionless coordinate ( $= r/h$ ).  
 $\tau_{rr}$  = radial normal stress (lb/in.<sup>2</sup>).

$\tau_{zz}$  = axial normal stress (lb/in.<sup>2</sup>).

$\tau_{rz}$  = shear stress (lb/in.<sup>2</sup>).

$\tau_{\theta\theta}$  = circumferential normal stress (lb/in.<sup>2</sup>).

$\phi$  = dimensionless pressure, defined in Equation 3.9.

$\phi^0$  = dimensionless pressure at center of contact.

$\phi_{i,j}$  ( $i = 1, \dots, n$ ;  $j = 1, \dots, m(i)$ ) = values of dimensionless pressure at grid points.

$\omega$  = Hankel transform variable.

$\Delta\xi$  = grid spacing in  $\xi$  direction ( $=1/(n-1)$ ).

$\Delta\eta$  = grid spacing in  $\eta$  direction ( $=\Delta\xi/\rho$ ).

## PART 1

### INTRODUCTION

Hertz's classical solution [1-3]\* for the contact stresses between deformable solids is frequently applied in the engineering analysis of load bearing mechanical elements such as ball and roller bearings, cams, and gears. Under Hertz's basic assumptions, the equations of linear elasticity apply, friction is absent, and each solid is treated as a halfspace under normal surface loading. In the contact zone, the relative normal surface displacement between the solids is prescribed by their deformation into contact. The contact pressure distribution, which is unknown, depends on this relative displacement through a singular integral equation whose kernel is the surface displacement of a halfspace due to a concentrated normal force. When the contact is between rounded surfaces over a small enough region, the undeformed normal separation can be approximated by a quadratic function; i.e., the separation is that between a plane and an elliptical paraboloid. The relative displacement profile in the contact zone is thus parabolic. For homogeneous isotropic solids, the pressure profile that satisfies the resulting integral equation was shown by Hertz [1-3] to be a semi-ellipsoid whose major to minor axis ratio in the surface of contact depends purely on the shape of the elliptical paraboloid defining the undeformed separation. The problem may be formulated in the same manner when one of the solids consists of an isotropic surface layer backed by an isotropic substrate of a different material. However, the integral equation will not have a simple analytical solution because the concentrated force solution for a layered halfspace is given by a Fourier or Hankel integral that requires numerical evaluation.

Current interest in the contact problem for layered solids follows from a need for analytical prediction of stresses and displacements in coated bearing elements. In some applications, a hard (high modulus) coating such as a ceramic may be used to increase the surface durability of an element; in others, a soft (low modulus) coating such as an

---

\*Numbers in brackets denote references listed at the end of the report.



elastomer can protect elements that experience impact. Water-lubricated marine bearings and gas-lubricated directional control gyroscopes are subjects of current research that fall into the latter category. Both applications involve a bearing surface consisting of a thin compliant elastomeric layer bonded to a relatively rigid substrate. Contact pressure distributions must be determined before one can compute the subsurface stresses developed in the layer under concentrated contact. When there is a large enough difference in elastic properties between layer and substrate, the true contact pressures can differ significantly from those predicted by the Hertz solution.

To date, any layered contact solutions available in the literature are limited to plane strain and axisymmetry [4-8]. For plane strain, the undeformed separation is that between a plane and an infinitely long parabolic cylinder; the kernel is the solution for a line load. For axisymmetry, the undeformed separation is that between a plane and a paraboloid of revolution; the kernel is the solution for a ring load. Except for differences in the mathematical form of the kernel, the integral equations for the two cases are the same. The unknown pressure is one-dimensional and the same general strategies can be used to obtain approximate numerical solutions to both problems. There are no solutions in the literature for the general case of three-dimensional contact for layered solids, in which the undeformed separation is that between a plane and an elliptical paraboloid. Here the kernel is the solution for a point load, and the unknown pressure is two-dimensional. The aim of the present study is to solve this problem numerically by extending to two dimensions a method that has been used for plane and axisymmetric problems.

The literature up to 1972 on plane and axisymmetric layered contact is listed by Chen and Engel [4]. Of the works listed, only that of Tu [5] has direct bearing on the method used in the present study. In obtaining a numerical solution to the axisymmetric contact of a plate pressed between two spheres, Tu represents the contact pressure distribution by values defined on a discrete set of concentric circles with the pressure varying linearly in radius between adjacent circles. The analogous treatment for plane problems was recently put forth by Gupta and Walowit [6] who treat the plane strain contact between a homogeneous elastic solid and a layered elastic solid. The plane contact pressure distribution

is represented by values defined at a discrete set of points with the pressure varying linearly between adjacent points. In both cases, the exact displacement at each discrete point due to the approximate pressure distribution is obtained in terms of Fourier integrals and matched to the prescribed contact displacement to produce a set of linear equations in the unknown discrete pressure values.

Chen and Engel [4], in treating the axisymmetric contact between a rigid paraboloid and a layered elastic solid, represent the unknown pressure distribution  $p(r)$  as a truncated series of base pressures:  $p_i(r) = A_i(1-r^2/a^2)^{i-1/2}$  (where  $A_i$  are undetermined coefficients and  $a$  is the contact radius). With exact surface displacements due to each base function computed from Fourier integrals, the coefficients  $A_i$  are determined by matching computed displacements to prescribed contact displacements according to an integral-least square or collocation criterion. Methods similar to this one are applied in many of the earlier works cited by Chen and Engel. In some instances, the form of the base pressures follows from a power series approximation of the kernel function. Here the calculated surface displacement due to the approximate pressure distribution is also approximate. Wu and Ling [7] use this approach to obtain approximate solutions for the axisymmetric contact between a rigid paraboloid and an elastic plate resting on a rigid foundation.

Methods that involve series approximations of the kernel are difficult to implement when the layer is very thin relative to the contact zone dimension. The number of terms needed for convergence increases rapidly as the layer thickness decreases [5]. Also, in the case of a hard layer on a soft substrate, the pressure profile shape can depart significantly from the elliptical shape of the Hertz solution. Pressure profiles given in References [4] and [6] for this case show a peak near the edge of contact that becomes sharper as the layer thickness decreases. An unwieldy number of base functions is presumably required to represent such a profile accurately. The discrete pressure methods of Tu [5] and of Gupta and Walowit [6] do not suffer from these limitations though they do require more computational labor than methods based on series approximations. The kernel evaluation is exact and pressure irregularities can be handled by increasing the number of discrete points in troublesome regions.

In the present study, a natural extension of the above discrete pressure methods is applied to the general three-dimensional contact between a layered elastic solid and a homogeneous elastic solid. The layered solid consists of a single isotropic layer in perfect adherence to an isotropic substrate. Since the unknown pressure distribution depends on two space variables, it is represented by values defined at discrete points on a two-dimensional grid. Following Tu [5] and Gupta and Walowit [6], adjacent grid points delineate elements of linearly varying pressure, but this time in two dimensions. The basic contact zone division is a right triangle; the elemental pressure distribution is a plane. The point load solution for the kernel comes from a Hankel transform analysis similar to that of Lamb, Terezawa, and Sneddon [8]. As in the one-dimensional methods, the exact evaluation of the kernel makes possible the exact computation of surface displacements due to the approximate pressure distribution. The procedure of matching computed displacements to prescribed contact displacements at each grid point is then employed to get the desired system of linear equations in the unknown pressures. The contact zone boundary prescribed in setting up the problem is approximate since by definition it follows the grid lines that bound the outermost pressure elements. Moreover, the true boundary is an unknown in the problem because it depends on the mathematical form of the pressure distribution. Since the approximate boundary has to be specified to calculate the approximate pressure distribution, the best approximate boundary for a given grid size is determined by an iterative process.

Numerical solutions are presented for three distinct material combinations over ranges of the contact zone halfwidth to layer thickness ratio and the contact zone aspect or ellipticity ratio. A discrete boundary prescribed to represent an ellipse gave satisfactory results in all cases. Checks on the accuracy of the method include comparison of computed results with the Hertz solution [1-3] and numerical results of Chen and Engel [4]. The solutions are presented graphically in dimensionless form with major and minor halfwidths, relative approach, and central pressure shown at a fixed load as functions of layer thickness and ratio of the principal radii of curvature of the parabolic separation profile.

The analytical foundations of the study are presented in Parts 2 and 3. Part 2 covers the Hankel transform analysis leading to the point load solution; Part 3 gives the derivation of the integral equation in dimensionless form. Details of the numerical solution procedure for the integral equation are given in Part 4, and Part 5 contains the numerical results. A simple example at the end of Part 5 demonstrates the application of the numerical results to an engineering problem.



## PART 2

SOLUTION FOR SURFACE DISPLACEMENT DUE TO CONCENTRATED NORMAL FORCE2.1 Formulation of Boundary Value Problem

Consider the layered elastic halfspace shown in Figure 2-1 consisting of an isotropic layer of thickness  $h$  with Young's Modulus and Poisson's Ratio  $E_1, \nu_1$ , bonded uniformly to an infinite isotropic substrate of properties  $E_2, \nu_2$ . The halfspace is described by the Cartesian coordinates  $x, y, z$ , and cylindrical coordinates  $r, \theta, z$ , with the  $x$ - $y$  and  $r$ - $\theta$  planes coinciding with the free surface, and with the  $z$  axis directed into the halfspace. In this section, an expression will be derived for the normal displacement at any point on the surface due to a concentrated force  $F$  acting normally inward at the origin. This solution will form the kernel of the integral equation for the contact problem to be dealt with subsequently.

In cylindrical coordinates  $r, z$ , begin with Love's stress function  $X$  for axisymmetric problems [2] satisfying

$$\left. \begin{aligned} \nabla^4 X &= \nabla^2(\nabla^2 X) = 0 \\ \nabla^2 &= \frac{\partial^2}{\partial r^2} + \frac{1}{r} \frac{\partial}{\partial r} + \frac{\partial^2}{\partial z^2} \end{aligned} \right\} \quad (2.1)$$

with stress components expressible in terms of  $X$ :

$$\begin{aligned} \tau_{rr} &= \frac{\partial}{\partial z} \left( \nu \nabla^2 - \frac{\partial^2}{\partial r^2} \right) X \\ \tau_{\theta\theta} &= \frac{\partial}{\partial z} \left( \nu \nabla^2 - \frac{1}{r} \frac{\partial}{\partial r} \right) X \\ \tau_{zz} &= \frac{\partial}{\partial z} \left[ (2 - \nu) \nabla^2 - \frac{\partial^2}{\partial z^2} \right] X \\ \tau_{rz} &= \frac{\partial}{\partial r} \left[ (1 - \nu) \nabla^2 - \frac{\partial^2}{\partial z^2} \right] X \end{aligned} \quad (2.2)$$

$$\tau_{r\theta} = \tau_{\theta z} = 0$$

and displacement components:

$$\left. \begin{aligned} u_r &= - \frac{1 + \nu}{E} \frac{\partial^2 X}{\partial r \partial z} \\ u_z &= \frac{1 + \nu}{E} \left[ 2(1 - \nu) \nabla^2 - \frac{\partial^2}{\partial z^2} \right] X \end{aligned} \right\} \quad (2.3)$$

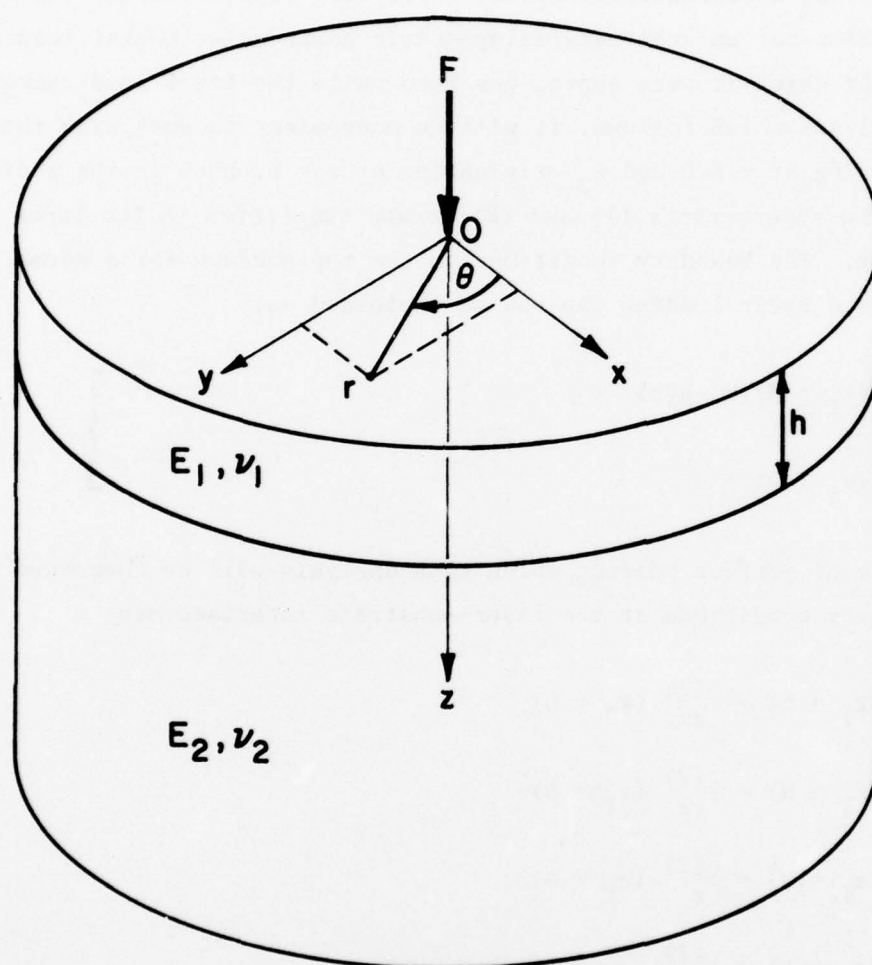


Fig. 2-1 Configuration for Concentrated Force Problem

It can be verified by direct substitution that Equations 2.3 satisfy the displacement form of the static equilibrium equations of isotropic linear elasticity when  $X$  satisfies Equations 2.1. By successive application of the strain-displacement and stress-strain relations, Equations 2.2 are obtained from Equations 2.3.

The solution for a concentrated normal force will be obtained as the limit of the solution for an arbitrary axisymmetric compressive normal loading as the area over which it acts approaches zero while the total load remains finite. For the analysis which follows, it will be convenient to work with the coordinates  $z_1$ , originating at  $z = 0$  and  $z_2$  originating at  $z = h$ , both in the  $z$  direction. Also, let the superscripts (1) and (2) denote quantities in the layer and substrate, respectively. The boundary conditions on the top surface for a normal loading  $p(r)$  with zero shear loading can now be expressed as:

$$\left. \begin{aligned} \tau_{zz}^{(1)}(z_1 = 0) &= -p(r) \\ \tau_{rz}^{(1)}(z_1 = 0) &= 0 \end{aligned} \right\} \quad (2.4)$$

For the case of perfect bonding which this analysis will be concerned with, the continuity conditions at the layer-substrate interface are:

$$\begin{aligned} \tau_{zz}^{(1)}(z_1 = h) &= \tau_{zz}^{(2)}(z_2 = 0) \\ \tau_{rz}^{(1)}(z_1 = h) &= \tau_{rz}^{(2)}(z_2 = 0) \\ u_r^{(1)}(z_1 = h) &= u_r^{(2)}(z_2 = 0) \\ u_z^{(1)}(z_1 = h) &= u_z^{(2)}(z_2 = 0) \end{aligned} \quad (2.5)$$

In addition, the stress components must satisfy

$$\begin{aligned} \tau_{zz} &\rightarrow 0 & \text{as } z &\rightarrow \infty \\ \tau_{rz} &\rightarrow 0 & \text{as } z, r &\rightarrow \infty \\ \tau_{rr} &\rightarrow 0 & \text{as } r &\rightarrow \infty \end{aligned}$$

in order that all surface tractions vanish at  $\infty$ .

## 2.2 Formal Solution by Integral Transforms

In many cases, partial differential equations can be reduced to ordinary ones through the use of integral transforms. For axisymmetric problems where the radial variable ranges from 0 to  $\infty$ , the Hankel Transform is generally applied. The formulation used here is similar to those of Lamb, Terezawa, and Sneddon [8] in obtaining solutions for half-space and plate problems with axial symmetry.

Let  $f(r)$  be a function which satisfies the sufficient conditions for representation by the Hankel Integral Formula [8]. Its Hankel Transform and inverse transform are given by

$$F(\omega) = \int_0^{\infty} r f(r) J_0(\omega r) dr$$

$$f(r) = \int_0^{\infty} \omega F(\omega) J_0(\omega r) d\omega$$

Before taking the Hankel Transforms of Equations 2.1 through 2.5, it will be helpful to rewrite them in terms of the dimensionless coordinates  $\bar{\rho} = r/h$ ,  $\bar{\zeta} = z/h$ , and the stress function  $\hat{X} = X/h^3$  which has the dimension of stress. Equations 2.1 become

$$\left. \begin{aligned} \nabla^4 \hat{X} &= \nabla^2 (\nabla^2 \hat{X}) = 0 \\ \nabla^2 &= \frac{\partial^2}{\partial \bar{\rho}^2} + \frac{1}{\bar{\rho}} \frac{\partial}{\partial \bar{\rho}} + \frac{\partial^2}{\partial \bar{\zeta}^2} \end{aligned} \right\} \quad (2.1a)$$

with the stresses and displacement from Equations 2.2 and 2.3

$$\begin{aligned} \tau_{rr} &= \frac{\partial}{\partial \bar{\zeta}} \left( \nu \nabla^2 - \frac{\partial^2}{\partial \bar{\rho}^2} \right) \hat{X} \\ \tau_{\theta\theta} &= \frac{\partial}{\partial \bar{\zeta}} \left( \nu \nabla^2 - \frac{1}{\bar{\rho}} \frac{\partial}{\partial \bar{\rho}} \right) \hat{X} \\ \tau_{zz} &= \frac{\partial}{\partial \bar{\zeta}} \left[ (2-\nu) \nabla^2 - \frac{\partial^2}{\partial \bar{\zeta}^2} \right] \hat{X} \\ \tau_{rz} &= \frac{\partial}{\partial \bar{\rho}} \left[ (1-\nu) \nabla^2 - \frac{\partial^2}{\partial \bar{\zeta}^2} \right] \hat{X} \end{aligned} \quad (2.2a)$$



$$\left. \begin{aligned} u_r &= -\frac{h(1+\nu)}{E} \frac{\partial^2 \hat{X}}{\partial \bar{\rho} \partial \zeta} \\ u_z &= \frac{h(1+\nu)}{E} \left[ 2(1-\nu) \nabla^2 - \frac{\partial^2}{\partial \zeta^2} \right] \hat{X} \end{aligned} \right\} \quad (2.3a)$$

The boundary and continuity conditions from Equations 2.4 and 2.5 can be written as

$$\left. \begin{aligned} \tau_{zz}^{(1)}(\zeta_1 = 0) &= -p(\bar{\rho}) \\ \tau_{rz}^{(1)}(\zeta_1 = 0) &= 0 \end{aligned} \right\} \quad (2.4a)$$

$$\begin{aligned} \tau_{zz}^{(1)}(\zeta_1 = 1) &= \tau_{zz}^{(2)}(\zeta_2 = 0) \\ \tau_{rz}^{(1)}(\zeta_1 = 1) &= \tau_{rz}^{(2)}(\zeta_2 = 0) \\ u_r^{(1)}(\zeta_1 = 1) &= u_r^{(2)}(\zeta_2 = 0) \\ u_z^{(1)}(\zeta_1 = 1) &= u_z^{(2)}(\zeta_2 = 0) \end{aligned} \quad (2.5a)$$

with  $\zeta_1$  and  $\zeta_2$  defined analogously to  $z_1$  and  $z_2$ .

Denoting the Hankel Transform of  $\hat{X}(\bar{\rho}, \zeta)$  by

$$G(\omega, \zeta) = \int_0^\infty \hat{X}(\bar{\rho}, \zeta) J_0(\rho\omega) d\bar{\rho},$$

and taking the transform of Equations 2.1a, one obtains

$$\left( \frac{d^2}{d\zeta^2} - \omega^2 \right)^2 G = 0$$

which has the general solution

$$G = (A + B\zeta)e^{-\omega\zeta} + (C + D\zeta)e^{\omega\zeta} \quad (2.6)$$

where the constant coefficients, A, B, C, and D, will generally depend on  $\omega$ . Taking the Hankel transforms of Equations 2.2a and 2.3a, and then inverting, one obtains the following expressions for the stresses and displacements in terms of G.

$$\begin{aligned}
\tau_{rr} &= \int_0^\infty \omega J_0(\bar{\rho}\omega) \left[ \nu \frac{d^3 G}{d\zeta^3} + (1-\nu) \omega^2 \frac{dG}{d\zeta} \right] d\omega - \frac{1}{\rho} \int_0^\infty \omega^2 J_1(\bar{\rho}\omega) \frac{dG}{d\zeta} d\omega \\
\tau_{\theta\theta} &= \nu \int_0^\infty \omega J_0(\bar{\rho}\omega) \left[ \frac{d^3 G}{d\zeta^3} - \omega^2 \frac{dG}{d\zeta} \right] d\omega + \frac{1}{\rho} \int_0^\infty \omega^2 J_1(\bar{\rho}\omega) \frac{dG}{d\zeta} d\omega \\
\tau_{zz} &= \int_0^\infty \omega J_0(\bar{\rho}\omega) \left[ (1-\nu) \frac{d^3 G}{d\zeta^3} - (2-\nu) \omega^2 \frac{dG}{d\zeta} \right] d\omega \\
\tau_{rz} &= \int_0^\infty \omega^2 J_1(\bar{\rho}\omega) \left[ \nu \frac{d^2 G}{d\zeta^2} + (1-\nu) \omega^2 G \right] d\omega \\
u_r &= \frac{h(1+\nu)}{E} \int_0^\infty \omega^2 J_1(\bar{\rho}\omega) \frac{dG}{d\zeta} d\omega \\
u_z &= \frac{h(1+\nu)}{E} \int_0^\infty \omega J_0(\bar{\rho}\omega) \left[ (1-2\nu) \frac{d^2 G}{d\zeta^2} - 2(1-\nu) \omega^2 G \right] d\omega
\end{aligned} \tag{2.7}$$

The function  $G$  will take the following forms in the layer and substrate, respectively:

$$\left. \begin{aligned}
G^{(1)} &= (A_1 + B_1 \zeta_1) e^{-\omega \zeta_1} + (C_1 + D_1 \zeta_1) e^{\omega \zeta_1}, \quad 0 \leq \zeta_1 \leq 1 \\
G^{(2)} &= (A_2 + B_2 \zeta_2) e^{-\omega \zeta_2} + (C_2 + D_2 \zeta_2) e^{\omega \zeta_2}, \quad 0 \leq \zeta_2 \leq \infty
\end{aligned} \right\} \tag{2.8}$$

In order for the tractions to vanish as  $\zeta_2 \rightarrow \infty$ ,  $C_2 = D_2 = 0$ . The remaining six constants are obtained from the two boundary and four continuity conditions in Equations 2.4a and 2.5a. Using Equations 2.7 to express these conditions in terms of  $G$  gives:

$$\begin{aligned}
\left[ (1-\nu_1) \frac{d^3 G^{(1)}}{d\zeta_1^3} - (2-\nu_1) \omega^2 \frac{dG^{(1)}}{d\zeta_1} \right]_{\zeta_1=0} &= -P(\omega) \\
\left[ \nu_1 \frac{d^2 G^{(1)}}{d\zeta_1^2} + (1-\nu_1) \omega^2 G^{(1)} \right]_{\zeta_1=0} &= 0
\end{aligned} \tag{2.9}$$

$$\left[ (1-\nu_1) \frac{d^3 G^{(1)}}{d\zeta_1^3} - (2-\nu_1) \omega^2 \frac{dG^{(1)}}{d\zeta_1} \right]_{\zeta_1=1} = \left[ (1-\nu_2) \frac{d^3 G^{(2)}}{d\zeta_2^3} - (2-\nu_2) \omega^2 \frac{dG^{(2)}}{d\zeta_2} \right]_{\zeta_2=0}$$

$$\left[ \nu_1 \frac{d^2 G^{(1)}}{d\zeta_1^2} + (1-\nu_1) \omega^2 G^{(1)} \right]_{\zeta_1=1} = \left[ \nu_2 \frac{d^2 G^{(2)}}{d\zeta_2^2} + (1-\nu_2) \omega^2 G^{(2)} \right]_{\zeta_2=0}$$

$$\frac{1+\nu_1}{E_1} \left[ \frac{dG^{(1)}}{d\zeta_1} \right]_{\zeta_1=1} = \frac{1+\nu_2}{E_2} \left[ \frac{dG^{(2)}}{d\zeta_2} \right]_{\zeta_2=0} \quad (2.9) \quad (\text{Cont'd.})$$

$$\frac{1+\nu_1}{E_1} \left[ (1-2\nu_1) \frac{d^2 G^{(1)}}{d\zeta_1^2} - 2(1-\nu_1) \omega^2 G^{(1)} \right]_{\zeta_1=1} = \frac{1+\nu_2}{E_2} \left[ (1-2\nu_2) \frac{d^2 G^{(2)}}{d\zeta_2^2} - 2(1-\nu_2) \omega^2 G^{(2)} \right]_{\zeta_2=0}$$

where  $P(\omega)$  is the Hankel transform of the normal loading  $p(\rho)$ :

$$P(\omega) = \int_0^\infty \rho p(\rho) J_0(\rho\omega) d\rho \quad (2.10)$$

Substituting from Equations 2.8 into Equations 2.9 yields six simultaneous equations in the six unknown constants  $A_1, B_1, C_1, D_1, A_2$ , and  $B_2$ . It is convenient to express the unknown constants as the quantities:

$$\begin{aligned} g_1 &= -A_1 [\omega^3/P(\omega)] \\ g_2 &= -B_1 [\omega^2/P(\omega)] \\ g_3 &= -C_1 [\omega^3/P(\omega)] \\ g_4 &= -D_1 [\omega^2/P(\omega)] \\ g_5 &= -A_2 [\omega^3/P(\omega)] \\ g_6 &= -B_2 [\omega^2/P(\omega)] \end{aligned} \quad (2.11)$$

which turn out to depend only on  $\omega$ ,  $\nu_1, \nu_2$ , and  $E_1/E_2$ . Table 2-1 gives the resulting simultaneous equations in  $g_1$  through  $g_6$  in matrix form.

At this point, Equations 2.7, 2.8, 2.10, and 2.11, and Table 2-1 could be applied to compute the stresses and displacements at any point in the halfspace due to the normal surface loading  $p(\bar{\rho})$ . However, the only quantity needed to formulate the contact problem is the normal surface displacement  $u_z^{(1)} (\zeta_1 = 0)$  which will be denoted by  $u_o$ . Substituting from the first of Equations 2.8 into the sixth of Equations 2.7, setting  $\zeta_1 = 0$ , and using Equations 2.11 and the second equation in Table 2-1 to simplify the result, the following expression is obtained:

$$u_o(\bar{\rho}) = \frac{2h(1-\nu_1^2)}{E_1} \int_0^{\infty} [g_2(\omega) - g_4(\omega)] P(\omega) J_0(\bar{\rho}\omega) d\omega \quad (2.12)$$

To obtain the specific form of  $P(\omega)$  for a concentrated normal force  $F$  at the origin, begin with the following loading:

$$p(\bar{\rho}) = \begin{cases} F/\pi a^2 & \bar{\rho} \leq a/h \\ 0 & \bar{\rho} > a/h \end{cases}$$

Equation 2.10 gives

$$P(\omega) = \frac{F}{\pi h^2} \frac{J_1(a\omega/h)}{(a\omega/h)}$$

for the Hankel transform of this normal loading. The limit of this expression as  $a \rightarrow 0$  is

$$P(\omega) = \frac{F}{2\pi h^2}$$

the Hankel transform of a normal loading consisting of a concentrated force of magnitude  $F$  at the origin. Setting  $F = 1$ , write Equation 2.12 for this particular  $P(\omega)$ . The desired end result, the surface displacement due to a unit concentrated force, is now obtained.

Denoting it by  $\delta_o$ , one has:

TABLE 2-1  
SIMULTANEOUS EQUATIONS IN CONSTANTS FOR HANKEL TRANSFORM SOLUTION

$$\begin{bmatrix} 1 & n_1 & -1 & n_1 & 0 & 0 \\ 1 & -2v_1 & 1 & 2v_1 & 0 & 0 \\ 1 & n_1 + \omega & -e^{2\omega} & (n_1 - \omega)e^{2\omega} & -e^{\omega} & -n_2 e^{\omega} \\ 1 & \omega - 2v_1 & e^{2\omega} & (\omega + 2v_1)e^{2\omega} & -e^{\omega} & 2v_2 e^{\omega} \\ -1 & 1 - \omega & e^{2\omega} & (1 + \omega)e^{2\omega} & \gamma e^{\omega} & -\gamma e^{\omega} \\ 1 & \omega + 2n_1 & e^{2\omega} & (\omega - 2n_1)e^{2\omega} & -\gamma e^{\omega} & -2\gamma n_2 e^{\omega} \end{bmatrix} \begin{bmatrix} g_1 \\ g_2 \\ g_3 \\ g_4 \\ g_5 \\ g_6 \end{bmatrix} = \begin{bmatrix} 1 \\ 0 \\ 0 \\ 0 \\ 0 \\ 0 \end{bmatrix}$$

$$n_1 = 1 - 2v_1$$

$$n_2 = 1 - 2v_2$$

$$\gamma = \frac{E_1}{E_2} \left( \frac{1 + v_2}{1 + v_1} \right)$$



$$\delta_o(\bar{\rho}) = \frac{1-v_1^2}{\pi E_1 h} \int_0^{\infty} [g_2(\omega) - g_4(\omega)] J_o(\bar{\rho} s) d\omega \quad (2.13)$$

To obtain algebraic solutions for  $g_2$  and  $g_4$  from the 6 x 6 system in Table 2-1, first solve the third and fourth equations for  $e^{\omega} g_5$  and  $e^{\omega} g_6$  and use the resulting expressions to eliminate  $g_5$  and  $g_6$  from the fifth and sixth equations. Then solve the first and second equations for  $g_1$  and  $g_3$ , and use the resulting expressions to eliminate  $g_1$  and  $g_3$  from the modified fifth and sixth equations. The resultant form of the fifth and sixth equations may now be solved for  $g_2$  and  $g_4$  to yield:

$$g_2(\omega) - g_4(\omega) = \frac{k_1(\ell_{21} + \ell_{22}) - k_2(\ell_{11} + \ell_{12})}{\ell_{11}\ell_{22} - \ell_{12}\ell_{21}} \quad (2.14)$$

$$\begin{aligned} \text{where } \ell_{11} &= 3 - 4v_1 - \bar{\gamma} + (1+\bar{\gamma})e^{2\omega} \\ \ell_{12} &= (1+\bar{\gamma})2\omega e^{2\omega} \\ \ell_{21} &= (1-\gamma)(3-4v_1-2\omega) + 2\gamma(2v_2 - 2v_1) + (1+\bar{\gamma})e^{2\omega} \\ \ell_{22} &= 1 - \gamma + e^{2\omega} [2 + 2\gamma(2v_2n_1 + 2v_1n_2 + 4v_1 - 1) - (1+\bar{\gamma})(4v_1 - 1 - 2\omega)] \\ k_1 &= (1+\bar{\gamma})e^{2\omega} \\ k_2 &= (1-\gamma) + (1+\bar{\gamma})e^{2\omega} \end{aligned} \quad (2.15)$$

$$\begin{aligned} \text{with } n_1 &= 1 - 2v_1 & ; & & n_2 &= 1 - 2v_2 \\ \gamma &= \frac{E_1}{E_2} \left( \frac{1+v_2}{1+v_1} \right) & ; & & \bar{\gamma} &= \gamma(3-4v_2) \end{aligned} \quad (2.16)$$

It is easily seen that for large  $\omega$ :

$$g_2(\omega) - g_4(\omega) = 1 + O(\omega^2 e^{-2\omega}) \quad (2.17)$$

This result permits recasting of the improper integral in Equation 2.13 to facilitate numerical evaluation. Add and subtract  $J_o(\bar{\rho}\omega)$  inside the integral and recall the basic result

$$\int_0^{\infty} J_o(\bar{\rho}\omega) d\omega = \frac{1}{\bar{\rho}}$$

to obtain

$$\delta_o(\bar{\rho}) = \frac{1 - \nu_1^2}{\pi E_1 h} \left[ \int_0^\infty [g_2(\omega) - g_4(\omega) - 1] J_0(\bar{\rho}\omega) d\omega + \frac{1}{\bar{\rho}} \right] \quad (2.18)$$

The  $1/\bar{\rho}$  term is the surface displacement for a homogeneous half-space of properties  $E_1$ ,  $\nu_1$ , and the integral contains the effect of layering. (Note from Equations 2.15 through 2.17 that  $g_2(\omega) - g_4(\omega) - 1 = 0$  for all  $\omega$  when  $E_1/E_2 = 1$  and  $\nu_1 = \nu_2$ .) It is clear from Equation 2.17 that the improper integral in Equation 2.18 converges like  $\omega^2 e^{-2\omega}$ . Thus, numerical evaluation to high accuracy is possible using an upper limit  $\omega_o$  of moderate magnitude. The error is given by:

$$\int_0^\infty [g_2(\omega) - g_4(\omega) - 1] J_0(\bar{\rho}\omega) d\omega = 0 \quad (\omega_o^2 e^{-2\omega_o}) \quad (2.19)$$

In this study,  $\omega_o$  was assigned a value of 10, leaving an error of the order of  $10^{-7}$ .

In terms of the dimensionless Cartesian coordinates:

$$\left. \begin{aligned} \xi &= x/a \\ \eta &= y/a \end{aligned} \right\} \quad (2.20)$$

where  $a$  will be a characteristic length for the contact problem, Equation 2.14 may be expressed as

$$\delta_o(\xi, \eta) = \frac{1 - \nu_1^2}{\pi E_1 a} \alpha K'(\alpha\xi, \alpha\eta) \quad (2.21)$$

where

$$K'(\xi, \eta) = \int_0^\infty [g_2(\omega) - g_4(\omega) - 1] J_0(\omega \sqrt{\xi^2 + \eta^2}) d\omega + \frac{1}{\sqrt{\xi^2 + \eta^2}} \quad (2.22)$$

and

$$\alpha = a/h \quad (2.23)$$

For notational simplicity, define:

$$\bar{K}'(\xi, \eta) = \alpha K'(\alpha\xi, \alpha\eta) \quad (2.24)$$

to give  $\delta_o$  the form:

$$\delta_o(\xi, \eta) = \frac{1 - \nu_1^2}{\pi E_1 a} \bar{K}'(\xi, \eta) \quad (2.25)$$

Equation 2.25 gives the normal surface displacement at  $\xi, \eta$  due to a unit concentrated normal force at the origin. For the same force positioned at  $\xi', \eta'$ , the displacement at  $\xi, \eta$  is simply:

$$\delta_o(\xi, \eta) = \frac{1 - \nu_1^2}{\pi E_1 a} \bar{K}'(\xi - \xi', \eta - \eta') \quad (2.26)$$

This relation will be used in Section 3.1 to obtain the displacement due to a non-axisymmetric pressure distribution, with the function  $\bar{K}'$  forming a portion of the kernel of the integral equation for the contact problem.

It is important to note from Equations 2.20 and 2.23 that the function  $\bar{K}'$  is singular when its arguments, the  $\xi$  and  $\eta$  positions of the point in question with respect to the position of the concentrated force, vanish. The singularity is isolated to the inverse square root term which was subtracted from the Hankel inversion integral in order to form an integrand which would die out exponentially for large  $\omega$ . The integral, as a result, is fully convergent for all values of the arguments of  $\bar{K}'$ . Letting  $R$  be the distance between the concentrated force and the point in question, the singular term is  $1/R$ . This is an integrable singularity in the sense that the singularity vanishes when Equation 2.24 is integrated to obtain the displacement due to a continuous pressure distribution over a finite region.



## PART 3

ANALYTICAL FORMULATION OF INTEGRAL EQUATION FOR CONTACT PROBLEM3.1 Surface Displacement Due to Non-Axisymmetric Pressure Distribution

To formulate the contact problem, an expression is needed for the normal surface displacements of a layered halfspace due to a pressure distribution such as that shown in Figure 3-1. The pressure is symmetric about the  $x$  and  $y$  axes and is bounded by a closed curve of the same symmetry with vertices at  $(\pm a, 0)$  and  $(0, \pm b)$ . The pressure vanishes everywhere on and outside the bounding curve.

Using the dimensionless coordinates  $\xi = x/a$  and  $\eta = y/a$  defined previously and letting  $\eta = \pm f(\xi)$ , (with  $f(-\xi) = f(\xi)$ ,  $f(0) = b/a$ , and  $f(\pm 1) = 0$ ), denote the upper and lower portions of the bounding curve. Equation 2.26 can be used to set-up the following integral expression for the normal surface displacement  $u_o(\xi, \eta)$  due to the pressure distribution in Figure 3-1:

$$u_o(\xi, \eta) = \frac{a(1-\nu_1^2)}{\pi E_1} \int_{-1}^1 \int_{-f(\xi')}^1 p(\xi', \eta') \bar{K}'(\xi - \xi', \eta - \eta') d\eta' d\xi' \quad (3.1)$$

which is the continuous sum over the pressure distribution of the displacements due to concentrated forces at  $(\xi', \eta')$  of magnitude  $p(\xi', \eta') a^2 d\eta' d\xi'$ . As discussed at the end of Section 2.2,  $u_o(\xi, \eta)$  is bounded and continuous everywhere despite the singularity of  $\bar{K}'$  at  $(\xi, \eta) = (\xi', \eta')$ . Of course the pressure  $p(\xi', \eta')$  must be continuous and sufficiently smooth.

3.2 Derivation of Integral Equation

Under the classical Hertzian assumptions [1-3], the problem of contact between two elastic solids can be reduced to a consideration of the contact between an elliptical paraboloid and a halfspace. Figure 3-2 shows the situation of interest here in which the paraboloid is a homogeneous solid of properties  $E_3, \nu_3$ , and the halfspace is the layered solid analyzed in Part 2. The load direction, parabolic axis of the paraboloid, and  $z$  axis of the layered halfspace are coincident. The  $x$  and  $y$  axes on the surface of the layered halfspace coincide,

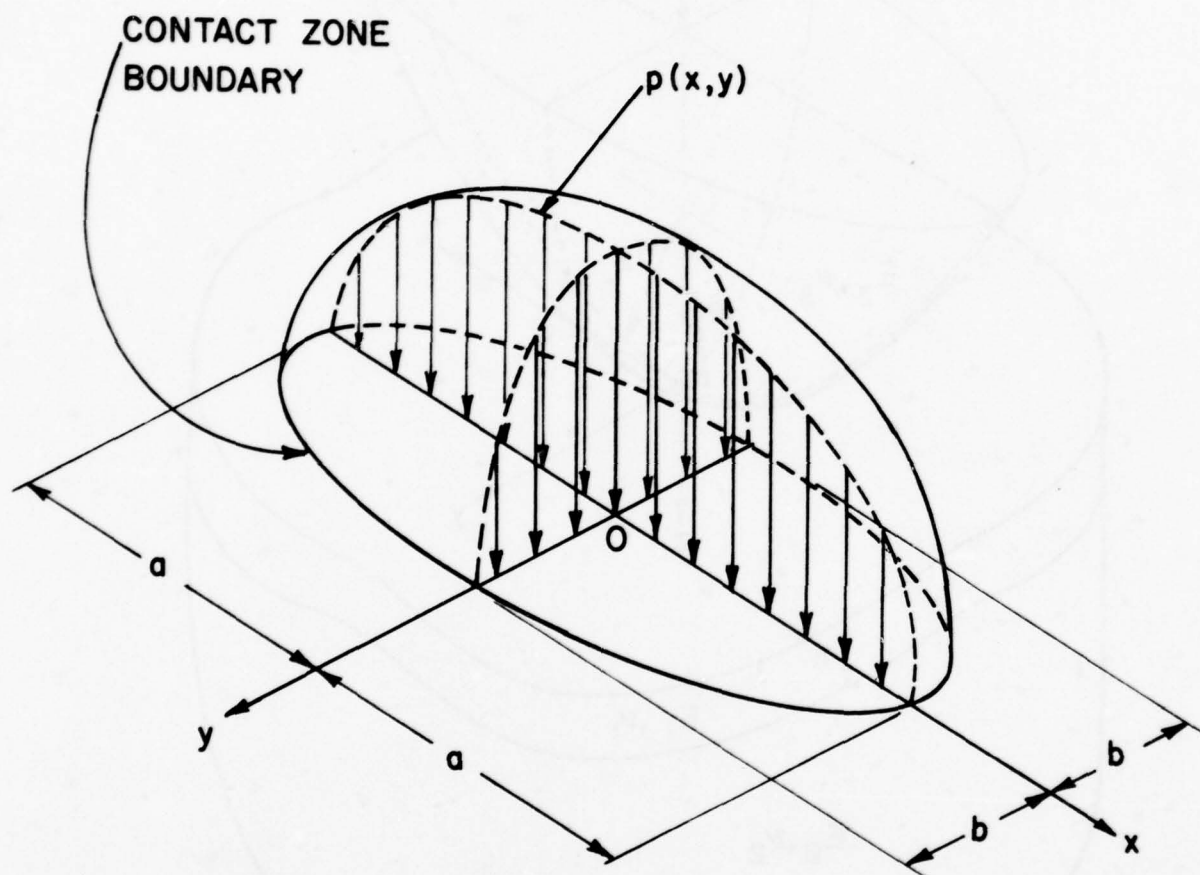


Fig. 3-1 Typical Contact Pressure Distribution

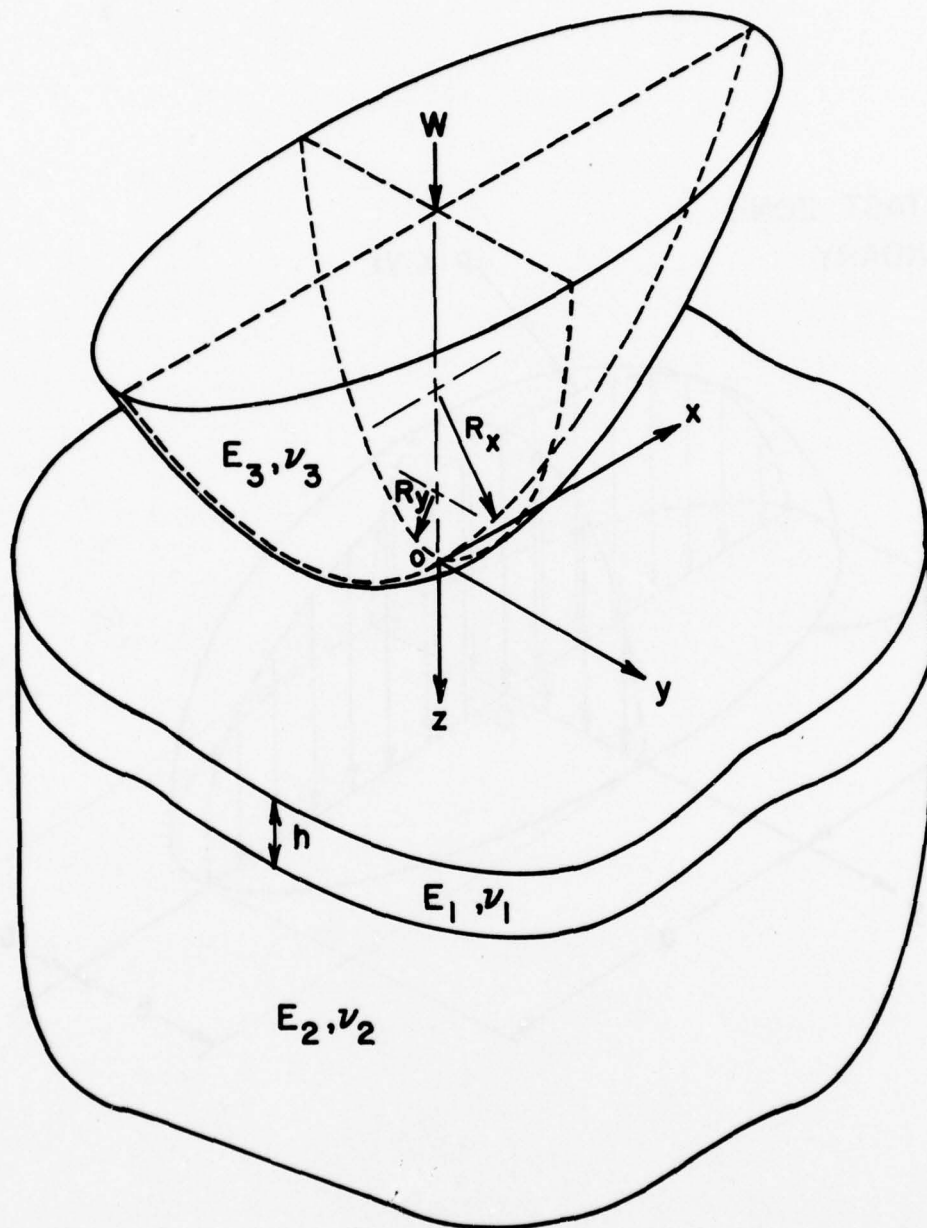


Fig. 3-2 Contact Between Elliptical Paraboloid and Layered Halfspace

respectively, with the major and minor elliptical axes of the paraboloid. In the unstressed state, the two solids are in point contact at the origin with the initial normal separation given by

$$U_i = \frac{x^2}{2R_x} + \frac{y^2}{2R_y}$$

where  $R_x$  and  $R_y$  are the radii of curvature at the vertex of the undeformed paraboloid in the  $x$ - $z$  and  $y$ - $z$  planes, respectively. When the solids are pressed together under a load  $W$ , the separation at any point  $x, y$  is decreased by the normal approach between the two solids and increased by the sum of their local normally inward surface displacements. Thus, the final separation under load is

$$U_f = U_i - d + u_o^I + u_o^{II}$$

where  $d$  is the normal approach;  $u_o^I$  and  $u_o^{II}$  are the surface displacements of the halfspace and paraboloid, respectively. The two solids will be in contact over a finite region centered at the origin in which  $U_f = 0$ , forcing the surface displacement to satisfy:

$$u_o^I + u_o^{II} = d - \frac{x^2}{2R_x} - \frac{y^2}{2R_y} \quad (3.2)$$

The load  $W$  is transmitted through the contact zone by a pressure distribution  $p(x, y)$  as shown in Figure 3-1 which acts normally inward on the surface of each solid, vanishing on and outside the contact zone boundary. As in the statement of the classical Hertz problem, no shear stress is transmitted between the contacting solids.

Equation 3.1 holds exactly as written for  $u_o^I$ , where  $p(\xi, \eta)$  is the contact pressure distribution;  $\eta = \pm f(\xi)$  is the contact zone boundary, and  $a$  and  $b$  are the major and minor contact zone halfwidths. The corresponding surface displacement of the homogeneous solid is given by:

$$u_o^{II}(\xi, \eta) = \frac{a(1-\nu_3^2)}{\pi E_3} \int_{-1}^1 \int_{-f(\xi')}^{f(\xi')} \frac{p(\xi', \eta')}{\sqrt{(\xi-\xi')^2 + (\eta-\eta')^2}} d\eta' d\xi' \quad (3.3)$$

Adding Equation 3.3 to Equation 3.1 for  $u_o^I$  yields:

$$u_o^I(\xi, \eta) + u_o^{II}(\xi, \eta) = \frac{a(1-v_1^2)}{\pi E_1} \int_{-1}^1 \frac{f(\xi')}{-f(\xi')} p(\xi', \eta') \bar{K}(\xi - \xi', \eta - \eta') d\eta' d\xi' \quad (3.4)$$

where the function  $\bar{K}$  is defined in terms of a basic kernel function  $K(\xi, \eta)$ :

$$K(\xi, \eta) = \int_0^\infty [g_2(\omega) - g_4(\omega) - 1] J_0(\omega \sqrt{\xi^2 + \eta^2}) d\omega + \frac{1 + \beta}{\sqrt{\xi^2 + \eta^2}} \quad (3.5)$$

with

$$\beta = \frac{E_1}{E_3} \left( \frac{1 - v_3^2}{1 - v_1^2} \right) \quad (3.6)$$

according to:

$$\bar{K}(\xi, \eta) = \alpha K(\alpha \xi, \alpha \eta) \quad (3.7)$$

Approximating the infinite integral in  $\omega$  as discussed in Section 2.2, the form of  $K(\xi, \eta)$  to be used in the subsequent numerical analysis is:

$$K(\xi, \eta) \approx \int_0^{\omega_o} [g_2(\omega) - g_4(\omega) - 1] J_0(\omega \sqrt{\xi^2 + \eta^2}) d\omega + \frac{1 + \beta}{\sqrt{\xi^2 + \eta^2}} \quad (3.8)$$

with an error of order  $\omega_o^2 e^{-2\omega_o}$  associated with this approximation.

By combining Equation 3.1 with Equation 3.4 and defining the dimensionless quantities:

$$\begin{aligned} \Gamma &= 2R_x d/a^2 \\ \epsilon &= R_x/R_y \\ \phi &= \frac{2R_x(1-v_1^2)p}{\pi E_1 a} \end{aligned} \quad (3.9)$$



one obtains the integral equation

$$\Gamma - \xi^2 - \epsilon\eta^2 = \int_{-1}^1 \frac{f(\xi')}{-f(\xi')} \phi(\xi', \eta') \bar{K}(\xi - \xi', \eta - \eta') d\eta' d\xi' \quad (3.10)$$

which holds for all  $\xi$  and  $\eta$  within the contact zone. Outside the contact zone and along its boundary,  $\phi(\xi, \eta) = 0$ .

Taking advantage of the symmetry of the problem, Equation 3.10 can be written as an integral over the first quadrant of the contact zone:

$$\Gamma - \xi^2 - \epsilon\eta^2 = \int_0^1 \int_0^1 \frac{f(\xi')}{f(\xi')} \phi(\xi', \eta') Q(\xi, \eta; \xi', \eta') d\eta' d\xi' \quad (3.11)$$

where

$$\begin{aligned} Q(\xi, \eta; \xi', \eta') &= \bar{K}(\xi - \xi', \eta - \eta') + \bar{K}(\xi + \xi', \eta - \eta') \\ &+ \bar{K}(\xi - \xi', \eta + \eta') + \bar{K}(\xi + \xi', \eta + \eta') \end{aligned} \quad (3.12)$$

A dimensionless contact load  $\bar{W}$  may be obtained from the integral of  $\phi(\xi, \eta)$  over the contact zone:

$$\bar{W} = 4 \int_0^1 \int_0^1 \frac{f(\xi)}{f(\xi)} \phi(\xi, \eta) d\eta d\xi \quad (3.13)$$

Taking the expression for the actual contact load  $W$ :

$$W = 4 \int_0^a \int_0^{af(x/a)} p(x, y) dy dx$$

and writing  $p$ ,  $x$ , and  $y$  in terms of  $\phi$ ,  $\xi$ , and  $\eta$ , respectively, gives the definition of  $\bar{W}$  as:

$$\bar{W} = \frac{2R_x (1 - \nu_1^2) W}{\pi E_1 a^3} \quad (3.14)$$

This study will be concerned with numerically solving a discretized form of Equation 3.11 to obtain approximate distributions of  $\phi(\xi, \eta)$  along with  $\Gamma$ ,  $\epsilon$ , and  $\bar{W}$  for various layered contact configurations. Before

proceeding with the numerical formulation, it is of some value to consider the classical Hertzian solution as a closed form analytical solution to Equation 3.11 and making use of that solution to define some dimensionless variables more amenable to direct physical interpretation than  $\phi$ ,  $\bar{W}$ , and  $\Gamma$ .

The problem at hand reduces to the classical Hertzian contact problem for homogeneous elastic solids when one sets  $E_1/E_2 = 1$  and  $\nu_1 = \nu_2$  in Equations 2.14 through 2.16 for  $[g_2(\omega) - g_4(\omega)]$ . It is easily verified that under these conditions  $g_2(\omega) - g_4(\omega) = 1$  for all  $\omega$ , so that the Hankel inversion integral in Equation 3.5 for  $K(\xi, \eta)$  vanishes identically, causing Equation 3.10 to reduce to:

$$\Gamma - \xi^2 - \epsilon \eta^2 = \frac{1}{-1 - f(\xi')} \int \frac{f(\xi')}{\sqrt{(\xi - \xi')^2 + (\eta - \eta')^2}} \frac{(1+\beta) \phi(\xi', \eta') d\eta' d\xi'}{\quad} \quad (3.15)$$

This is the integral equation solved analytically by Hertz [1], with the well known result consisting of an ellipsoidal pressure distribution and elliptical contact zone boundary:

$$\begin{aligned} \phi(\xi, \eta) &= \phi^0 \sqrt{1 - \xi^2 - \rho^2 \eta^2} \\ f(\xi) &= \frac{1}{\rho} \sqrt{1 - \xi^2} \end{aligned} \quad (3.16)$$

where

$$\rho \equiv a/b \quad (3.17)$$

Due to the ellipsoidal form of  $\phi$ :

$$\bar{W} = \frac{2\pi\phi^0}{3\rho} \quad (3.18)$$

The constants  $\epsilon$ ,  $\Gamma$ , and  $\phi^0$  are given in terms of complete elliptic integrals whose arguments depend on  $\rho$ :

$$\epsilon = \frac{\rho^2 E(\mu) - K(\mu)}{K(\mu) - E(\mu)} \quad (3.19)$$

$$\Gamma = \frac{\mu K(\mu)}{K(\mu) - E(\mu)} \quad (3.20)$$

$$\phi^0 = \frac{\rho\mu}{\pi(1+\beta)[K(\mu) - E(\mu)]} \quad (3.21)$$

where

$$\mu \equiv \frac{\rho^2 - 1}{\rho^2}, \quad \rho \geq 1 \quad (3.22)$$

$K(\mu)$  and  $E(\mu)$  are complete elliptic integrals of the first and second kind, respectively, defined by:

$$\left. \begin{aligned} K(\mu) &= \int_0^{\pi/2} (1 - \mu \sin^2 \theta)^{-1/2} d\theta \\ E(\mu) &= \int_0^{\pi/2} (1 - \mu \sin^2 \theta)^{1/2} d\theta \end{aligned} \right\} \quad (3.23)$$

Tables and polynomial approximations of these functions are found in Reference [ 9 ].

For the axisymmetric case, the contact zone is circular and  $\rho = 1$ . The constants reduce to:

$$\begin{aligned} \varepsilon &= 1 \\ \Gamma &= 2 \\ \phi^0 &= \frac{4}{\pi^2(1+\beta)} \\ \bar{W} &= \frac{8}{3\pi(1+\beta)} \end{aligned} \quad (3.24)$$

In most physical situations to which contact theory can usefully be applied, the load  $W$  and curvature ratio  $\varepsilon$  are known. Typically, one wishes to determine the normal pressures  $p(x,y)$ , major and minor half-widths  $a, b$ , and approach  $d$ . Denoting by  $p_0(x,y)$ ,  $a_0$ , and  $d_0$ , the

values of these quantities for the case of an axisymmetric Hertzian contact, where the layered halfspace shown in Figure 3-2 is homogeneous in the layer properties  $E_1$ ,  $\nu_1$ , the second, third, and fourth of Equation 3.24 may be equated, respectively, to the first and third of Equation 3.9 and Equation 3.14 to give:

$$d_o = \frac{a_o^2}{R_x} \quad (3.25)$$

$$p_o^o \equiv p_o(0,0) = \frac{2a_o E_1}{\pi R_x (1+\beta)(1-\nu_1^2)} \quad (3.26)$$

$$a_o = \left[ \frac{3R_x W(1+\beta)(1-\nu_1^2)}{4E_1} \right]^{1/3} \quad (3.27)$$

These three equations can be combined, respectively, with the first and third of Equation 3.9 and Equation 3.14 to yield the dimensionless quantities:

$$d/d_o = \frac{1}{2} (a/a_o)^2 \Gamma \quad (3.28)$$

$$p/p_o^o = \frac{1}{4} \pi^2 (1+\beta) (a/a_o) \phi \quad (3.29)$$

$$a/a_o = 2 \left[ 3\pi(1+\beta)\bar{W} \right]^{-1/3} \quad (3.30)$$

In addition, a dimensionless minor halfwidth and layer thickness are clearly given by:

$$b/a_o = \frac{a/a_o}{\rho} \quad (3.31)$$

$$a_o/h = \frac{\alpha}{a/a_o} \quad (3.32)$$

Through the direct mathematical solution to Equations 3.11 and 3.13, one obtains the dependent variables of the problem:  $\phi(\xi, \eta)$ ,  $\bar{W}$ ,  $\Gamma$ , and  $\epsilon$ , as functions of the independent variables:  $E_1/E_2$ ,  $E_1/E_3$ ,  $\nu_1$ ,  $\nu_2$ ,  $\nu_3$ ,  $\alpha$ , and  $\rho$ . However, since the quantities  $a_o$ ,  $d_o$ , and  $p_o^o$  are functions of known physical variables through Equations 3.25 through 3.27, Equations 3.28 through 3.32 provide a useful physical interpretation of this solution, whereby the dependent variables are taken as  $p/p_o^o$ ,  $a/a_o$ ,

$b/a_o$ , and  $d/d_o$ , with the independent variables  $E_1/E_2$ ,  $E_1/E_3$ ,  $v_1$ ,  $v_2$ ,  $v_3$ ,  $a_o/h$ , and  $\epsilon$ .

When the solution is viewed in this manner, all of the independent variables are functions of generally known physical parameters:  $W$ ,  $h$ ,  $R_x$ ,  $R_y$ ,  $E_1$ ,  $E_2$ ,  $E_3$ ,  $v_1$ ,  $v_2$ , and  $v_3$ . The dependent variables consist of the unknowns:  $p$ ,  $a$ ,  $b$ , and  $d$ , each scaled on a function of the known physical parameters. Unfortunately,  $a_o/h$  and  $\epsilon$ , while independent variables physically, are dependent mathematically. Thus, to obtain a solution for particular values of  $a_o/h$  and  $\epsilon$ , one must perform an interpolation of solutions to Equation 3.11 over ranges of the mathematically independent variables  $\alpha$  and  $\rho$ .

Equations 3.18 through 3.21 may be combined with Equations 3.28 through 3.31 to yield for elliptical Hertzian contact:

$$\begin{aligned}\frac{a}{a_o} &= \left[ \frac{4}{\pi} \left( \frac{K(\mu) - E(\mu)}{\mu} \right) \right]^{1/3} \\ \frac{d}{d_o} &= \frac{\mu K(\mu)}{8} \left( \frac{a}{a_o} \right)^{-1} \\ \frac{p_o}{p_o} &= \rho \left( \frac{a}{a_o} \right)^{-2}\end{aligned}\tag{3.33}$$

For this case, Equation 3.19, together with Equations 3.22 and 3.33, must be solved iteratively to determine  $\rho$  given a value of  $\epsilon$ . The desired quantities are then determined directly from Equations 3.33 and 3.31.



## PART 4

## NUMERICAL FORMULATION

## 4.1 Discretized Integral Equation and Method of Solution

Equation 3.11, which is the integral equation to be solved for the contact pressure distribution  $\phi(\xi, \eta)$ , is discretized by dividing the first quadrant of the contact zone into a rectangular mesh as shown in Figure 4-1 with  $n-1$  uniform divisions between  $\xi = 0$  and  $\xi = 1$ , and the same number of uniform divisions between  $\eta = 0$  and  $\eta = b/a$ . The mesh point positions are denoted by  $(\xi_i, \eta_j)$ ,  $i = 1 \dots n$ ;  $j = 1 \dots m(i)$ , with  $\eta_{m(i)}$  locating the mesh point at the discretized boundary for each  $\xi_i$ . The quantities  $\Delta\xi$  and  $\Delta\eta$  denote the respective lengths of the  $\xi$  and  $\eta$  divisions, with:

$$\left. \begin{aligned} \Delta\xi &= \frac{1}{n-1} \\ \Delta\eta &= (b/a)\Delta\xi \end{aligned} \right\} \quad (4.1)$$

The contact pressure distribution is modeled by assigning a value of  $\phi$  at each mesh point:

$$\phi_{i,j} \quad , \quad i=1, \dots, n \quad ; \quad j=1, \dots, m(i)$$

with  $\phi$  varying linearly in  $\xi$  and  $\eta$  between adjacent mesh points. This linear variation is achieved over each rectangular element bounded by adjacent horizontal and vertical mesh lines by dividing the element along a diagonal into two right triangular segments over which the distribution of  $\phi$  is planar. This is shown in Figure 4-2 for a single element, and Figure 4-3 shows an example of a complete pressure distribution comprised of such elements. Referring to the orientation of Figure 4-1, the dividing diagonals connect the mesh points at the upper-left and lower-right corners of each element. Alternatively, dividing diagonals connecting mesh points at the lower-left and upper-right corners of each element could just as easily have been used, but were ruled out because they appeared less convenient for modeling a contact zone boundary of the general shape shown in Figure 4-1.

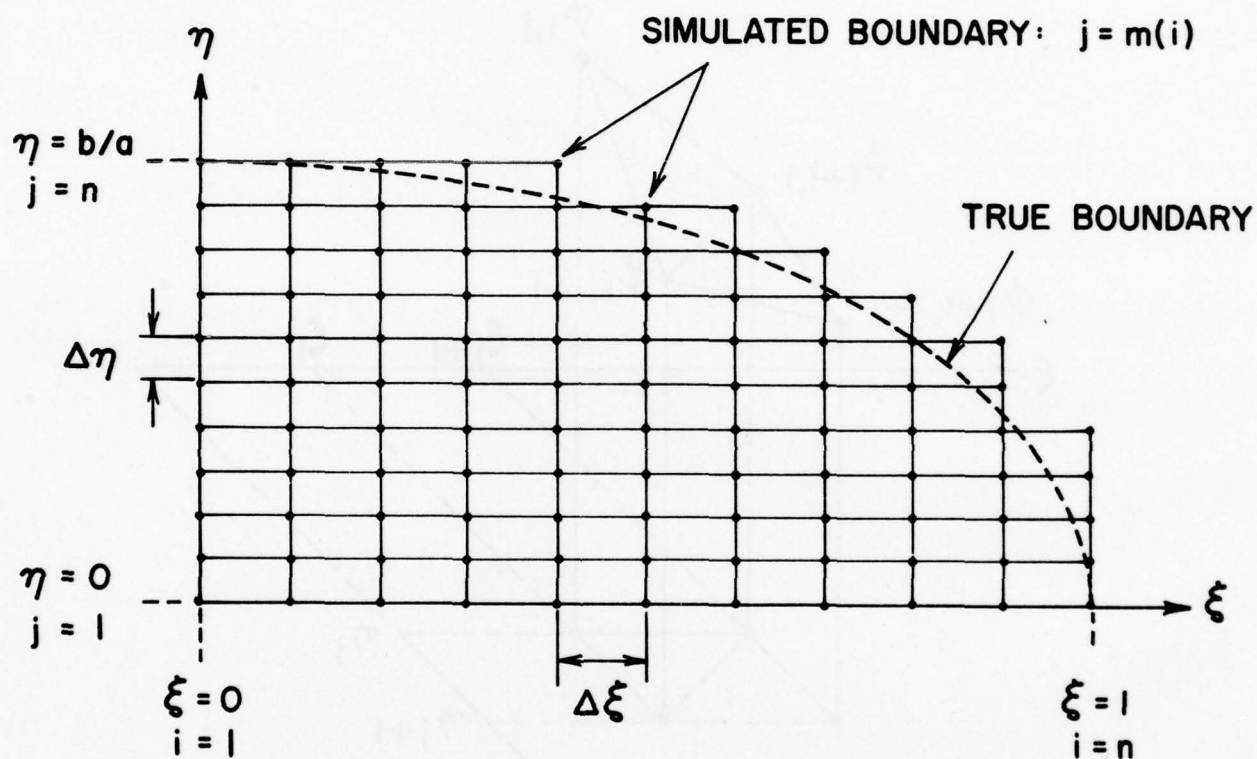


Fig. 4-1 Discretization of Contact Zone

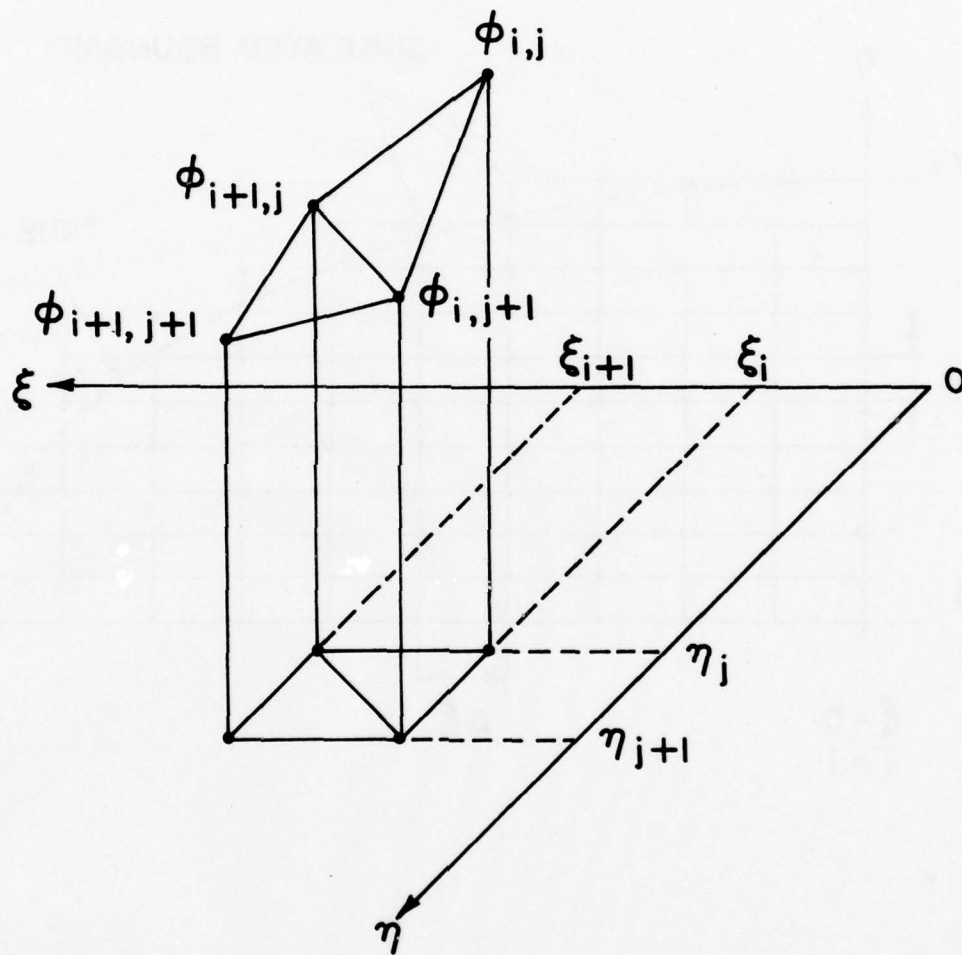


Fig. 4-2 Element of Linear Pressure Variation

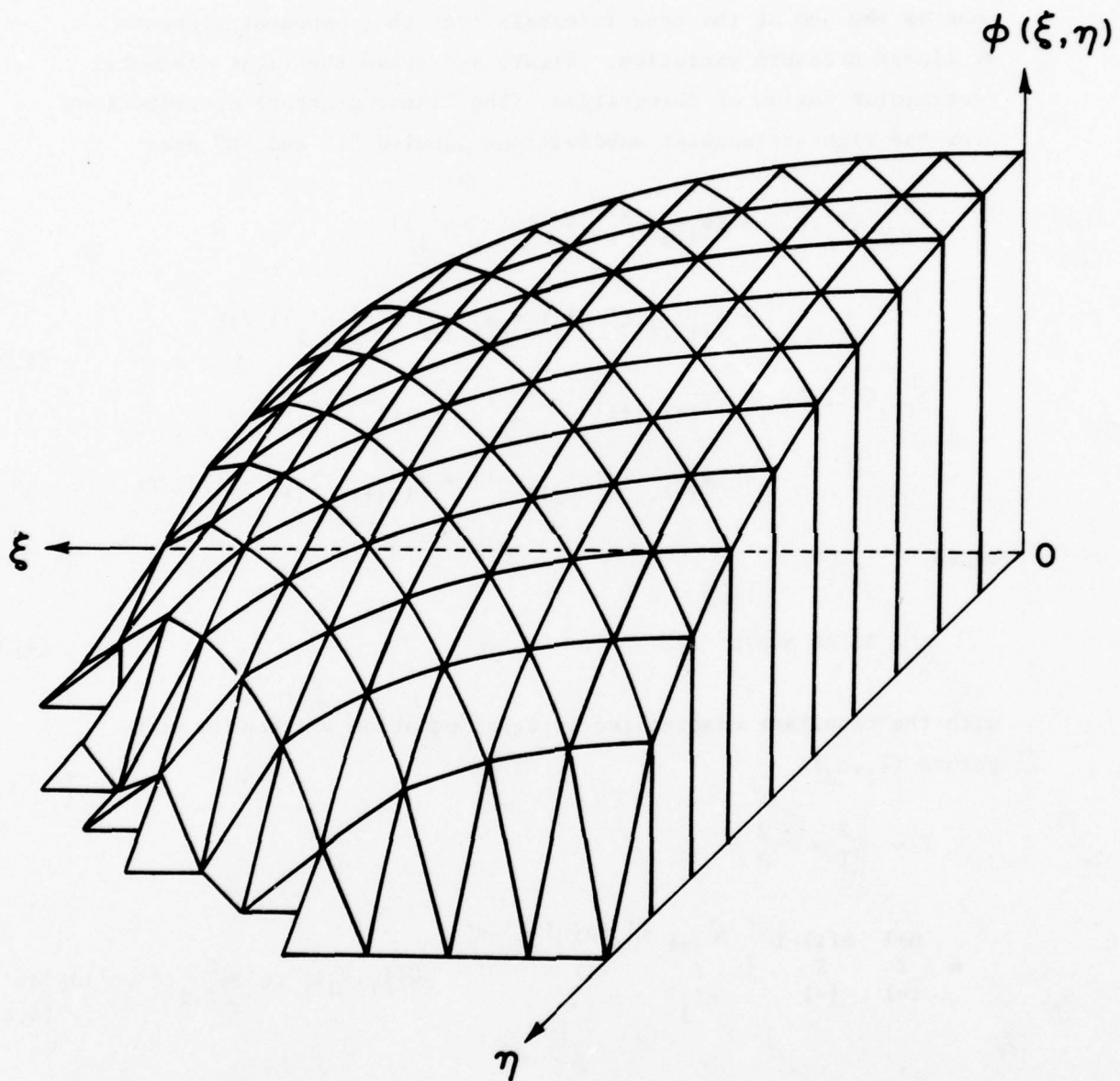


Fig. 4-3 Discretized Pressure Distribution

The discretized form of Equation 3.11 may now be written for the sum of the normal displacements of the two solids at each contact zone mesh point by expressing the area integral over the contact zone as the sum of the area integrals over the component elements of linear pressure variation. Figure 4-4 shows the (i,j) elemental rectangular region of integration. The linear pressure distributions over the right-triangular subdivisions labeled "L" and "U" are:

$$\begin{aligned}
 \phi_{i,j}^L(\xi', \eta') &= \{ \phi_{i,j} [\xi'_{i+1} - \xi' + \rho(\eta' - \eta'_j)] \\
 &\quad + \phi_{i+1,j}(\xi' - \xi'_i) + \phi_{i,j+1} \rho(\eta' - \eta'_j) \} / \Delta \xi \\
 \phi_{i,j}^U(\xi', \eta') &= \{ \phi_{i+1,j+1} [\xi' - \xi'_i + \rho(\eta'_{j+1} - \eta')] \\
 &\quad + \phi_{i+1,j} \rho(\eta'_{j+1} - \eta') + \phi_{i,j+1} (\xi'_{i+1} - \xi') \} / \Delta \xi
 \end{aligned} \tag{4.2}$$

where

$$\rho \equiv \Delta \xi / \Delta \eta = a/b \tag{4.3}$$

with the resultant discretized integral equation written for mesh points  $(\xi_I, \eta_J)$ :

$$\begin{aligned}
 \Gamma - \xi_I^2 - \eta_J^2 &= \sum_{i=1}^{n-1} \sum_{j=1}^{m(i)-1} \left[ \int_{\eta'_j}^{\eta'_{j+1}} \int_{\xi'_i}^{\xi'_{i+1} + \rho(\eta'_{j+1} - \eta')} Q(\xi_I, \eta_J; \xi', \eta') \phi_{i,j}^L(\xi', \eta') d\xi' d\eta' \right. \\
 &\quad \left. + \int_{\eta'_j}^{\eta'_{j+1}} \int_{\xi'_i + \rho(\eta'_{j+1} - \eta')}^{\xi'_{i+1}} Q(\xi_I, \eta_J; \xi', \eta') \phi_{i,j}^U(\xi', \eta') d\xi' d\eta' \right]
 \end{aligned} \tag{4.4}$$

$$I=1, \dots, n \quad ; \quad J=1, \dots, m(I)$$



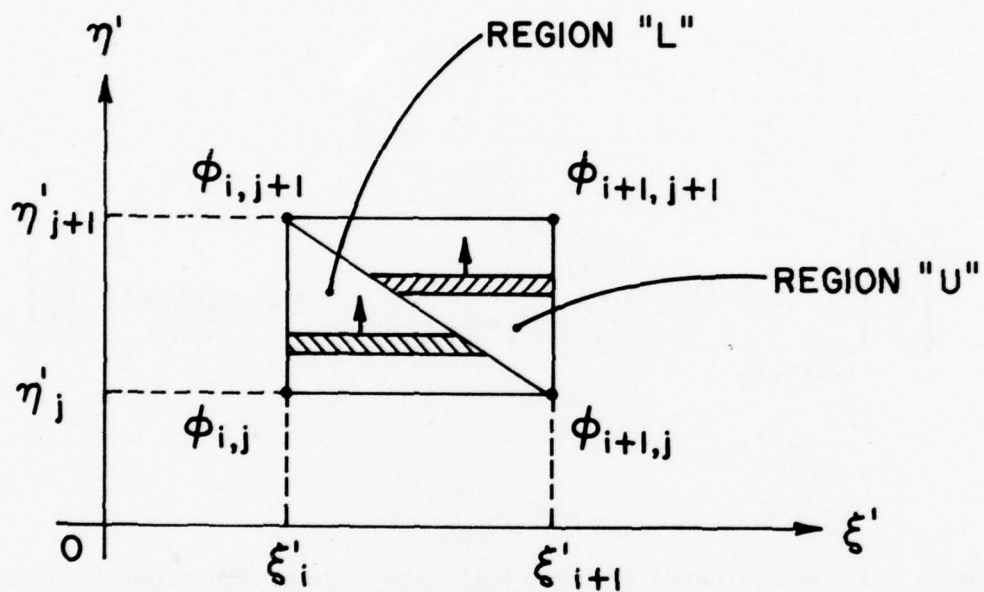


Fig. 4-4 Elemental Region of Integration for Discretized Integral Equation

Defining the quantities:

$$\left\{ \begin{matrix} \alpha_L \\ \beta_L \\ \gamma \end{matrix} \right\}_{I,J;i,j} = \frac{1}{\Delta \xi} \int_{\eta'_j}^{\eta'_{j+1}} \int_{\xi'_i}^{\xi'_i + \rho(\eta'_{j+1} - \eta')} Q(\xi_I, \eta_J; \xi', \eta') \left\{ \begin{matrix} 1 \\ \xi' \\ \eta' \end{matrix} \right\} d\xi' d\eta' \quad (4.5)$$

$$\left\{ \begin{matrix} \alpha_U \\ \beta_U \\ \gamma \end{matrix} \right\}_{I,J;i,j} = \frac{1}{\Delta \xi} \int_{\eta'_j}^{\eta'_{j+1}} \int_{\xi'_i}^{\xi'_{i+1} + \rho(\eta'_{j+1} - \eta')} Q(\xi_I, \eta_J; \xi', \eta') \left\{ \begin{matrix} 1 \\ \xi' \\ \eta' \end{matrix} \right\} d\xi' d\eta'$$

which will be evaluated by numerical integration, Equations 4.4 take the form:

$$\begin{aligned} \Gamma - \xi_I^2 - \epsilon \eta_J^2 = & \sum_{i=1}^{n-1} \sum_{j=1}^{m(i)-1} \{ \phi_{i,j} [ \xi'_{i+1} \alpha_{I,J;i,j}^L - \beta_{I,J;i,j}^L - \rho(\gamma_{I,J;i,j}^L - \eta'_j \alpha_{I,J;i,j}^L) ] \\ & + \phi_{i+1,j} [ \beta_{I,J;i,j}^L - \xi'_i \alpha_{I,J;i,j}^L + \rho(\eta'_{j+1} \alpha_{I,J;i,j}^U - \gamma_{I,J;i,j}^U) ] \\ & + \phi_{i,j+1} [ \rho(\gamma_{I,J;i,j}^L - \eta'_j \alpha_{I,J;i,j}^L) + \xi'_{i+1} \alpha_{I,J;i,j}^U - \beta_{I,J;i,j}^U ] \\ & + \phi_{i+1,j+1} [ \beta_{I,J;i,j}^U - \xi'_i \alpha_{I,J;i,j}^U - \rho(\eta'_{j+1} \alpha_{I,J;i,j}^U - \gamma_{I,J;i,j}^U) ] \} \end{aligned}$$

$$I=1, \dots, n \quad ; \quad J=1, \dots, m(I)$$

By adjusting the summation indices in the second, third, and fourth lines of this expression, one obtains:

$$\begin{aligned}
 \Gamma - \xi_I^2 - \varepsilon \eta_J^2 = & \sum_{i=1}^{n-1} \sum_{j=1}^{m(i)-1} \phi_{i,j} C_{I,J;i,j}^{(1)} + \sum_{i=2}^n \sum_{j=1}^{m(i-1)-1} \phi_{i,j} C_{I,J;i,j}^{(2)} \\
 & + \sum_{i=1}^{n-1} \sum_{j=2}^{m(i)} \phi_{i,j} C_{I,J;i,j}^{(3)} + \sum_{i=2}^n \sum_{j=2}^{m(i-1)} \phi_{i,j} C_{I,J;i,j}^{(4)} \\
 & i=1, \dots, n \quad ; \quad J=1, \dots, m(I)
 \end{aligned} \tag{4.6}$$

where

$$\begin{aligned}
 C_{I,J;i,j}^{(1)} &= (\xi'_{i+1} + \rho \eta'_j) \alpha_{I,J;i,j}^L - \beta_{I,J;i,j}^L - \rho \gamma_{I,J;i,j}^L \\
 C_{I,J;i,j}^{(2)} &= -\xi'_{i-1} \alpha_{I,J;i-1,j}^L + \beta_{I,J;i-1,j}^L + \rho (\eta'_{j+1} \alpha_{I,J;i-1,j}^U - \gamma_{I,J;i-1,j}^U) \\
 C_{I,J;i,j}^{(3)} &= \xi'_{i+1} \alpha_{I,J;i,j-1}^U - \beta_{I,J;i,j-1}^U - \rho (\eta'_{j-1} \alpha_{I,J;i,j-1}^L - \\
 & \quad \gamma_{I,J;i,j-1}^L) \\
 C_{I,J;i,j}^{(4)} &= -(\xi'_{i-1} + \rho \eta'_j) \alpha_{I,J;i-1,j-1}^U + \beta_{I,J;i-1,j-1}^U + \\
 & \quad \rho \gamma_{I,J;i-1,j-1}^U
 \end{aligned} \tag{4.7}$$

It is assumed that the boundary contour  $\eta = f(\xi)$  is monotonically decreasing over  $0 \leq \xi \leq 1$  so that the discretized boundary will always satisfy:

$$\begin{aligned}
 m(1) &= m(2) = n \\
 m(i+1) &\leq m(i) \quad i=2, \dots, n-1
 \end{aligned} \tag{4.8}$$

Applying this condition while combining the four double summations in Equation 4.6, one obtains:

$$\Gamma - \xi_I^2 - \epsilon \eta_J^2 = \sum_{i=1}^n \sum_{j=1}^{m(i)} C_{I,J;i,j} \phi_{i,j} \quad (4.9)$$

$$I=1, \dots, n ; J=1, \dots, m(I)$$

with the influence coefficients  $C_{I,J;i,j}$  given by Table 4-1 in terms of the quantities  $C_{I,J;i,j}^{(1)}$  defined by Equation 4.7. The subscripts  $I, J; i, j$  are left off for conciseness in Table 4-1.

Equation 4.9 constitutes  $N$  simultaneous linear equations in the  $N$  discrete pressures  $\phi_{i,j}$  where

$$N = \sum_{i=1}^n m(i) \quad (4.10)$$

For given values of the elastic properties  $E_1/E_2$ ,  $E_1/E_3$ ,  $\nu_1$ ,  $\nu_2$ , and  $\nu_3$ , geometric ratios  $a/h$  and  $a/b$ , and contact zone mesh parameter  $n$ , the integrals in Equation 4.5 are computed and tabulated for all mesh coordinates:

$$(\xi_I, \eta_J; \xi'_i, \eta'_j) \begin{cases} I=1, \dots, n ; J=1, \dots, n \\ i=1, \dots, n-1 ; j=1, \dots, n-1 \end{cases}$$

using procedures to be presented in Section 4.2. Then, from Equation 4.7 and Table 4-1, the set of influence coefficients  $C_{I,J;i,j}$  may be obtained for contact zones of any discretized boundary shape satisfying the conditions given by Equation 4.8.

For computational purposes, the following notation is adopted for Equation 4.9:

$$\delta_p = \sum_{q=1}^N C_{p;q} \phi_q \quad p=1, \dots, N \quad (4.11)$$

with

$$\delta_p = \Gamma - \xi_I^2 - \epsilon \eta_J^2 \quad (4.12)$$

TABLE 4-1  
INFLUENCE COEFFICIENTS FOR EQUATION 4.9

i	j	C	Restrictions
1	1	$C^{(1)}$	
	2, ..., n-1	$C^{(1)} + C^{(3)}$	
	n	$C^{(3)}$	
2, ..., n-1	1	$C^{(1)} + C^{(2)}$	
	2, ..., m(i+1)-1	$C^{(1)} + C^{(2)} + C^{(3)} + C^{(4)}$	$m(i+1) > 2$
	m(i+1)	$C^{(2)} + C^{(3)} + C^{(4)}$	$m(i+1) < m(i)$
	m(i+1)	$C^{(3)} + C^{(4)}$	$m(i+1) = m(i)$
	m(i+1)+1, ..., m(i)-1	$C^{(2)} + C^{(4)}$	$m(i+1) < m(i) - 1$
	m(i)	$C^{(4)}$	$m(i+1) < m(i)$
n	1	$C^{(2)}$	
	2, ..., m(n)-1	$C^{(2)} + C^{(4)}$	$m(n) > 2$
	m(n)	$C^{(4)}$	



$$C_{p;q} = C_{I,J;i,j}$$

(4.12)

$$\phi_q = \phi_{i,j}$$

(Cont'.d)

where the indices  $p$  and  $q$  replace, respectively, the pairs of indices  $(I,J)$  and  $(i,j)$  according to:

$$p = \begin{cases} J & I=1; J=1, \dots, n \\ J + \sum_{k=1}^{I-1} m(k) & I=2, \dots, n ; J=1, \dots, m(I) \end{cases}$$

(4.13)

$$q = \begin{cases} j & i=1; j=1, \dots, n \\ j + \sum_{k=1}^{i-1} m(k) & i=2, \dots, n ; j=1, \dots, m(i) \end{cases}$$

Since any discretized boundary allowed by Equation 4.8 contains the vertices  $(\xi = 0, \eta = b/a)$  and  $(\xi = 1, \eta = 0)$ , the pressure is implicitly constrained to vanish at these two points. The criteria for satisfactory selection of the boundary shape between the vertices is that the discretized pressure distribution obtained as a solution to Equation 4.11 vanish along the correct boundary. Clearly, this boundary selection is an iterative process.

For consistency with the above-mentioned constraint, the vertex pressures  $\phi_n$  and  $\phi_{n-m(n)+1}$  must be set to zero in each of Equations 4.11. With some minor rearrangement, this leaves the following system of  $N$  linear equations in the  $N-2$  unknown pressures along with the unknown parameters  $\Gamma$  and  $\epsilon$ :

$$\bar{\delta}_p = \sum_{q=1}^N \bar{C}_{p;q} \bar{\phi}_q \quad p=1, \dots, N \quad (4.14)$$

with

$$\bar{\delta}_p = -\xi_I^2 \quad p=1, \dots, N \quad (4.15)$$

$$\bar{\phi}_q = \begin{cases} \Gamma & q = n \\ \epsilon & q = N-m(n)+1 \\ \phi_q & \text{all other } q \end{cases} \quad (4.15)$$

$$\bar{C}_{p;q} \quad (p=1, \dots, N) = \begin{cases} -1 & q = n \\ \eta_J^2 & q = N-m(n)+1 \\ C_{p;q} & \text{all other } q \end{cases} \quad (\text{Cont'd.})$$

In selecting the discretized boundary to approximate a continuous curve as shown in Figure 4-1, the pressures at mesh points outside the continuous curve are set to zero and the members of Equation 4.14 prescribing the contact surface displacement conditions at these points are effectively discarded. Letting such a point be denoted by:

$$(i_o, j_o) = (I_o, J_o) = p_o = q_o, \quad ,$$

this is accomplished by setting:

$$\bar{C}_{p_o;q} = \begin{cases} 1 & q = p_o \\ 0 & \text{all other } q \end{cases}$$

$$\bar{\delta}_{p_o} = 0$$

which replaces the  $p_o$ th member of Equation 4.14 with the equation

$$\bar{\phi}_{p_o} = 0.$$

The resulting system of Equation 4.14 is solved for the  $N \phi_q$ 's using a standard Gaussian elimination technique, and the solution is inspected for approximate satisfaction of the condition  $\phi = 0$  along the selected boundary contour.

The dimensionless load  $\bar{W}$ , defined by Equation 3.14, is obtained from the discretized distribution of  $\phi$  by forming the summation over the contact zone of the volumes of each rectangular pressure element such as shown in Figure 4-2. Letting  $w_{i,j}$  denote the volume of such an element:

$$\bar{W} = 4 \sum_{i=1}^{n-1} \sum_{j=1}^{m(i)-1} w_{i,j} \quad (4.16)$$

where it is clear from Figure 4-2 and basic concepts of solid geometry that

$$w_{i,j} = \frac{1}{6} \Delta\eta\Delta\xi (\phi_{i,j} + 2\phi_{i+1,j} + 2\phi_{i,j+1} + \phi_{i+1,j+1})$$

Substituting this expression for  $w_{i,j}$  into Equation 4.16, one obtains the relation which may be used directly to compute  $\bar{W}$  from the solution to Equation 4.14:

$$\bar{W} = \frac{2}{3} \Delta\eta\Delta\xi \sum_{i=1}^{n-1} \sum_{j=1}^{m(i)-1} (\phi_{i,j} + 2\phi_{i+1,j} + 2\phi_{i,j+1} + \phi_{i+1,j+1}) \quad (4.17)$$

with Equation 4.13 used to convert from the solution notation  $\phi_q$  to  $\phi_{i,j}$ . With  $\epsilon$ ,  $\Gamma$ ,  $\bar{W}$ , and the  $\phi$  distribution available from this discretized solution, Equations 3.28 through 3.32 are used to obtain the quantities:  $a_o/h$ ,  $a/a_o$ ,  $b/a_o$ ,  $d/d_o$ , and  $p/p_o^o$ .

## 4.2 Evaluation of Influence Coefficients for Discretized Integral Equation

### 4.2.1 Formulation in Terms of Integral Functions

The integrals appearing in Equation 4.5 of the function,

$$Q(\xi_I, \eta_J; \xi', \eta') = \bar{K}(\xi_I - \xi', \eta_J - \eta') + \bar{K}(\xi_I + \xi', \eta_J - \eta') \\ + \bar{K}(\xi_I + \xi', \eta_J + \eta') + \bar{K}(\xi_J + \xi', \eta_J + \eta')$$

defined by Equation 3.12, must be evaluated numerically in order to determine the influence coefficients  $C_{I,J;i,j}$  from Equation 4.7 and Table 4-1. Equation 4.5 can be broken down into the integral functions,

$$\begin{Bmatrix} \bar{H} \\ \bar{I} \\ \bar{J} \end{Bmatrix} (\xi, \eta) = \int_0^\eta \int_0^\xi \bar{K}(u, v) \begin{Bmatrix} 1 \\ u \\ v \end{Bmatrix} du dv \quad (4.2.1)$$

$$\begin{Bmatrix} \bar{H}^* \\ \bar{I}^* \\ \bar{J}^* \end{Bmatrix} (\xi, \eta, \pm \rho) = \int_0^{\eta} \int_{\xi}^{\xi \pm \rho} \bar{K}(u, v) \begin{Bmatrix} 1 \\ u \\ v \end{Bmatrix} dudv \quad (4.2.1) \quad (\text{Cont'd.})$$

which are naturally amenable to systematic numerical computation and tabulation. To express Equation 4.5 in terms of these integrals, first substitute the above expression for  $Q$  into the first three of Equation 4.5 and change the variables of integration in each term such that they are the same as the arguments of  $\bar{K}$  to obtain:

$$\begin{aligned} \begin{Bmatrix} \alpha^L \\ \beta^L \\ \gamma^L \end{Bmatrix}_{I,J;i,j} &= \frac{1}{\Delta \xi} \int_{\eta_J - \eta'_j}^{\eta_J - \eta'_{j+1}} \int_{\xi_I - \xi'_i}^{[\xi_I - \xi'_i + \rho(\eta_J - \eta'_{j+1})] - \rho v} \bar{K}(u, v) \cdot \begin{Bmatrix} -1 \\ \xi_I - u \\ \eta_J - v \end{Bmatrix} dudv \\ &+ \frac{1}{\Delta \xi} \int_{\eta_J - \eta'_j}^{\eta_J - \eta'_{j+1}} \int_{\xi_I + \xi'_i}^{[\xi_I + \xi'_i - \rho(\eta_J - \eta'_{j+1})] + \rho v} \bar{K}(u, v) \cdot \begin{Bmatrix} 1 \\ \xi_I - u \\ v - \eta_J \end{Bmatrix} dudv \\ &+ \frac{1}{\Delta \xi} \int_{\eta_J + \eta'_j}^{\eta_J + \eta'_{j+1}} \int_{\xi_I - \xi'_i}^{[\xi_I - \xi'_i - \rho(\eta_J + \eta'_{j+1})] + \rho v} \bar{K}(u, v) \cdot \begin{Bmatrix} -1 \\ u - \xi_I \\ \eta_J - v \end{Bmatrix} dudv \\ &+ \frac{1}{\Delta \xi} \int_{\eta_J + \eta'_j}^{\eta_J + \eta'_{j+1}} \int_{\xi_I + \xi'_i}^{[\xi_I + \xi'_i + \rho(\eta_J + \eta'_{j+1})] - \rho v} \bar{K}(u, v) \cdot \begin{Bmatrix} 1 \\ u - \xi_I \\ v - \eta_J \end{Bmatrix} dudv \end{aligned} \quad (4.2.2)$$

It should be clear that this expression can be applied to the latter three of Equation 4.5 by changing the sign of each integral and replacing  $\xi'_i$  with  $\xi'_{i+1}$  in the lower limit of the  $u$  integration for each term. Now separate Equation 4.2.2 into integrals over rectangular regions denoted as:

$$\begin{aligned} \begin{Bmatrix} A \\ B \\ C \end{Bmatrix}_{I,J;i,j} &= - \int_{\eta_J - \eta'_j}^{\eta_J - \eta'_{j+1}} \int_0^{\xi_I - \xi'_i} \bar{K}(u, v) \begin{Bmatrix} 1 \\ \xi_I - u \\ \eta_J - v \end{Bmatrix} dudv \\ &- \int_{\eta_J - \eta'_j}^{\eta_J - \eta'_{j+1}} \int_0^{\xi_I + \xi'_i} \bar{K}(u, v) \begin{Bmatrix} -1 \\ \xi_I - u \\ v - \eta_J \end{Bmatrix} dudv \end{aligned} \quad (4.2.3)$$

$$- \int_{\eta_J + \eta'_j}^{\eta_J + \eta'_{j+1}} \int_0^{\xi_I - \xi'_i} \bar{K}(u, v) \cdot \begin{Bmatrix} -1 \\ u - \xi_I \\ \eta_J - v \end{Bmatrix} dudv$$

(4.2.3)  
(Cont'd.)

$$- \int_{\eta_J + \eta'_j}^{\eta_J + \eta'_{j+1}} \int_0^{\xi_I + \xi'_i} \bar{K}(u, v) \cdot \begin{Bmatrix} 1 \\ u - \xi_I \\ v - \eta_J \end{Bmatrix} dudv$$

and integrals over trapezoidal regions denoted as:

$$\begin{aligned} \begin{Bmatrix} A^* \\ B^* \\ G^* \end{Bmatrix}_{I, J; i, j} &= \int_{\eta_J - \eta'_j}^{\eta_J - \eta'_{j+1}} \int_0^{[\xi_I - \xi'_i + \rho(\eta_J - \eta'_{j+1})] - \rho v} \bar{K}(u, v) \cdot \begin{Bmatrix} 1 \\ \xi_I - u \\ \eta_J - v \end{Bmatrix} dudv \\ &+ \int_{\eta_J - \eta'_j}^{\eta_J - \eta'_{j+1}} \int_0^{[\xi_I + \xi'_i - \rho(\eta_J - \eta'_{j+1})] + \rho v} \bar{K}(u, v) \cdot \begin{Bmatrix} -1 \\ \xi_I - u \\ v - \eta_J \end{Bmatrix} dudv \\ &+ \int_{\eta_J + \eta'_j}^{\eta_J + \eta'_{j+1}} \int_0^{[\xi_I - \xi'_i - \rho(\eta_J + \eta'_{j+1})] + \rho v} \bar{K}(u, v) \cdot \begin{Bmatrix} -1 \\ u - \xi_I \\ \eta_J - v \end{Bmatrix} dudv \\ &+ \int_{\eta_J + \eta'_j}^{\eta_J + \eta'_{j+1}} \int_0^{[\xi_I + \xi'_i + \rho(\eta_J + \eta'_{j+1})] - \rho v} \bar{K}(u, v) \cdot \begin{Bmatrix} 1 \\ u - \xi_I \\ v - \eta_J \end{Bmatrix} dudv \end{aligned} \quad (4.2.4)$$

to obtain the following convenient representation of all six of Equation 4.5:

$$\begin{aligned} \begin{Bmatrix} \alpha^L \\ \beta^L \\ \gamma^L \end{Bmatrix}_{I, J; i, j} &= \frac{1}{\Delta \xi} \cdot \begin{Bmatrix} A \\ B \\ G \end{Bmatrix}_{I, J; i, j} + \frac{1}{\Delta \xi} \cdot \begin{Bmatrix} A^* \\ B^* \\ G^* \end{Bmatrix}_{I, J; i, j} \\ \begin{Bmatrix} \alpha^U \\ \beta^U \\ \gamma^U \end{Bmatrix}_{I, J; i, j} &= \frac{1}{\Delta \xi} \cdot \begin{Bmatrix} A \\ B \\ G \end{Bmatrix}_{I, J; i+1, j} - \frac{1}{\Delta \xi} \cdot \begin{Bmatrix} A^* \\ B^* \\ G^* \end{Bmatrix}_{I, J; i, j} \end{aligned} \quad (4.2.5)$$



Equation 4.2.3 for A, B, and G can be written in terms of the integral functions  $\bar{H}$ ,  $\bar{I}$ , and  $\bar{J}$  to yield:

$$\begin{aligned}
 \begin{Bmatrix} A \\ B \\ G \end{Bmatrix}_{I,J;i,j} &+ - \begin{Bmatrix} \bar{H} \\ \xi_I \bar{H} - \bar{I} \\ \eta_J \bar{H} - \bar{J} \end{Bmatrix} (\xi_I - \xi'_i, \eta_J - \eta'_{j+1}) + \begin{Bmatrix} \bar{H} \\ \xi_I \bar{H} - \bar{I} \\ \eta_J \bar{H} - \bar{J} \end{Bmatrix} (\xi_I - \xi'_i, \eta_J - \eta'_j) \\
 &- \begin{Bmatrix} -\bar{H} \\ \xi_I \bar{H} - \bar{I} \\ \bar{J} - \eta_J \bar{H} \end{Bmatrix} (\xi_I + \xi'_i, \eta_J - \eta'_{j+1}) + \begin{Bmatrix} -\bar{H} \\ \xi_I \bar{H} - \bar{I} \\ \bar{J} - \eta_J \bar{H} \end{Bmatrix} (\xi_I + \xi'_i, \eta_J - \eta'_j) \\
 &- \begin{Bmatrix} -\bar{H} \\ \bar{I} - \xi_I \bar{H} \\ \eta_J \bar{H} - \bar{J} \end{Bmatrix} (\xi_I - \xi'_i, \eta_J + \eta'_{j+1}) + \begin{Bmatrix} -\bar{H} \\ \bar{I} - \xi_I \bar{H} \\ \eta_J \bar{H} - \bar{J} \end{Bmatrix} (\xi_I - \xi'_i, \eta_J + \eta'_j) \\
 &- \begin{Bmatrix} \bar{H} \\ \bar{I} - \xi_I \bar{H} \\ \bar{J} - \eta_J \bar{H} \end{Bmatrix} (\xi_I + \xi'_i, \eta_J + \eta'_{j+1}) + \begin{Bmatrix} \bar{H} \\ \bar{I} - \xi_I \bar{H} \\ \bar{J} - \eta_J \bar{H} \end{Bmatrix} (\xi_I + \xi'_i, \eta_J + \eta'_j)
 \end{aligned} \tag{4.2.6}$$

Similarly  $A^*$ ,  $B^*$ , and  $G^*$  may be expressed in terms of  $\bar{H}^*$ ,  $\bar{I}^*$ , and  $\bar{J}^*$ :

$$\begin{aligned}
 \begin{Bmatrix} A^* \\ B^* \\ G^* \end{Bmatrix}_{I,J;i,j} &= \begin{Bmatrix} \bar{H}^* \\ \xi_I \bar{H}^* - \bar{I}^* \\ \eta_J \bar{H}^* - \bar{J}^* \end{Bmatrix} (\xi^{(1)}, \eta_J - \eta'_{j+1}, -\rho) - \begin{Bmatrix} \bar{H}^* \\ \xi_I \bar{H}^* - \bar{I}^* \\ \eta_J \bar{H}^* - \bar{J}^* \end{Bmatrix} (\xi^{(1)}, \eta_J - \eta'_j, -\rho) \\
 &+ \begin{Bmatrix} -\bar{H}^* \\ \xi_I \bar{H}^* - \bar{I}^* \\ \bar{J}^* - \eta_J \bar{H}^* \end{Bmatrix} (\xi^{(2)}, \eta_J - \eta'_{j+1}, +\rho) - \begin{Bmatrix} -\bar{H}^* \\ \xi_I \bar{H}^* - \bar{I}^* \\ \bar{J}^* - \eta_J \bar{H}^* \end{Bmatrix} (\xi^{(2)}, \eta_J - \eta'_j, +\rho) \\
 &+ \begin{Bmatrix} -\bar{H}^* \\ \bar{I}^* - \xi_I \bar{H}^* \\ \eta_J \bar{H}^* - \bar{J}^* \end{Bmatrix} (\xi^{(3)}, \eta_J + \eta'_{j+1}, +\rho) - \begin{Bmatrix} -\bar{H}^* \\ \bar{I}^* - \xi_I \bar{H}^* \\ \eta_J \bar{H}^* - \bar{J}^* \end{Bmatrix} (\xi^{(3)}, \eta_J + \eta'_j, +\rho) \\
 &+ \begin{Bmatrix} \bar{H}^* \\ \bar{I}^* - \xi_I \bar{H}^* \\ \bar{J}^* - \eta_J \bar{H}^* \end{Bmatrix} (\xi^{(4)}, \eta_J + \eta'_{j+1}, -\rho) - \begin{Bmatrix} \bar{H}^* \\ \bar{I}^* - \xi_I \bar{H}^* \\ \bar{J}^* - \eta_J \bar{H}^* \end{Bmatrix} (\xi^{(4)}, \eta_J + \eta'_j, -\rho)
 \end{aligned} \tag{4.2.7}$$

with

$$\begin{aligned}
 \xi^{(1)} &= \xi_I - \xi'_i + \rho(\eta_J - \eta'_{j+1}) \\
 \xi^{(2)} &= \xi_I + \xi'_i - \rho(\eta_J - \eta'_{j+1}) \\
 \xi^{(3)} &= \xi_I - \xi'_i - \rho(\eta_J + \eta'_{j+1}) \\
 \xi^{(4)} &= \xi_I + \xi'_i + \rho(\eta_J + \eta'_{j+1})
 \end{aligned}
 \tag{4.2.8}$$

Equation 4.2.5 together with Equations 4.2.6 and 4.2.7 give the desired expression of the quantities  $\alpha^L$ ,  $\beta^L$ ,  $\gamma^L$ ,  $\alpha^U$ ,  $\beta^U$ , and  $\gamma^U$  in terms of  $\bar{H}$ ,  $\bar{I}$ ,  $\bar{J}$ ,  $\bar{H}^*$ ,  $\bar{I}^*$ , and  $\bar{J}^*$ .

Recalling from Equation 3.7 that  $\bar{K}(\xi, \eta) = \alpha K(\alpha\xi, \alpha\eta)$  with  $\alpha = a/h$  and  $K(u, v)$  the kernel function given by Equation 3.5, it is seen that  $\bar{H}$ ,  $\bar{I}$ ,  $\bar{J}$ ,  $\bar{H}^*$ ,  $\bar{I}^*$ , and  $\bar{J}^*$  are obtainable from computations of the basic integral functions:

$$\begin{Bmatrix} H \\ I \\ J \end{Bmatrix} (s, t) = \int_0^t \int_0^s K(u, v) \begin{Bmatrix} 1 \\ u \\ v \end{Bmatrix} dudv
 \tag{4.2.9}$$

$$\begin{Bmatrix} H^* \\ I^* \\ J^* \end{Bmatrix} (s, t, \pm\rho) = \int_0^t \int_0^{s \pm \rho v} K(u, v) \begin{Bmatrix} 1 \\ u \\ v \end{Bmatrix} dudv$$

with

$$\begin{aligned}
 \bar{H}(\xi, \eta) &= (1/\alpha) H(\alpha\xi, \alpha\eta) \\
 \bar{I}(\xi, \eta) &= (1/\alpha^2) I(\alpha\xi, \alpha\eta) \\
 \bar{J}(\xi, \eta) &= (1/\alpha^2) J(\alpha\xi, \alpha\eta) \\
 \bar{H}^*(\xi, \eta, \pm\rho) &= (1/\alpha) H^*(\alpha\xi, \alpha\eta, \pm\rho) \\
 \bar{I}^*(\xi, \eta, \pm\rho) &= (1/\alpha^2) I^*(\alpha\xi, \alpha\eta, \pm\rho) \\
 \bar{J}^*(\xi, \eta, \pm\rho) &= (1/\alpha^2) J^*(\alpha\xi, \alpha\eta, \pm\rho)
 \end{aligned}
 \tag{4.2.10}$$

From Equation 3.5, it is clear that:

$$K(u,v) = K(-u,v) = K(u,-v) = K(-u,-v)$$

and as a consequence of this symmetry:

$$\begin{aligned} H(s,t) &= \text{Sgn}(st) H(|s|, |t|) \\ I(s,t) &= \text{Sgn}(t) I(|s|, |t|) \\ J(s,t) &= \text{Sgn}(s) J(|s|, |t|) \\ H^*(s,t,\pm\rho) &= \text{Sgn}(st) H^* [|s|, |t|, \pm\rho \text{Sgn}(st)] \\ I^*(s,t,\pm\rho) &= \text{Sgn}(t) I^* [|s|, |t|, \pm\rho \text{Sgn}(st)] \\ J^*(s,t,\pm\rho) &= \text{Sgn}(s) J^* [|s|, |t|, \pm\rho \text{Sgn}(st)] \end{aligned} \quad (4.2.11)$$

where

$$\text{Sgn}(x) \equiv \begin{cases} -1 & x < 0 \\ +1 & x \geq 0 \end{cases} \quad (4.2.12)$$

so that the basic integral functions defined by Equation 4.2.9 need only be computed for positive values of  $s$  and  $t$ . By combining Equations 4.2.10 and 4.2.11, one obtains the relations:

$$\begin{aligned} \bar{H}(\xi,\eta) &= (1/\alpha) \text{Sgn}(\xi\eta) H(\alpha|\xi|, \alpha|\eta|) \\ \bar{I}(\xi,\eta) &= (1/\alpha^2) \text{Sgn}(\eta) J(\alpha|\xi|, \alpha|\eta|) \\ \bar{J}(\xi,\eta) &= (1/\alpha^2) \text{Sgn}(\xi) J(\alpha|\xi|, \alpha|\eta|) \\ \bar{H}^*(\xi,\eta,\pm\rho) &= (1/\alpha) \text{Sgn}(\xi\eta) H^*[\alpha|\xi|, \alpha|\eta|, \pm\rho \text{Sgn}(\xi\eta)] \\ \bar{I}^*(\xi,\eta,\pm\rho) &= (1/\alpha^2) \text{Sgn}(\eta) I^*[\alpha|\xi|, \alpha|\eta|, \pm\rho \text{Sgn}(\xi\eta)] \\ \bar{J}^*(\xi,\eta,\pm\rho) &= (1/\alpha^2) \text{Sgn}(\xi) J^*[\alpha|\xi|, \alpha|\eta|, \pm\rho \text{Sgn}(\xi\eta)] \end{aligned} \quad (4.2.13)$$

which will be used to obtain the values of  $\bar{H}$ ,  $\bar{I}$ ,  $\bar{J}$ ,  $\bar{H}^*$ ,  $\bar{I}^*$ , and  $\bar{J}^*$  required in Equations 4.2.6 and 4.2.7 from computed values of  $H$ ,  $I$ ,  $J$ ,  $H^*$ ,  $I^*$ , and  $J^*$ .

Equations 4.2.6, 4.2.7, and 4.2.8, together with Equation 4.2.13, must now be closely examined to determine all arguments  $s, t$  for which  $H$ ,  $I$ ,  $J$ ,  $H^*$ ,  $I^*$ , and  $J^*$  must be evaluated in order to provide the values of  $\bar{H}$ ,  $\bar{I}$ ,  $\bar{J}$ ,  $\bar{H}^*$ ,  $\bar{I}^*$ , and  $\bar{J}^*$  at all arguments  $\xi, \eta$  called for in Equations

4.2.6 and 4.2.7. First, note that the quantities  $(A,B,G)_{I,J;i,j}$  given by Equation 4.2.6 and  $(A^*,B^*,G^*)_{I,J;i,j}$  given by Equation 4.2.7 must be obtained for all the integer subscripts  $I=1,\dots,n$ ;  $J=1,\dots,n$ ;  $i=1,\dots,n-1$ ;  $j=1,\dots,n-1$ , in order to obtain all of the influence coefficients  $C_{I,J;i,j}$  from Equation 4.2.5, Equation 4.7, and Table 4-1. Thus, the mesh coordinates  $\xi_I, \eta_J$ ;  $\xi'_i, \eta'_j$ , will take on their full range of values:

$$\xi_I = (I-1)\Delta\xi \quad I=1,\dots,n$$

$$\eta_J = (J-1)\Delta\eta \quad J=1,\dots,n$$

$$\xi'_i = (i-1)\Delta\xi \quad i=1,\dots,n$$

$$\eta'_j = (j-1)\Delta\eta \quad j=1,\dots,n$$

in forming the arguments for which  $\bar{H}$ ,  $\bar{I}$ ,  $\bar{J}$ ,  $\bar{H}^*$ ,  $\bar{I}^*$ , and  $\bar{J}^*$  will be needed in Equations 4.2.6 and 4.2.7. Clearly, for any values of  $[\bar{H}, \bar{I}, \bar{J}]$   $(\xi, \eta)$  and  $[\bar{H}^*, \bar{I}^*, \bar{J}^*]$   $(\xi, \eta, \pm\rho)$  required in Equations 4.2.6 and 4.2.7, the argument  $\xi$  will be a positive or negative integer multiple of  $\Delta\xi$  and the argument  $\eta$  will be a positive or negative integer multiple of  $\Delta\eta$ . For the corresponding values of  $[H, I, J]$   $(s, t)$  and  $[H^*, I^*, J^*]$   $(s, t, \pm\rho)$  called for in Equation 4.2.13, the arguments  $s$  and  $t$  will be positive integer multiples of  $\alpha\Delta\xi$  and  $\alpha\Delta\eta$ , respectively. Computations of  $[H, I, J]$   $(s, t)$  and  $[H^*, I^*, J^*]$   $(s, t, \pm\rho)$  are thus required over particular ranges of  $s$  at intervals of  $\alpha\Delta\xi$  and  $t$  at intervals of  $\alpha\Delta\eta$ . By noting the extreme values of the arguments of  $\bar{H}$ ,  $\bar{I}$ ,  $\bar{J}$ ,  $\bar{H}^*$ ,  $\bar{I}^*$ , and  $\bar{J}^*$  in Equations 4.2.6 and 4.2.7 over the full range of values of the mesh coordinates, and using Equation 4.2.13 to determine the corresponding extreme values of the arguments of  $H$ ,  $I$ ,  $J$ ,  $H^*$ ,  $I^*$ , and  $J^*$ , one can establish the following ranges on  $s$  and  $t$  for computation at respective intervals of  $\alpha\Delta\xi$  and  $\alpha\Delta\eta$ :

$$\begin{aligned} [H, I, J] (s, t) & \begin{cases} 0 \leq s \leq 2(n-1)\alpha\Delta\xi \\ 0 \leq t \leq 2(n-1)\alpha\Delta\eta \end{cases} \\ [H^*, I^*, J^*] (s, t, \pm\rho) & \begin{cases} 0 \leq s \leq 2(n-1)\alpha\Delta\xi - \rho t \\ 0 \leq t \leq (n-1)\alpha\Delta\eta \end{cases} \end{aligned} \quad (4.2.14)$$

$$[H^*, I^*, J^*] (s, t, -\rho) \begin{cases} 0 \leq s \leq 4(n-1)\alpha\Delta\xi \\ 0 \leq t \leq (n-1)\alpha\Delta\eta \\ \rho t - (n-1)\alpha\Delta\xi \leq s \leq 4(n-1)\alpha\Delta\xi \\ n\alpha\Delta\eta \leq t \leq 2(n-1)\alpha\Delta\eta \end{cases} \quad \begin{matrix} (4.2.14) \\ (\text{Cont'd.}) \end{matrix}$$

By utilizing the computational methods derived in Section 4.2.2, the desired arrays of values of  $[H, I, J] (s, t)$  and  $[H^*, I^*, J^*] (s, t, \pm\rho)$  are obtained over these ranges. These numerical arrays, together with Equations 4.2.13, 4.2.6, 4.2.7, 4.2.5, and 4.7, and Table 4-1, provide for the complete determination of the array of influence coefficients  $C_{I, J; i, j}$  in the discretized integral equation given by Equation 4.9.

#### 4.2.2 Evaluation of Integral Functions

Substituting from Equation 3.8 for the approximate form of  $K(u, v)$  in the integral functions defined by Equation 4.2.9 and separately defining the integrals of the Hankel inversion integral and inverse square root parts of  $K(u, v)$ , one obtains:

$$\begin{Bmatrix} H \\ I \\ J \end{Bmatrix} (s, t) \approx \begin{Bmatrix} H_1 \\ I_1 \\ J_1 \end{Bmatrix} (s, t) + (1+\beta) \cdot \begin{Bmatrix} H_0 \\ I_0 \\ J_0 \end{Bmatrix} (s, t) \quad (4.2.15)$$

$$\begin{Bmatrix} H^* \\ I^* \\ J^* \end{Bmatrix} (s, t, \pm\rho) \approx \begin{Bmatrix} H_1^* \\ I_1^* \\ J_1^* \end{Bmatrix} (s, t, \pm\rho) + (1+\beta) \cdot \begin{Bmatrix} H_0^* \\ I_0^* \\ J_0^* \end{Bmatrix} (s, t, \pm\rho)$$

with

$$\begin{Bmatrix} H_1 \\ I_1 \\ J_1 \end{Bmatrix} (s, t) = \int_0^{\omega_0} [g_2(\omega) - g_4(\omega) - 1] \int_0^t \int_0^s J_0(\omega \sqrt{u^2 + v^2}) \begin{Bmatrix} 1 \\ u \\ v \end{Bmatrix} du dv d\omega \quad (4.2.16)$$

$$\begin{Bmatrix} H_1^* \\ I_1^* \\ J_1^* \end{Bmatrix} (s, t, \pm\rho) = \int_0^{\omega_0} [g_2(\omega) - g_4(\omega) - 1] \int_0^t \int_0^{s \pm \rho v} J_0(\omega \sqrt{u^2 + v^2}) \begin{Bmatrix} 1 \\ u \\ v \end{Bmatrix} du dv d\omega$$



and,

$$\begin{Bmatrix} H_o \\ I_o \\ J_o \end{Bmatrix} (s, t) = \int_0^t \int_0^s (u^2 + v^2)^{-1/2} \begin{Bmatrix} 1 \\ u \\ v \end{Bmatrix} dudv \quad (4.2.17)$$

$$\begin{Bmatrix} H_o^* \\ I_o^* \\ J_o^* \end{Bmatrix} (s, t, \pm \rho) = \int_0^t \int_0^{s \pm \rho v} (u^2 + v^2)^{-1/2} \begin{Bmatrix} 1 \\ u \\ v \end{Bmatrix} dudv$$

where in Equation 4.2.16, the natural order of integration has been switched by moving the  $\omega$  integration to the outside.

The  $u$ - $v$  double integration in Equation 4.2.17 is performed analytically by following the procedure described in Appendix I. Defining the quantities:

$$\begin{aligned} \sigma &= \sqrt{1 + \rho^2} \\ R^o &= \sqrt{s^2 + t^2} \\ s^{\pm} &= s \pm \rho t \\ R^{\pm} &= \sqrt{s^{\pm 2} + t^2} \end{aligned} \quad (4.2.18)$$

the resulting closed-form expressions in  $s$  and  $t$  take the form:

$$\begin{aligned} H_o(s, t) &= s \log \frac{R^o + t}{s} + t \log \frac{R^o + s}{t} \\ I_o(s, t) &= \frac{1}{2} s^2 \log \frac{R^o + t}{s} + \frac{1}{2} t(R^o - t) \\ J_o(s, t) &= \frac{1}{2} s(R^o - s) + \frac{1}{2} t^2 \log \frac{R^o + s}{t} \\ H_o^*(s, t, \pm \rho) &= \frac{s}{\sigma} \log \frac{(\sigma \pm \rho)(\sigma t + R^{\pm})}{\sigma s^{\pm} \mp \rho R^{\pm}} \\ &\quad + \text{Sgn}(s^{\pm}) t \log \frac{R^{\pm} + |s^{\pm}|}{t} \end{aligned} \quad (4.2.19)$$

$$I_o^* (s, t, \pm \rho) = \frac{1}{2} \left( \frac{s}{\sigma} \right)^2 \left[ \frac{\pm \rho (R^+ - s)}{s} + \frac{1}{\sigma} \log \frac{(\sigma \mp \rho)(\sigma t + R^+)}{\sigma s^+ \mp R^+} \right] + \frac{1}{2} t (R^+ - t) \quad (4.2.19)$$

(Cont'd.)

$$J_o^* (s, t, \pm \rho) = \frac{1}{2} \left( \frac{s}{\sigma} \right)^2 \left[ \frac{R^+ - s}{s} \mp \frac{\rho}{\sigma} \log \frac{(\sigma \mp \rho)(\sigma t + R^+)}{\sigma s^+ \mp R^+} \right] + \text{Sgn}(s^+) \frac{1}{2} t^2 \log \frac{R^+ + |s^+|}{t}$$

The  $u$ - $v$ - $\omega$  triple integration must be carried out numerically in evaluating the functions defined by Equation 4.2.16. It is seen that each  $s, t$  argument pair within the ranges given by Equation 4.2.14 defines a region of  $u$ - $v$  integration of one of six types shown in Figure 4-5. Decomposing these regions in the manner shown, a numerical scheme is derived for evaluating the functions at intervals of  $\alpha \Delta \xi$  in  $s$  and  $\alpha \Delta \eta$  in  $t$ . For Region I, this decomposition allows  $[H_1, I_1, J_1] (s, t)$  to be expressed in the form:

$$\begin{aligned} \begin{Bmatrix} H_1 \\ I_1 \\ J_1 \end{Bmatrix} (s, t) &= \int_0^\omega [g_2(\omega) - g_4(\omega) - 1] \int_{t-\alpha \Delta \eta}^t \int_{s-\alpha \Delta \xi}^s J_o(\omega \sqrt{u^2 + v^2}) \begin{Bmatrix} 1 \\ u \\ v \end{Bmatrix} dudvd\omega \\ &+ \begin{Bmatrix} H_1 \\ I_1 \\ J_1 \end{Bmatrix} (s, t - \alpha \Delta \eta) \begin{Bmatrix} H_1 \\ I_1 \\ J_1 \end{Bmatrix} (s - \alpha \Delta \xi, t) - \begin{Bmatrix} H_1 \\ I_1 \\ J_1 \end{Bmatrix} (s - \alpha \Delta \xi, t - \alpha \Delta \eta) \end{aligned} \quad (4.2.20)$$

Considering Regions II through V,  $[H_1^*, I_1^*, J_1^*] (s, t, -\rho)$  can be expressed in a similar manner for the various ranges of  $s$ :

$$\begin{aligned} \underline{s = \rho t} \\ \begin{Bmatrix} H_1^* \\ I_1^* \\ J_1^* \end{Bmatrix} (\rho t, t, -\rho) &= \int_0^\omega [g_2(\omega) - g_4(\omega) - 1] \int_{t-\alpha \Delta \eta}^t \int_0^{\rho t - \rho v} J_o(\omega \sqrt{u^2 + v^2}) \begin{Bmatrix} 1 \\ u \\ v \end{Bmatrix} dudvd\omega \end{aligned} \quad (4.2.21)$$

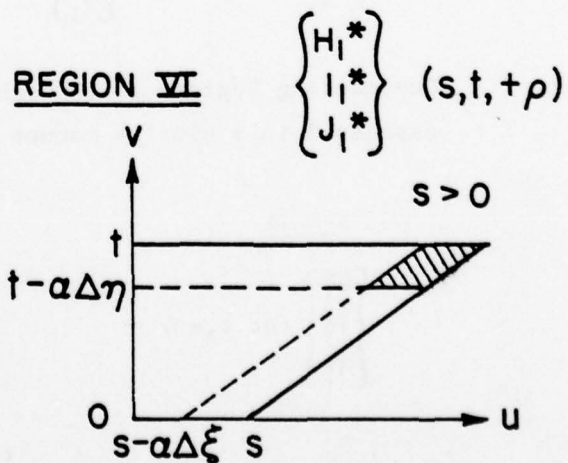
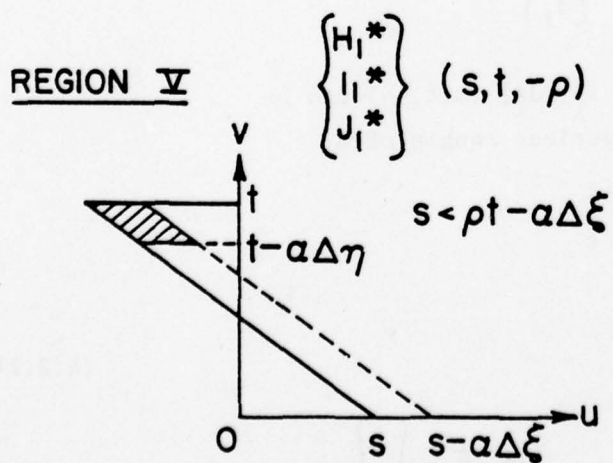
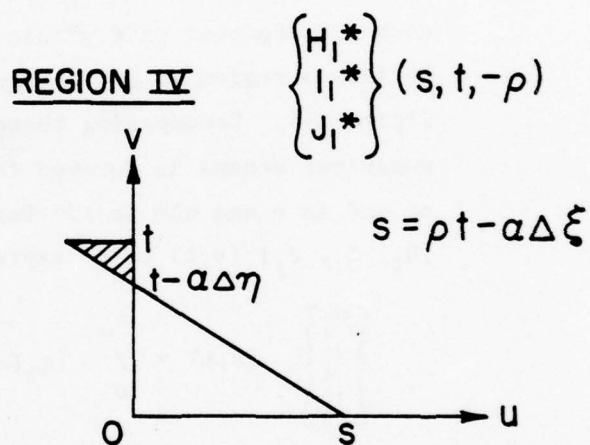
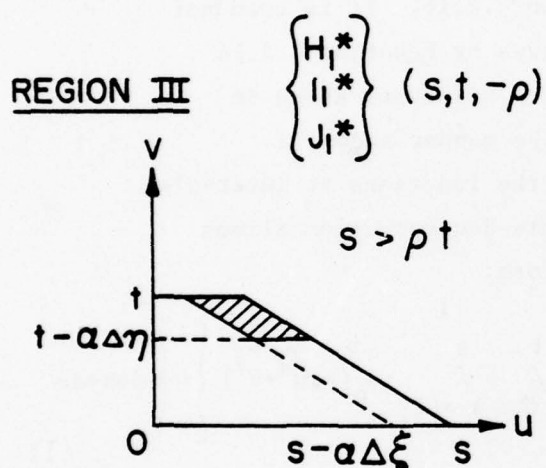
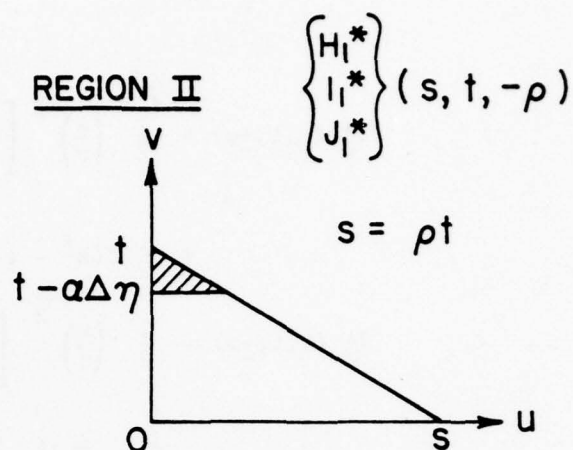
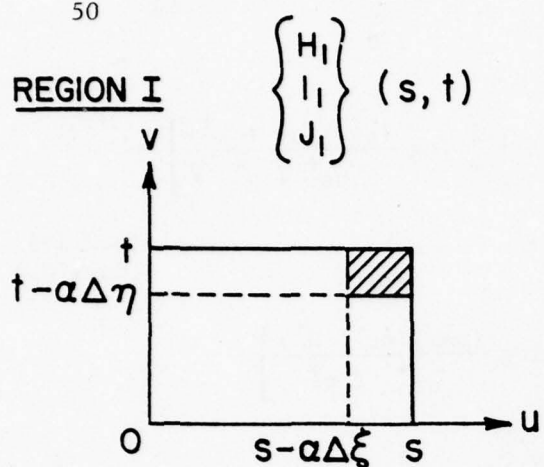


Fig. 4-5 Classes of  $u-v$  Regions of Integration for Hankel Inversion Integrals

$$+ \begin{Bmatrix} H_1^* \\ I_1^* \\ J_1^* \end{Bmatrix} (\rho t, t - \alpha \Delta \eta, -\rho) \quad (4.2.21) \quad (\text{Cont'd.})$$

$$s > \rho t$$

$$\begin{Bmatrix} H_1^* \\ I_1^* \\ J_1^* \end{Bmatrix} (s, t, -\rho) = \int_0^{\omega_0} [g_2(\omega) - g_4(\omega) - 1] \int_{t-\alpha\Delta\xi}^t \int_{s-\alpha\Delta\xi-\rho v}^{s-\rho v} J_0(\omega \sqrt{u^2+v^2}) \begin{Bmatrix} 1 \\ u \\ v \end{Bmatrix} dudvd\omega$$

$$+ \begin{Bmatrix} H_1^* \\ I_1^* \\ J_1^* \end{Bmatrix} (s, t - \alpha \Delta \eta, -\rho) + \begin{Bmatrix} H_1^* \\ I_1^* \\ J_1^* \end{Bmatrix} (s - \alpha \Delta \xi, t, -\rho) - \begin{Bmatrix} H_1^* \\ I_1^* \\ J_1^* \end{Bmatrix} (s - \alpha \Delta \xi, t - \alpha \Delta \eta, -\rho) \quad (4.2.22)$$

$$s = \rho t - \alpha \Delta \xi$$

$$\begin{Bmatrix} H_1^* \\ I_1^* \\ J_1^* \end{Bmatrix} (\rho t - \alpha \Delta \xi, t, -\rho) =$$

$$- \int_0^{\omega_0} [g_2(\omega) - g_4(\omega) - 1] \int_{t-\alpha\Delta\eta}^t \int_{\rho t - \alpha \Delta \xi - v}^0 J_0(\omega \sqrt{u^2+v^2}) \begin{Bmatrix} 1 \\ u \\ v \end{Bmatrix} dudvd\omega \quad (4.2.23)$$

$$+ \begin{Bmatrix} H_1^* \\ I_1^* \\ J_1^* \end{Bmatrix} (\rho t - \alpha \Delta \xi, t - \alpha \Delta \eta, -\rho)$$

$$s < \rho t - \alpha \Delta \xi$$

$$\begin{Bmatrix} H_1^* \\ I_1^* \\ J_1^* \end{Bmatrix} (s, t, -\rho) =$$

$$- \int_0^{\omega_0} [g_2(\omega) - g_4(\omega) - 1] \int_{t-\alpha\Delta\eta}^t \int_{s-\rho v}^{s+\alpha\Delta\xi-\rho v} J_0(\omega \sqrt{u^2+v^2}) \begin{Bmatrix} 1 \\ u \\ v \end{Bmatrix} dudvd\omega \quad (4.2.24)$$

$$+ \begin{Bmatrix} H_1^* \\ I_1^* \\ J_1^* \end{Bmatrix} (s, t - \alpha \Delta \eta, -\rho) + \begin{Bmatrix} H_1^* \\ I_1^* \\ J_1^* \end{Bmatrix} (s + \alpha \Delta \xi, t, -\rho) - \begin{Bmatrix} H_1^* \\ I_1^* \\ J_1^* \end{Bmatrix} (s + \alpha \Delta \xi, t - \alpha \Delta \eta, -\rho)$$

Finally, for Region VI:

$$\begin{aligned}
 & \begin{Bmatrix} H_1^* \\ I_1^* \\ J_1^* \end{Bmatrix} (s, t, +\rho) = \\
 & \int_0^{\omega_0} [g_2(\omega) - g_4(\omega) - 1] \int_{t-\alpha\Delta\eta}^t \int_{s-\alpha\Delta\xi+\rho v}^{s+\rho v} J_0(\omega \sqrt{u^2 + v^2}) \begin{Bmatrix} 1 \\ u \\ v \end{Bmatrix} du dv d\omega \quad (4.2.25) \\
 & + \begin{Bmatrix} H_1^* \\ I_1^* \\ J_1^* \end{Bmatrix} (s, t - \alpha\Delta\eta, +\rho) + \begin{Bmatrix} H_1^* \\ I_1^* \\ J_1^* \end{Bmatrix} (s - \alpha\Delta\xi, t, +\rho) - \begin{Bmatrix} H_1^* \\ I_1^* \\ J_1^* \end{Bmatrix} (s - \alpha\Delta\xi, t - \alpha\Delta\eta, +\rho)
 \end{aligned}$$

In addition, note the following from inspection of Equation 4.2.16:

$$\begin{Bmatrix} H_1 \\ I_1 \\ J_1 \end{Bmatrix} (s, 0) = \begin{Bmatrix} H_1 \\ I_1 \\ J_1 \end{Bmatrix} (0, t) = \begin{Bmatrix} H_1^* \\ I_1^* \\ J_1^* \end{Bmatrix} (s, 0, +\rho) = \begin{Bmatrix} 0 \\ 0 \\ 0 \end{Bmatrix} \quad (4.2.26)$$

$$\begin{Bmatrix} H_1^* \\ I_1^* \\ J_1^* \end{Bmatrix} (0, t, +\rho) = \begin{Bmatrix} -H_1^* \\ I_1^* \\ -J_1^* \end{Bmatrix} (0, t, -\rho) \quad (4.2.27)$$

Equations 4.2.20 through 4.2.27 are applied directly in evaluating the functions at successive increments of  $\alpha\Delta\xi$  in  $s$  and  $\alpha\Delta\eta$  in  $t$  between the limiting values given in Equation 4.2.14. Each function evaluation entails a numerical quadrature over the shaded segment of one of the regions shown in Figure 4-5, with quadrature over the remainder of the region having occurred for function evaluations at preceding values of  $s$  and  $t$ .

Since the integrands requiring numerical quadrature are smoothly varying continuous functions of  $\omega$ ,  $u$ , and  $v$ , standard single-variable Gaussian quadratures are used to integrate in each variable in the order shown. To avoid any numerical difficulties arising from the oscillation of  $J_0$ , the  $\omega$  region (0 to  $\omega_0$ ) is divided into uniform



intervals, roughly equal in length to a period of  $J_0(\bar{R}\omega)$  where  $\bar{R}$  is an estimated mean value of  $\sqrt{u^2+v^2}$  over the  $u-v$  region. A ten-point quadrature in  $\omega$  is then used to integrate over each interval. At each quadrature abscissa in  $\omega$ ,  $[g_2(\omega)-g_4(\omega)]$  is obtained from Equations 2.14 through 2.16, and the  $u-v$  integration is performed with a quadrature in  $u$  providing the value of the integrand at each abscissa of a quadrature in  $v$ . Polynomial approximations given in Reference [9] are used to compute  $J_0$  to eight-place accuracy in the  $u$  quadrature.

It is seen from Equations 4.2.20 through 4.2.25 that the  $u-v$  limits of integration span regions of at most  $\alpha\Delta\xi$  and  $\alpha\Delta\eta$ , respectively. For all values of  $\alpha$ ,  $\Delta\xi$ , and  $\Delta\eta$  considered in this study, and, with  $\omega_0 = 10$ , the argument of  $J_0$  always varied less than a period between the  $u-v$  limits. Consequently, convergence to seven places was attainable by dividing the  $\omega$  region as described above and using 5-point quadratures over the full  $u$  and  $v$  regions. Treating the oscillation of  $J_0$  as approximately sinusoidal, the number of  $\omega$  divisions,  $n_d$ , was determined from the formula:

$$n_d = \frac{\omega_0 \bar{R}}{2\pi}$$

with the constraint,  $n_d \leq 6$ . Tables of abscissas and weight factors used for the 5- and 10-point quadratures are given in Reference [9].

It should be noted that for fixed  $\Delta\xi$  and  $\Delta\eta$ , with  $\Delta\xi = 1/(n-1)$  and  $\Delta\eta = \Delta\xi/\rho$  from Equation 4.1, the magnitude of each value of  $s$  and  $t$  for which the integral functions are to be evaluated is proportional to the ratio  $\alpha = a/h$ . Thus, each  $\bar{R}$  and consequently each  $n_d$  is also proportional to  $\alpha$ ; and, since the number of abscissa points in  $\omega$  between the limits 0 and  $\omega_0$  is  $10 n_d$ , the computing time required to evaluate each triple integral is similarly proportional to  $\alpha$ . This is an important consideration in planning a parametric study of the effect of  $\alpha$  on the behavior of the contact zone.

Once all the values of  $H_1$ ,  $I_1$ ,  $J_1$ ,  $H_1^*$ ,  $I_1^*$ , and  $J_1^*$  have been computed and tabulated using the above methods, they are combined according to Equation 4.2.15 with the corresponding values of  $H_0$ ,  $I_0$ ,  $J_0$ ,  $H_0^*$ ,  $I_0^*$ , and  $J_0^*$  computed directly from Equations 4.2.19 and 4.2.18, to give the desired array of values of the integral functions  $H$ ,  $I$ ,  $J$ ,  $H^*$ ,  $I^*$ , and  $J^*$  needed to form the quantities considered in Section 4.2.1 above.

At this point, it is worth noting that the elastic properties of the homogeneous solid,  $E_1/E_3$  and  $\nu_3$ , enter the numerically formulated contact problem only in Equation 4.2.15 through the parameter  $\beta$  defined by Equation 3.6. The elastic properties of the layered solid,  $E_1/E_2$ ,  $\nu_1$ , and  $\nu_2$ , determine the functions  $H_1$ ,  $I_1$ ,  $J_1$ ,  $H_1^*$ ,  $I_1^*$ , and  $J_1^*$  through  $g_2(\omega)$ - $g_4(\omega)$  given by Equations 2.14 through 2.16.

### 4.3 Computer Programs

Two FORTRAN programs, HIJPRG and PSØLV, implement the computational scheme derived in Sections 4.1 and 4.2. Both programs are written for a CDC 6600 computing system with the NOS Operating System. Input and output descriptions and listings are given in Appendices III through VI.

In HIJPRG, the arrays of integral functions  $H_1$ ,  $I_1$ ,  $J_1$ ,  $H_1^*$ ,  $I_1^*$ , and  $J_1^*$ , computed by numerical quadrature are obtained for prescribed values of  $E_1/E_2$ ,  $\nu_1$ ,  $\nu_2$ ,  $\alpha$ ,  $\rho$ , and  $n$  as described in Section 4.2.2. In PSØLV, the influence coefficients  $C_{I,J;i,j}$  are generated from these arrays through Equations 4.2.19, 4.2.15, 4.2.13, 4.2.6, 4.2.7, 4.2.5, and 4.7 and Table 4-1. With Equation 4.9 expressed in the notation of Equation 4.14, a standard matrix inversion subroutine yields the dimensionless contact pressure distribution  $\phi_{i,j}$ , approach  $\Gamma$ , curvature ratio  $\epsilon$ , and, through Equation 4.17, load  $\bar{W}$ . Finally, the quantities  $a_0/h$ ,  $a/a_0$ ,  $b/a_0$ ,  $d/d_0$ , and  $p^0/p_0^0$  are obtained from Equations 3.28 through 3.32. The analysis contained in PSØLV pertains to prescribed values of  $E_1/E_3$ ,  $\nu_3$ , boundary shape  $m(i)$   $I=1,\dots,n$ , and boundary points  $(i,j)$  of zero pressure.

## PART 5

### NUMERICAL RESULTS

#### 5.1 Test for Numerical Accuracy

With the integral functions  $H_1$ ,  $I_1$ ,  $J_1$ ,  $H_1^*$ ,  $I_1^*$ , and  $J_1^*$  computed to seven-decimal-place accuracy, the numerical formulation is grounded on the essentially exact computation of surface displacements due to the discretized pressure distribution. The error in the solution is due to the truncation error in approximating the true continuous pressure distribution, an error that in principle can be made as small as desired by using a fine enough mesh to construct the approximate distribution. To keep computer time and storage at moderate levels in the present study, the mesh was limited to ten divisions along the major and minor halfwidths ( $n=11$ ). The truncation error associated with this mesh will now be examined by comparing numerical predictions for the limiting cases of elliptical Hertz contact of homogeneous solids and axisymmetric contact of layered solids with available exact solutions. These comparisons serve as an overall check on the validity of the numerical formulation.

As discussed in Section 3.2, the formulation for layered contact reduces to the Hertz problem for homogeneous solids when one prescribes  $E_1/E_2 = 1$  and  $\nu_1 = \nu_2$ . This reduction occurs in the numerical formulation through Equations 4.2.15 and 4.2.16, where the integral functions  $H_1$ ,  $I_1$ ,  $J_1$ ,  $H_1^*$ ,  $I_1^*$ , and  $J_1^*$  vanish identically for all arguments. With  $n=11$ , the elliptical boundary for any ellipticity ratio  $\rho$  is prescribed by:

i	1	2	3	4	5	6	7	8	9	10	11
m(i)	11	11	11	11	11	10	10	9	8	7	5

This is the boundary exhibited by the example contact zone mesh shown in Figure 4-1. The pressure is set to zero at the following boundary mesh points  $(\xi_i, \eta_j)$  which fall outside the true elliptical contour:

(i, j) = (2,11)	(3,11)	(4,11)	(5,11)	(6,10)
(7,10)	(7,9)	(8,9)	(9,8)	(9,7)
(10,7)	(10,6)	(11,5)	(11,4)	(11,3)
(11,2)				

With  $E_1/E_3 = 0$  completing the definition of this approximate Hertz problem, numerical solutions were obtained at ellipticity ratios of 1, 2, 5, and 10. Table 5-1 shows the resulting values of  $\epsilon$ ,  $\Gamma$ ,  $\phi^\circ$ ,  $\bar{W}$ ,  $a/a_0$ ,  $p^\circ/p_0^\circ$ , and  $d/d_0$  along with the exact values given by Equations 3.18 through 3.23 and 3.33. Note the improved agreement in  $a/a_0$  and  $d/d_0$  relative to the corresponding quantities  $\bar{W}$  and  $\Gamma$ . This is explained in part by the proportionality of  $a/a_0$  to  $\bar{W}^{-1/3}$  through Equation 3.30.

A second comparison is provided by an essentially exact computation of surface displacements for a layered solid due to an axisymmetric ellipsoidal pressure distribution. In terms of the dimensionless variables  $\tilde{u}_0 = u_0 R_x / a^2$  for surface displacement and  $\lambda = r/a =$

$\sqrt{\xi^2 + \eta^2}$  for radius, Equation II.1 of Appendix II takes the form:

$$u_0(\lambda) = \frac{\pi^2 \phi^\circ}{4} \left[ \frac{8\alpha}{\pi} \int_0^\infty \frac{[g_2(\omega) - g_4(\omega) - 1] J_0(\alpha\lambda\omega) (\sin\alpha\omega - \alpha\omega\cos\alpha\omega)}{+ 2 - \lambda^2} \frac{ds}{(\alpha\omega)^3} \right] \quad (5.1)$$

$\lambda \leq 1$

for the surface displacement due to pressure distribution:

$$\phi(\lambda) = \begin{cases} \phi^\circ \sqrt{1-\lambda^2} & \lambda \leq 1 \\ 0 & \lambda \geq 1 \end{cases}$$

For a given value of  $\lambda$ , the integral in Equation 5.1 is evaluated to 7-place accuracy by dividing the truncated region of integration (0 to 10) into a suitable number of intervals as discussed in Section 4.2.2 and using a 10-point Gaussian quadrature to integrate numerically over each interval. This exact computation of  $\tilde{u}_0(\lambda)$  is compared with the result obtained by computing the right-hand side of Equation 4.9 for:

$$\phi_{i,j} = \begin{cases} \phi^\circ \sqrt{1-\xi_i^2-\eta_j^2} & \xi_i^2 + \eta_j^2 \leq 1 \\ 0 & \xi_i^2 + \eta_j^2 \geq 1 \end{cases}$$

with influence coefficients obtained for  $\rho = 1$ ,  $\beta = 0$ , and the  $m(i)$ 's given above for a general elliptical boundary. Computations were performed for the case of an incompressible layer ( $\nu_1 = 0.5$ ) on a rigid substrate ( $E_1/E_2 = 0$ ) with  $\alpha = 1, 2$ , and 4.  $\phi^\circ$  was assigned a value



TABLE 5-1  
COMPARISON BETWEEN NUMERICAL AND EXACT  
SOLUTIONS FOR HERTZ CONTACT

$\rho$	1	2	5	10	
$\epsilon$	1.000	2.855	11.95	37.05	Computed
	1.000	2.843	11.83	36.54	Exact
	0.0	+0.4	+1.0	+1.4	% Error
$\Gamma$	1.96	1.68	1.46	1.36	Computed
	2.00	1.71	1.47	1.37	Exact
	-2.0	-1.8	-0.7	-0.7	% Error
$\phi^o$	0.402	0.502	0.777	1.180	Computed
	0.405	0.505	0.777	1.176	Exact
	-0.7	-0.6	0.0	+0.3	% Error
$\bar{W}$	0.825	0.515	0.320	0.243	Computed
	0.849	0.529	0.326	0.246	Exact
	-2.8	-2.6	-1.8	-1.2	% Error
$a/a_o$	1.010	1.181	1.385	1.517	Computed
	1.000	1.171	1.376	1.511	Exact
	+1.0	+0.9	+0.7	+0.4	% Error
$p^o/p_o^o$	1.002	1.464	2.656	4.42	Computed
	1.000	1.459	2.640	4.38	Exact
	+0.2	+0.3	+0.6	+0.9	% Error
$d/d_o$	1.000	1.173	1.396	1.560	Computed
	1.000	1.173	1.395	1.557	Exact
	0.0	0.0	+0.1	+0.2	% Error



of  $4/\pi^2$  to normalize the coefficient of Equation 5.1. Table 5-2 shows the resulting exact and numerically computed values of  $\tilde{u}_0(\lambda)$  for  $\lambda$  between 0 and 1 in increments of 0.2. As expected from the nature of the discretized pressure distribution, agreement is good near the center ( $\lambda = 0$ ) and relatively poor at the edge ( $\lambda = 1$ ) where the gradients of the actual pressure distribution are high and not adequately represented by the discretized model. The difficulty at the edge is obvious from an inspection of Figure 4-3 which illustrates the discretized model of an ellipsoidal pressure distribution for  $n=11$ .

The final comparison is provided by the solutions reported by Chen and Engel [4] for axisymmetric layered contact. As discussed in Part 1, these are approximate solutions to a one-dimensional integral equation. Nevertheless, the accuracy level verified by the authors is high enough that the solutions can be assumed exact for purposes of this comparison. The reported solutions consist of tabulated values of a dimensionless load  $p^* = 3\pi\bar{W}/8$  and approach  $\delta^* = \Gamma/2$  over ranges of  $\alpha$  and  $E_1/E_2$  with  $E_1/E_3 = 0$  and  $\nu_1 = \nu_3 = 1/3$ . Values of  $\bar{W}$  and  $\Gamma$  computed by the present method for  $\alpha = 1, 5, E_1/E_2 = 0.1, 10$  are shown in Table 5-3 along with the corresponding reported values. Also shown in this table are the values of  $a/a_0$  and  $d/d_0$  obtained from  $\bar{W}$  and  $\Gamma$  through Equations 3.30 and 3.28. Relative error magnitudes are notably similar to those shown in Table 5-1 for contact of homogeneous solids. Again note the small errors in  $a/a_0$  and  $d/d_0$  relative to those in  $\bar{W}$  and  $\Gamma$ .

The comparisons with the Hertz solution and the axisymmetric analysis of Chen and Engel show an error of roughly 1 percent in the solution quantities of primary physical importance: curvature ratio  $\epsilon$ , major halfwidth  $a/a_0$ , approach  $d/d_0$ , and central pressure  $p^0/p_0^0$ . The edge discrepancies in the comparison between exact and computed displacement profiles are representative of local errors that can be expected in computed pressures near the edge of the contact zone. Thus, the present formulation with  $n=11$ , while providing a fairly accurate computation of  $\epsilon$ ,  $a/a_0$ ,  $d/d_0$ , and  $p^0/p_0^0$ , does not give an accurate prediction of either the pressure profile shape near the boundary or the shape of the boundary contour. A finer mesh would be required to accurately determine these shapes.

TABLE 5-2  
COMPARISON BETWEEN NUMERICAL AND EXACT  
SOLUTIONS FOR SURFACE DISPLACEMENTS DUE TO  
AXISYMMETRIC ELLIPSOIDAL PRESSURE DISTRIBUTION

$\alpha$	0	1	2	4	
$\bar{u}_0 (\lambda=0)$	-	0.755	0.264	0.0579	Computed
	2.00	0.755	0.263	0.0574	Exact
	-	0.0	+0.4	+0.9	% Error
$\lambda=0.2$	-	0.732	0.261	0.0583	Computed
	1.96	0.732	0.260	0.0578	Exact
	-	0.0	+0.4	+0.9	% Error
$\lambda=0.4$	-	0.659	0.247	0.0593	Computed
	1.84	0.660	0.246	0.0587	Exact
	-	-0.2	0.4	+1.0	% Error
$\lambda=0.6$	-	0.532	0.212	0.0591	Computed
	1.64	0.535	0.212	0.0583	Exact
	-	-0.6	0.0	+1.4	% Error
$\lambda=0.8$	-	0.342	0.130	0.0453	Computed
	1.36	0.348	0.133	0.0456	Exact
	-	-1.7	-2.3	-0.7	% Error
$\lambda=1.0$	-	0.077	-0.030	-0.0356	Computed
	1.00	0.090	-0.020	-0.0286	Exact
	-	-14	+50	+24.5	% Error

Elastic Properties:  $E_1/E_2 = 0$   
 $\nu_1 = 0.5$

Pressure Distribution:  $\phi = \begin{cases} (4/\pi^2) \sqrt{1-\lambda^2} & \lambda \leq 1 \\ 0 & \lambda \geq 1 \end{cases}$

TABLE 5-3

COMPARISON OF NUMERICAL SOLUTIONS FOR AXISYMMETRIC LAYERED CONTACT  
WITH RESULTS OF CHEN AND ENGEL [4]

$$E_1/E_3 = 0$$

$$\nu_1 = \nu_2 = 1/3$$

$\alpha$	$E_1/E_2$	$\bar{W}$	$\Gamma$	$a/a_o$	$d/d_o$	
1	0.1	1.012	1.349	0.943	0.600	Computed
		1.045	1.374	0.933	0.598	Chen and Engel*
		-3.2	-1.8	+1.1	+0.4	% Error
5	0.1	2.539	1.312	0.694	0.316	Computed
		2.615	1.334	0.687	0.315	Chen and Engel
		-2.9	-1.7	+1.0	+0.2	% Error
1	10	0.490	4.564	1.201	3.293	Computed
		0.500	4.645	1.193	3.305	Chen and Engel
		-2.1	-1.7	+0.7	-0.3	% Error
5	10	0.144	2.658	1.807	4.337	Computed
		0.149	2.720	1.787	4.343	Chen and Engel
		-3.3	-2.3	+1.1	-0.1	% Error

\*Data from Reference [4].

## 5.2 Numerical Solutions

Numerical solutions over ranges of  $\alpha$  and  $\rho$  have been obtained for three sets of elastic property ratios in order to determine the influence of layer thickness and curvature ratio on the major and minor halfwidths, approach, and central pressure for a given load. The elastic property ratios pertain to (i) contact between a rigid solid and an incompressible layer backed by a rigid substrate, (ii) contact between a rigid solid and a high modulus layer backed by a low modulus substrate, and (iii) contact between a low modulus solid and a high modulus layer backed by a low modulus substrate. The following values represent these configurations:

	$E_1/E_2$	$E_1/E_3$	$\nu_1$	$\nu_2$	$\nu_3$
(i)	0	0	0.5	-	-
(ii)	10	0	0.25	0.25	-
(iii)	10	10	0.25	0.25	0.25

Computations were performed with values of 1, 2, 3, 4, and 5 assigned to  $\alpha$  and with values assigned to  $\rho$  in increments of 0.5 from 1.0 to the first value resulting in a computed curvature ratio  $\epsilon$  of 10 or above. In all cases, a discretized elliptical boundary, specified according to the values of  $m(i)$  and points of zero pressure given in Section 5-1 for  $n=11$ , resulted in a qualitatively well behaved pressure distribution in the sense that pressures fell to zero at the boundary without any unexpected irregularities. In other words, any departure of the boundary from the ellipse of the Hertz solution could not be distinguished due to the boundary truncation error associated with the  $n=11$  mesh.

Figures 5-1, 5-2, and 5-3 show the computed axisymmetric ( $\rho = \epsilon = 1$ ) pressure profiles for the three material combinations. The limiting cases of  $\alpha = 0$  and  $\alpha = \infty$  correspond to the Hertz solutions for an infinitely thick layer and a vanishing layer. The variation of these pressure profiles with  $\alpha$  represents the variation with layer thickness of the load required to maintain a fixed contact zone radius  $a$ . When each profile is normalized by its center value, the profile shapes shown in Figures 5-4, 5-5, and 5-6 are obtained. Those in Figure 5-4



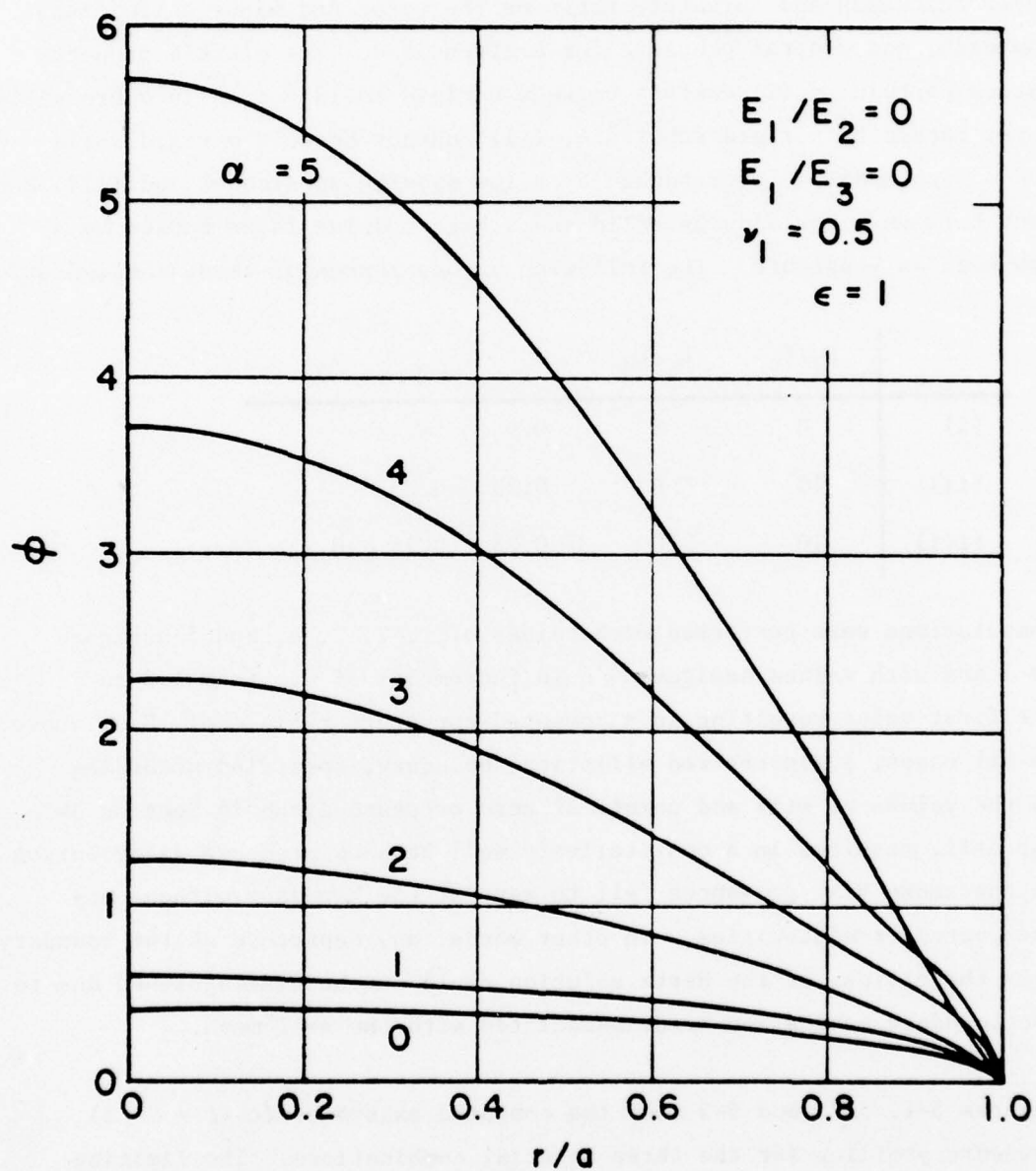


Fig. 5-1 Axisymmetric Pressure Profiles, Material Combination (i).



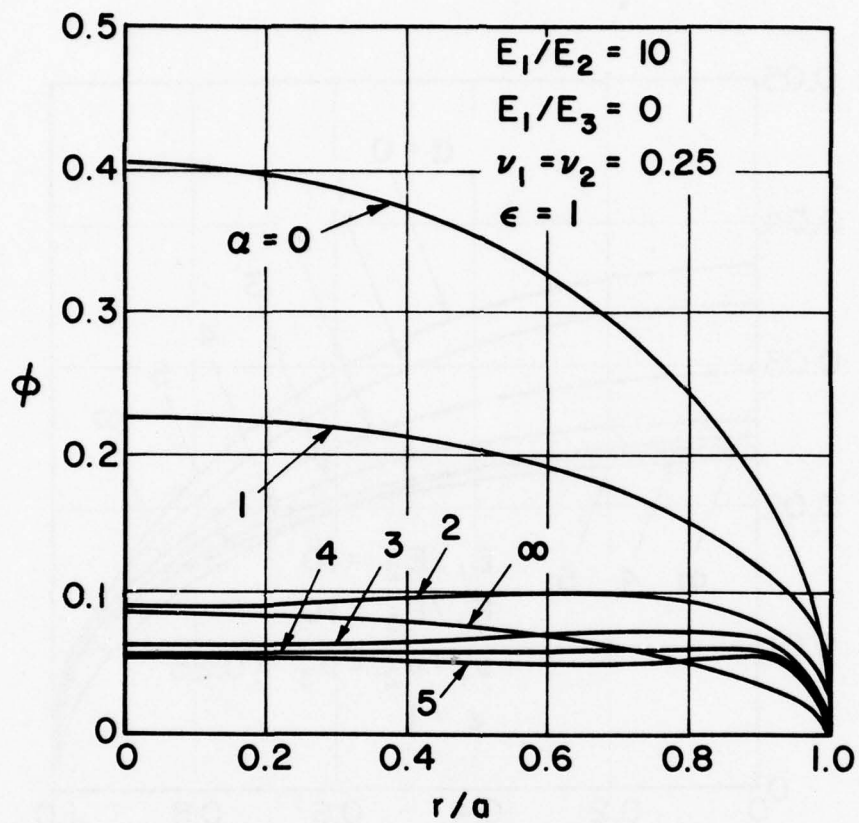


Fig. 5-2 Axisymmetric Pressure Profiles,  
Material Combination (ii)

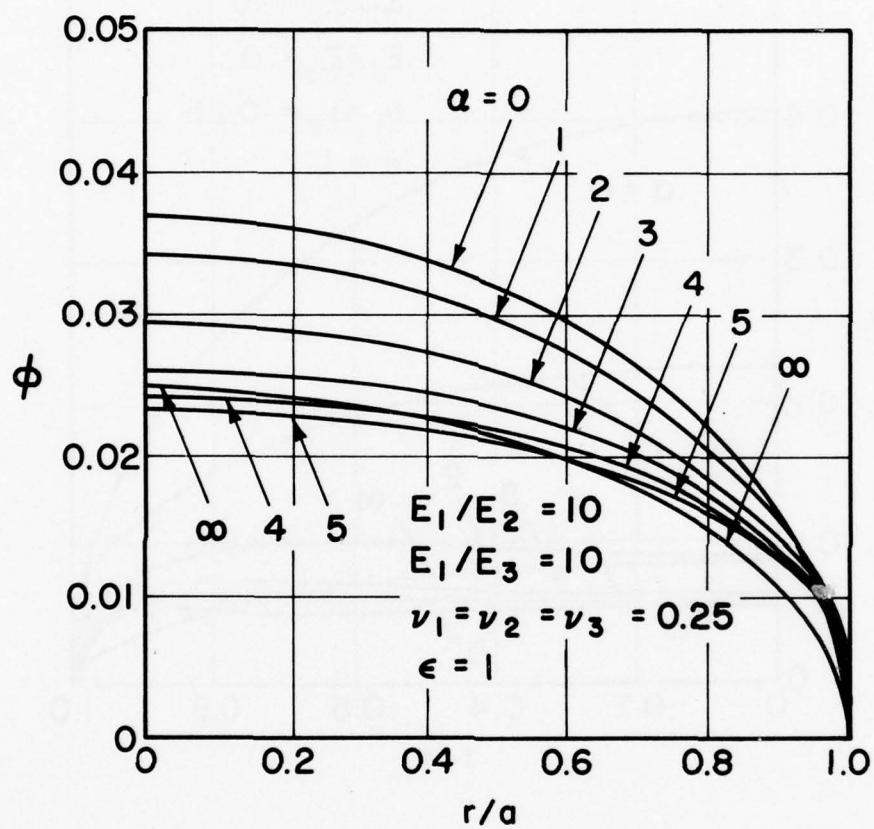


Fig. 5-3 Axisymmetric Pressure Profiles,  
Material Combination (iii)

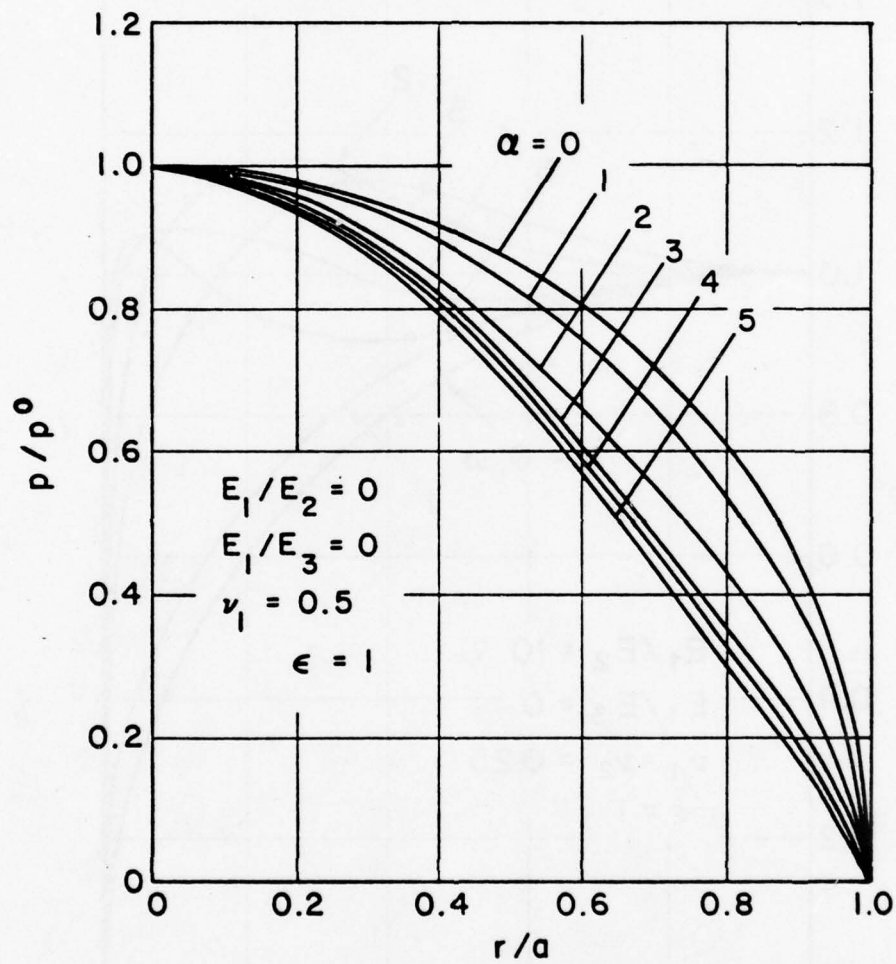


Fig. 5-4 Axisymmetric Pressure Profile Shapes,  
Material Combination (i).

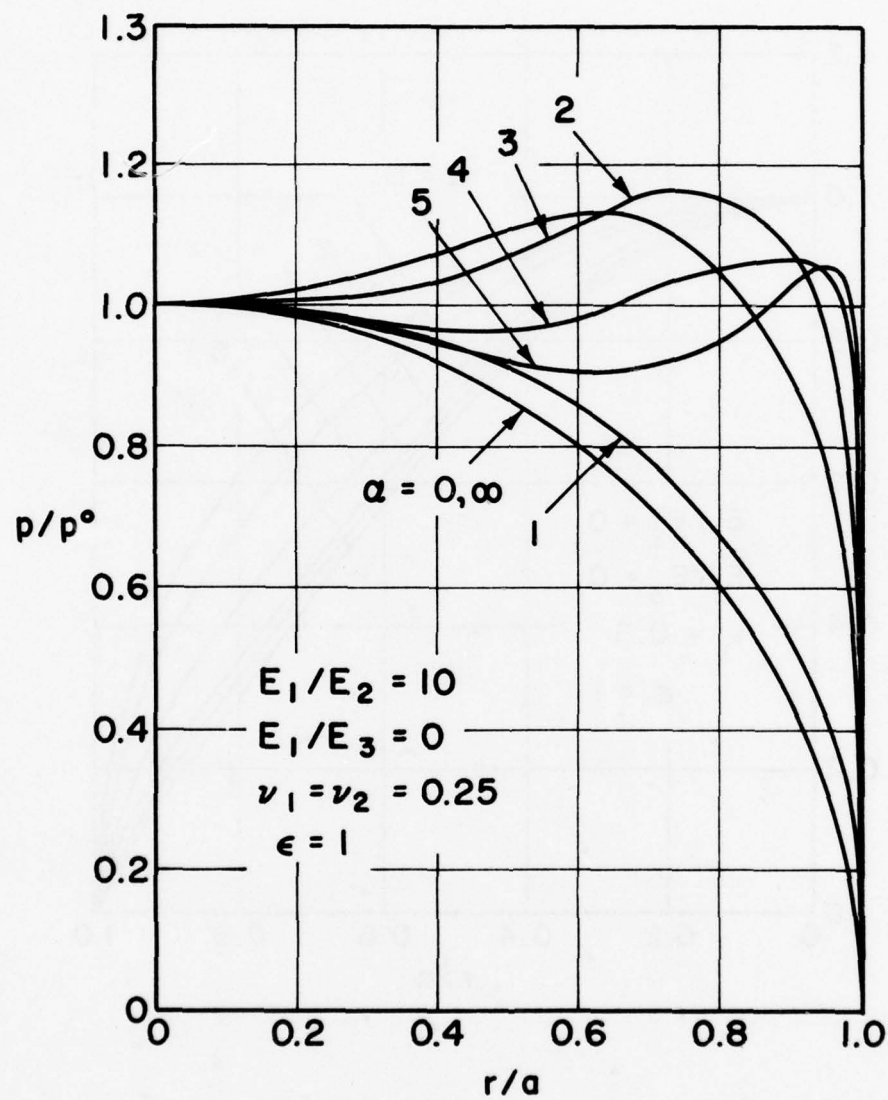


Fig. 5-5 Axisymmetric Pressure Profile Shapes, Material Combination (ii)

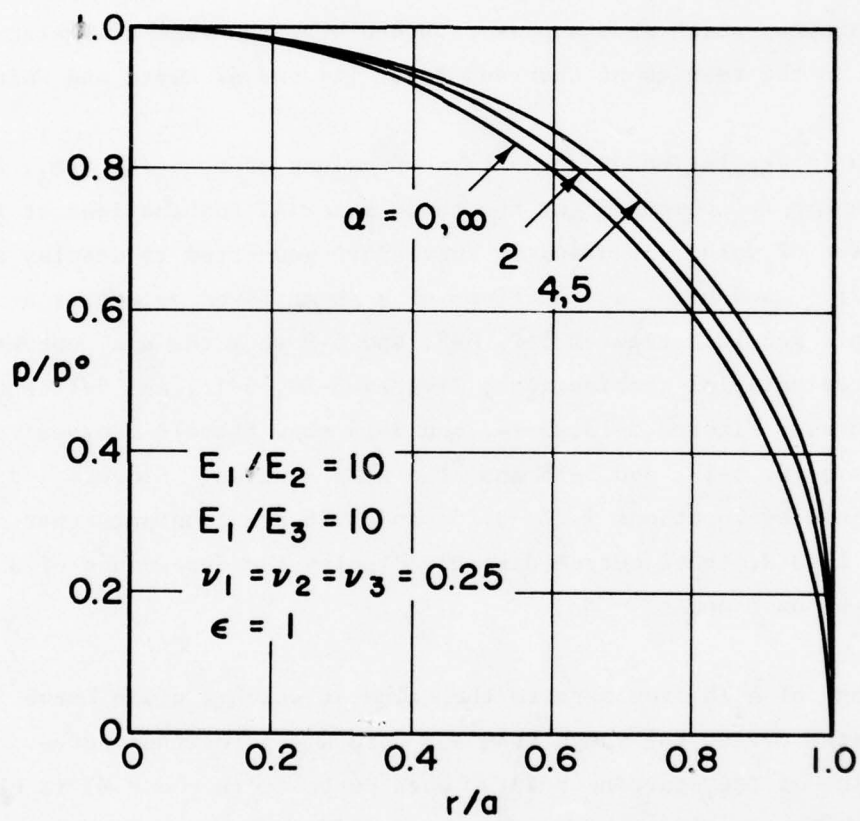


Fig. 5-6 Axisymmetric Pressure Profile Shapes,  
Material Combination (iii)



for material combination (i) appear to approach a parabolic shape with increasing  $\alpha$ . For material combination (iii) in Figure 5-6, very little change from the Hertz profile shape is evident. This is because the relative surface displacement is dominated by the low modulus homogeneous solid. The profile shapes in Figure 5-5 for material combination (ii) show a substantial departure from the Hertz ellipse. These shapes, which show a peak pressure near the edge of contact, also appear in the results of Chen and Engel [4] and of Gupta and Walowit [6].

Through interpolation of the arrays of values of  $\epsilon$ ,  $a_o/h$ ,  $a/a_o$ ,  $b/a_o$ ,  $d/d_o$ , and  $p^o/p_o^o$  computed for the three material combinations at the above set of values of  $\alpha$  and  $\rho$ , curves are generated to display  $a/a_o$ ,  $b/a_o$ ,  $d/d_o$ , and  $p^o/p_o^o$  as functions of  $a_o/h$  at fixed values of  $\epsilon$  between 1 and 10. Figures 5-7, 5-8, and 5-9 show the  $a/a_o$  curves for the three material combinations; Figures 5-10, 5-11, and 5-12 show the  $b/a_o$  curves; Figures 5-13, 5-14, and 5-15 show the  $d/d_o$  curves; and Figures 5-16, 5-17, and 5-18 show the  $p^o/p_o^o$  curves. Since  $a_o$ ,  $d_o$ , and  $p_o^o$  defined by Equations 3.27, 3.25, and 3.26 are constants that depend on the load  $W$ , these curves directly display the dependence of  $a$ ,  $b$ ,  $d$ , and  $p_o^o$  on  $h$  and  $\epsilon$ .

The range of  $a_o/h$  from zero to the value at which a given curve terminates covers the range from  $\alpha = 0$  to  $\alpha = 5$  for that curve. The value of the starting point of each curve ( $a_o/h = \alpha = 0$ ) is obtained from the Hertz solution for a layer of infinite thickness. In the limit  $a_o/h \rightarrow \infty$  which means a vanishing layer, material combination (i) is representing a contact between two rigid solids; for any curvature ratio the contact zone is becoming a point with major and minor half-widths and approach vanishing and the central pressure becoming infinite. In the same limit for material combinations (ii) and (iii), the layered solid is becoming a homogeneous solid of the elastic substrate material. The values of  $a/a_o$ ,  $b/a_o$ ,  $d/d_o$ , and  $p^o/p_o^o$  from the Hertz solution for the substrate material are shown as limiting values approached by the curves for material combinations (ii) and (iii).

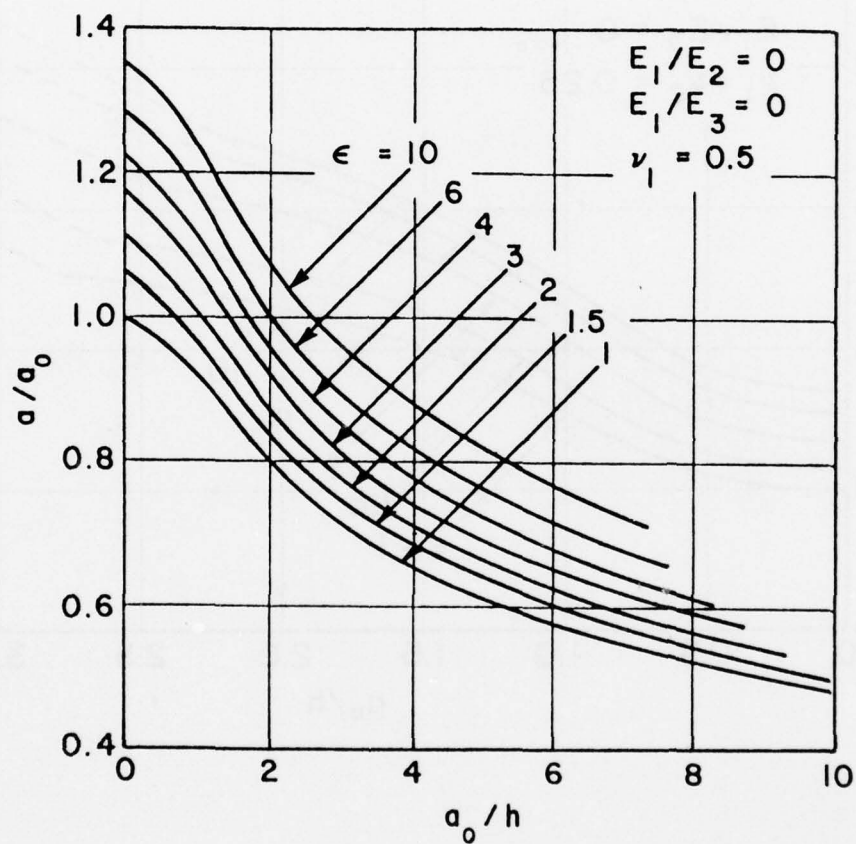


Fig. 5-7 Major Halfwidth versus Layer Thickness at Fixed Curvature Ratio, Material Combination (i).

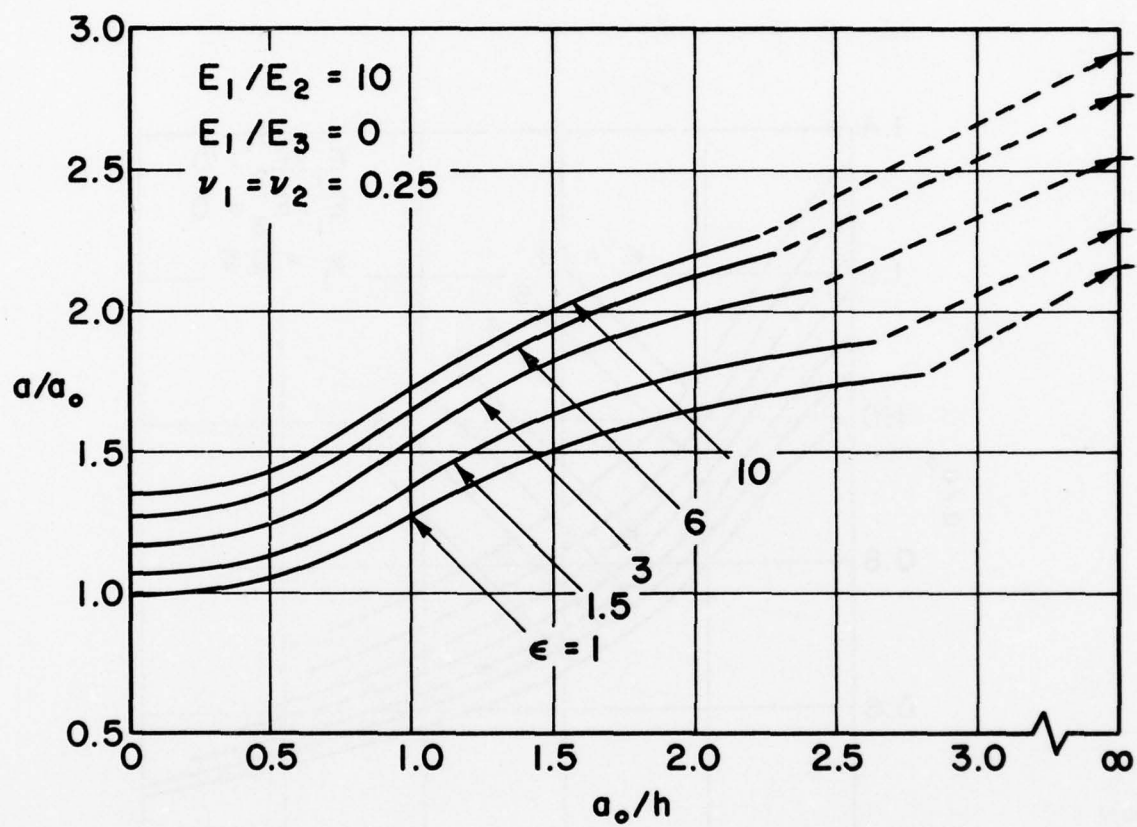


Fig. 5-8 Major Halfwidth versus Layer Thickness at Fixed Curvature Ratio, Material Combination (ii)

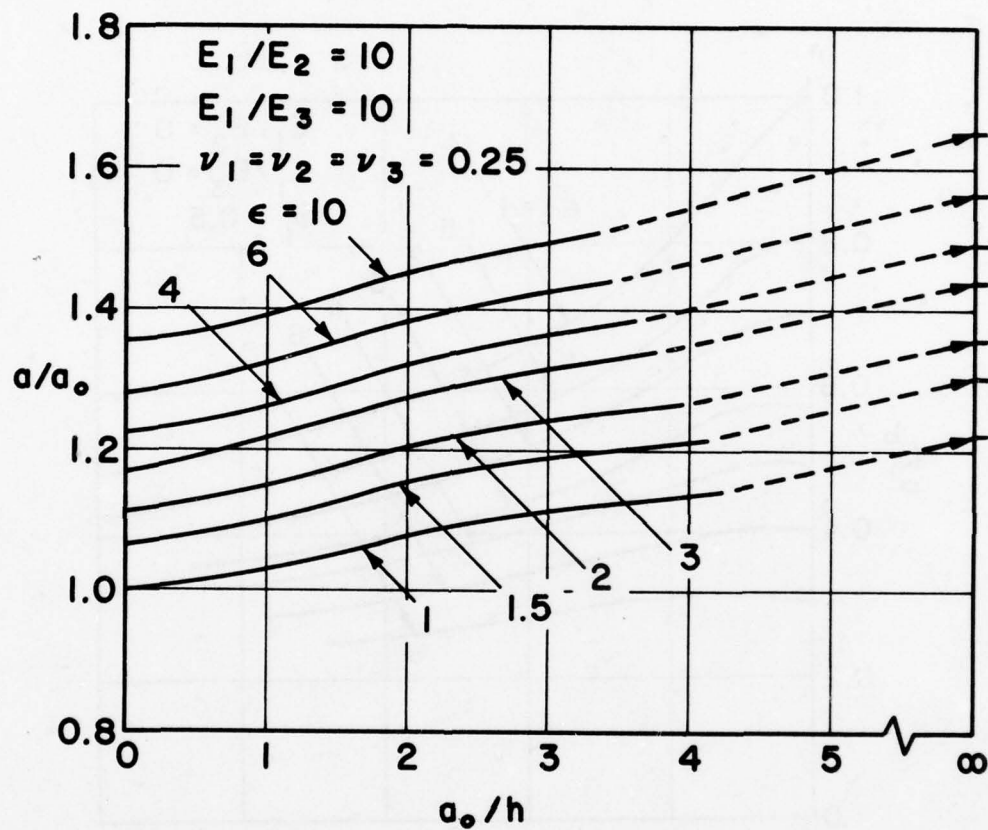


Fig. 5-9 Major Halfwidth versus Layer Thickness  
at Fixed Curvature Ratio, Material  
Combination (iii)

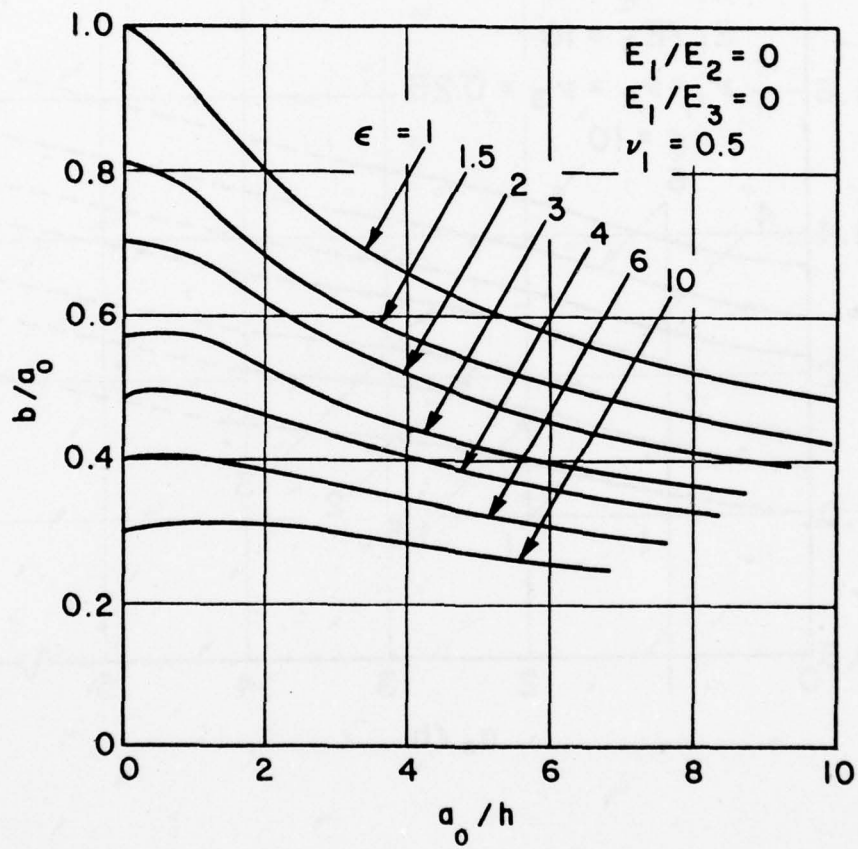


Fig. 5-10 Minor Halfwidth versus Layer Thickness at Fixed Curvature Ratio, Material Combination (i).



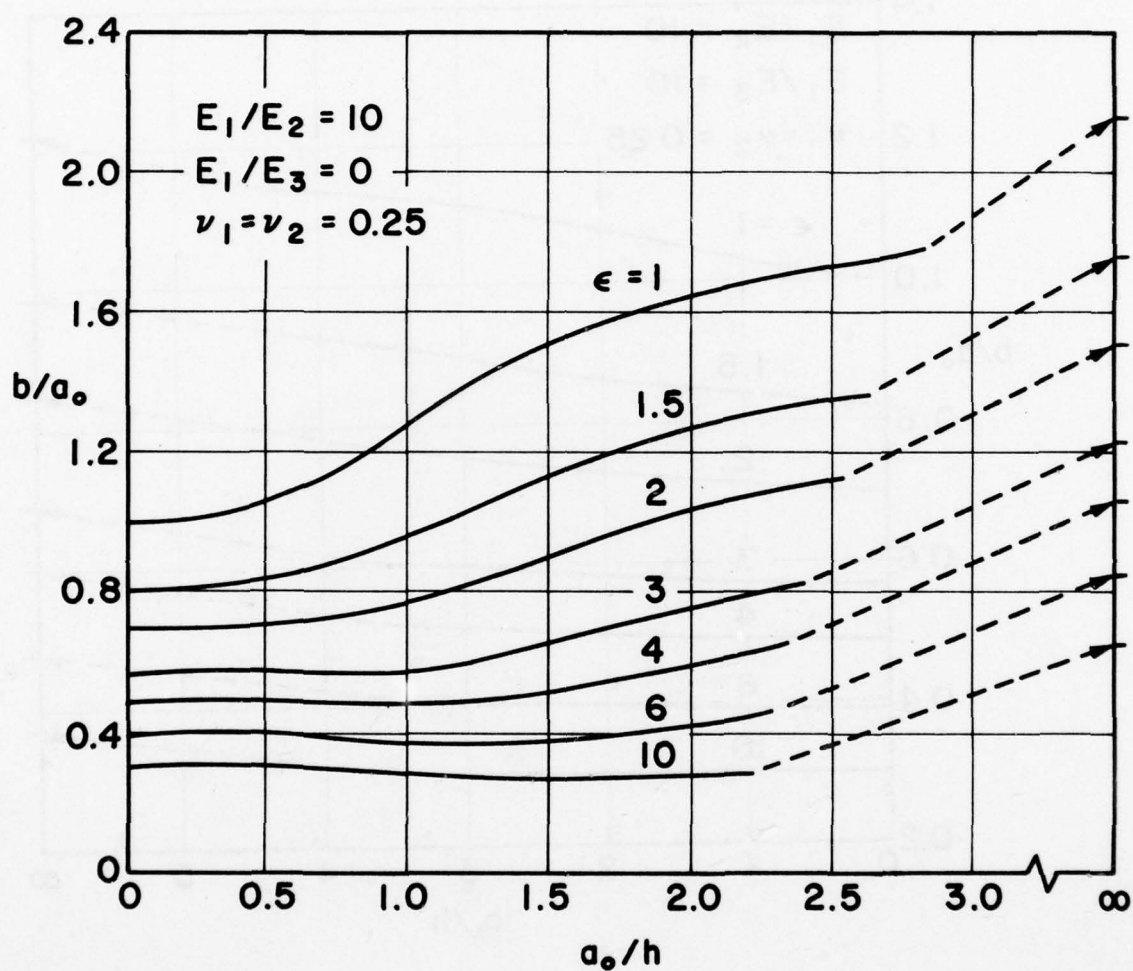


Fig. 5-11 Minor Halfwidth versus Layer Thickness at Fixed Curvature Ratio, Material Combination (ii)

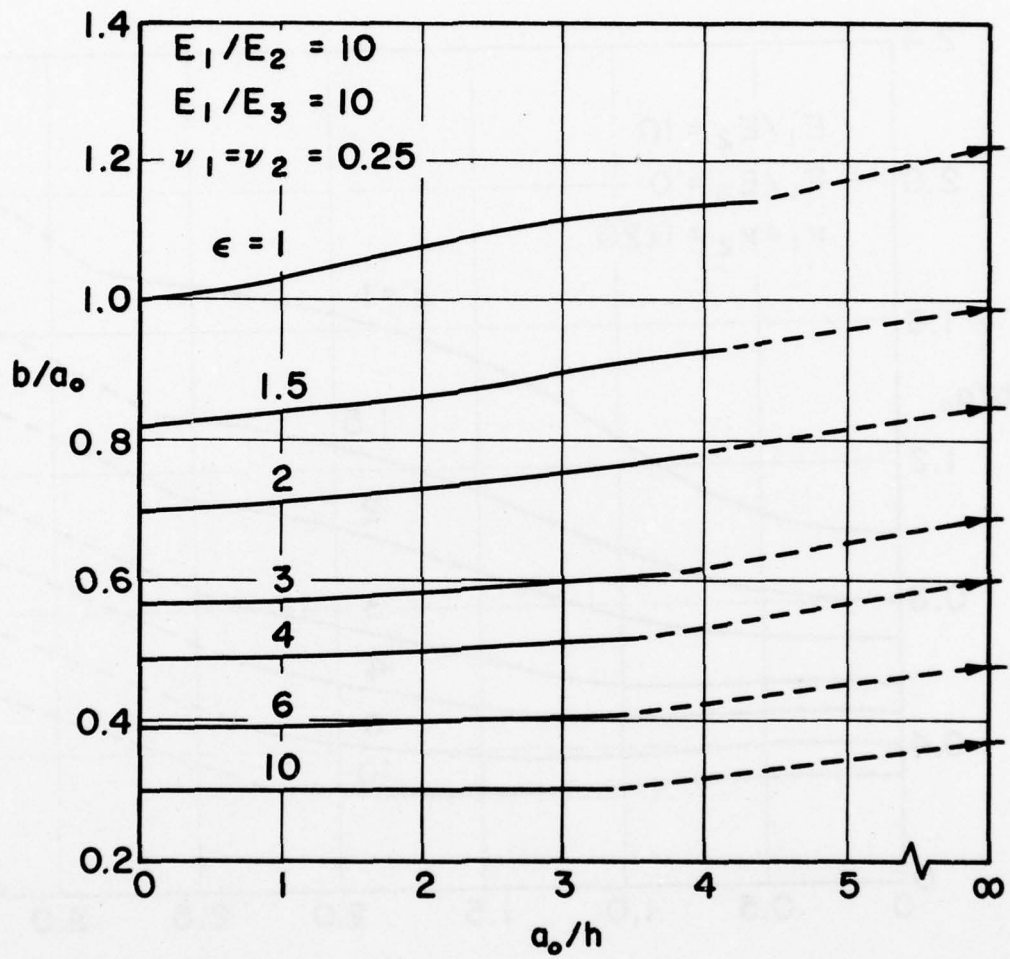


Fig. 5-12 Minor Halfwidth versus Layer Thickness at Fixed Curvature Ratio, Material Combination (iii)

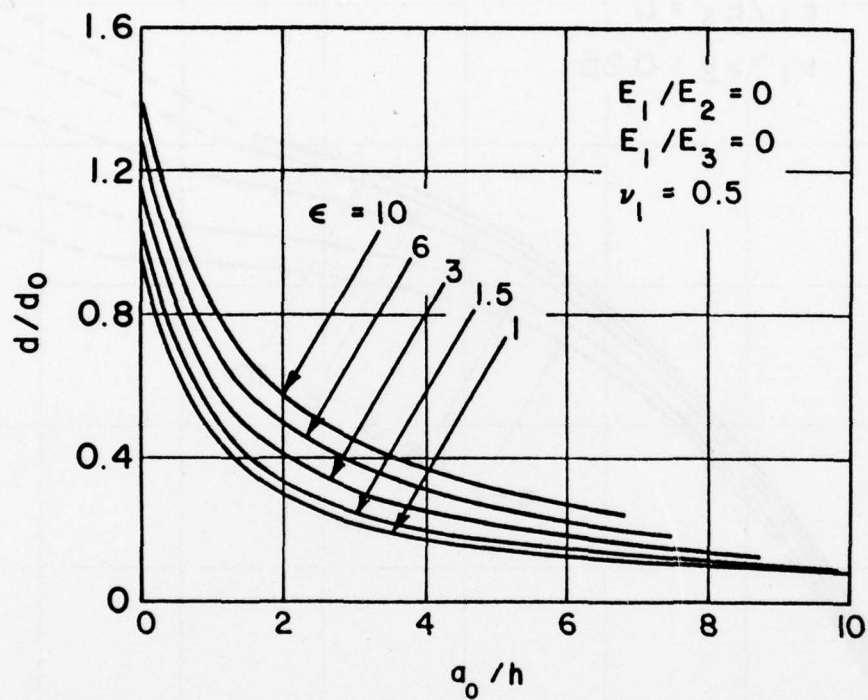


Fig. 5-13 Approach versus Layer Thickness at Fixed Curvature Ratio, Material Combination (i).

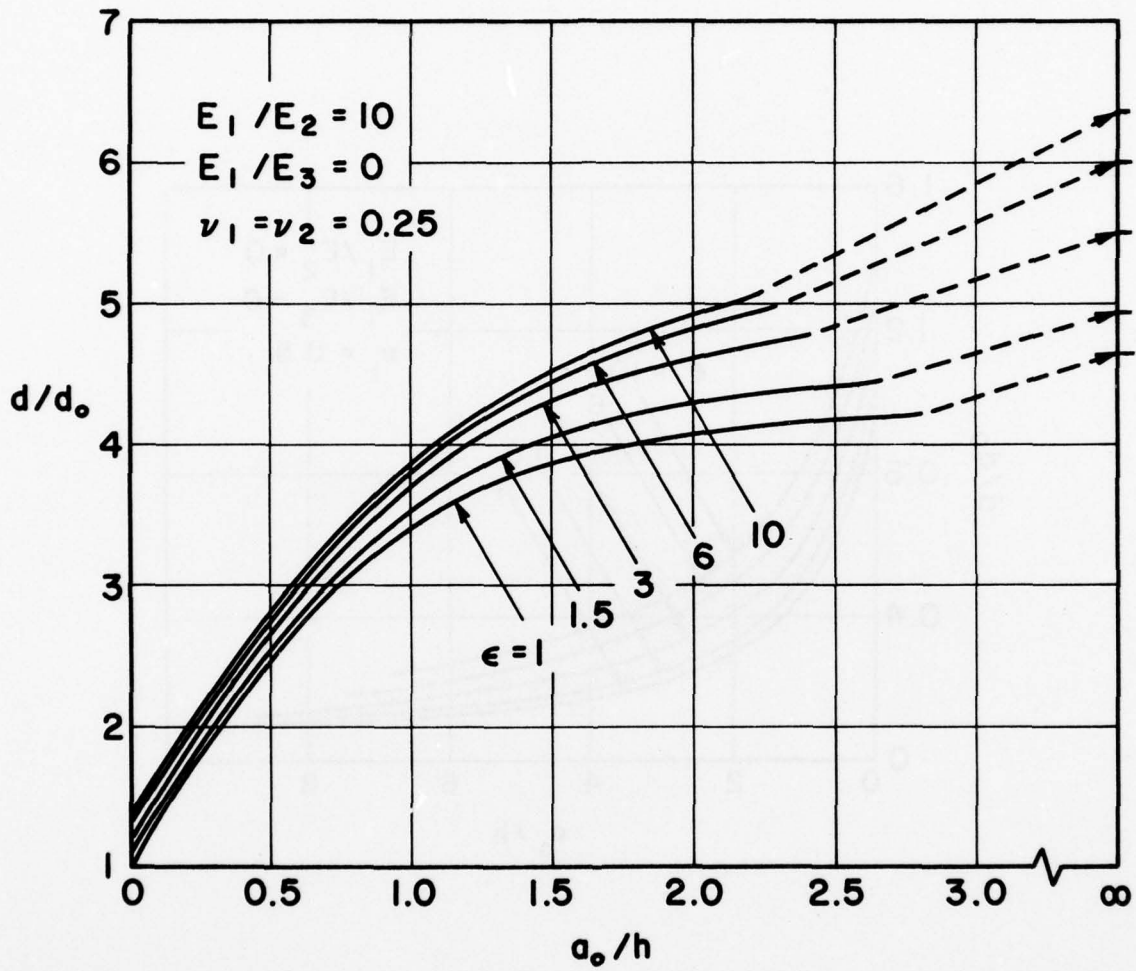


Fig. 5-14 Approach versus Layer Thickness at Fixed Curvature Ratio, Material Combination (ii)

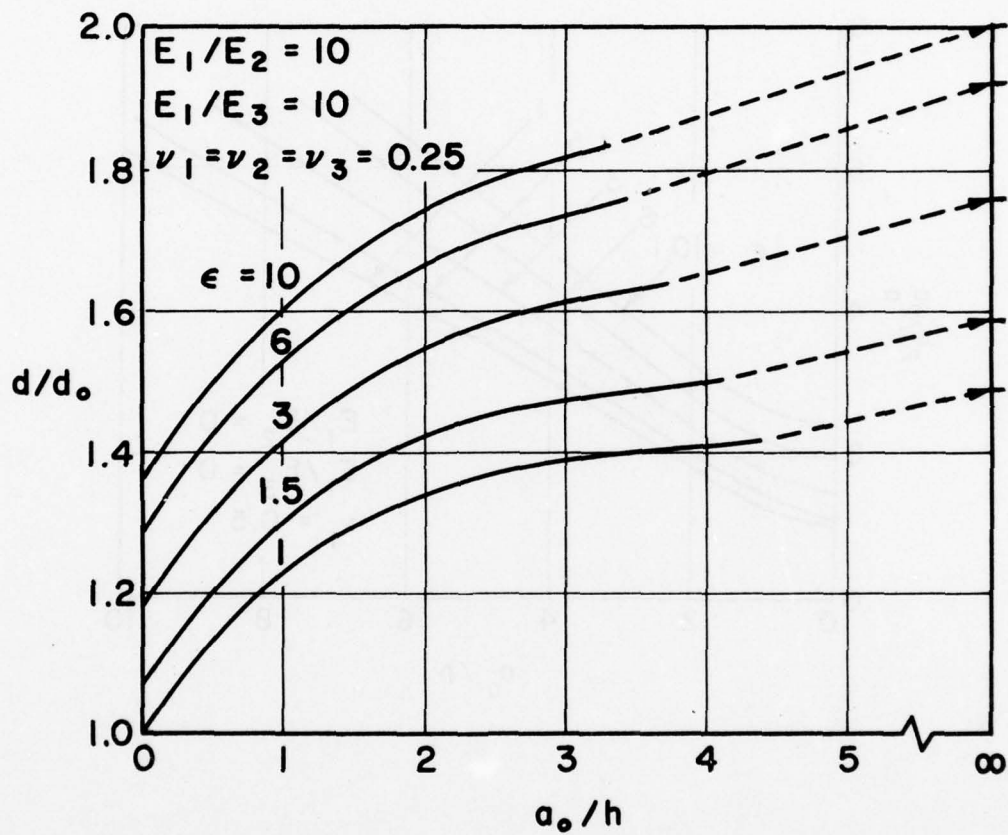


Fig. 5-15 Approach versus Layer Thickness at Fixed Curvature Ratio, Material Combination (iii)



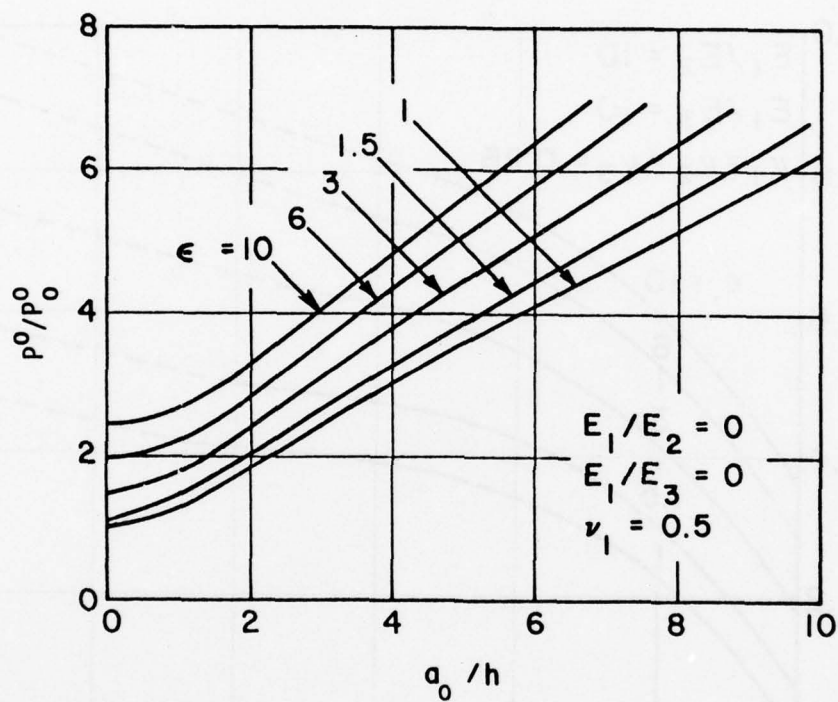


Fig. 5-16 Central Pressure versus Layer Thickness at Fixed Curvature Ratio, Material Combination (i).

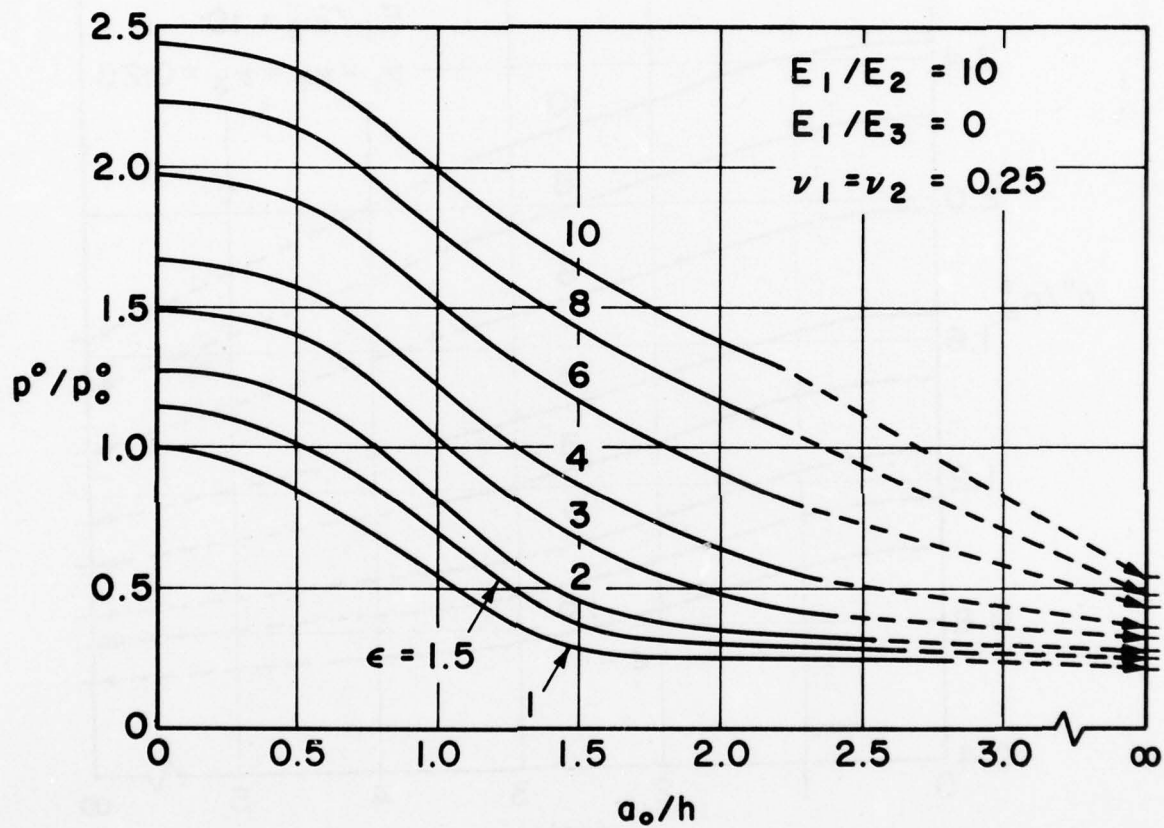


Fig. 5-17 Central Pressure versus Layer Thickness at Fixed Curvature Ratio, Material Combination (ii)

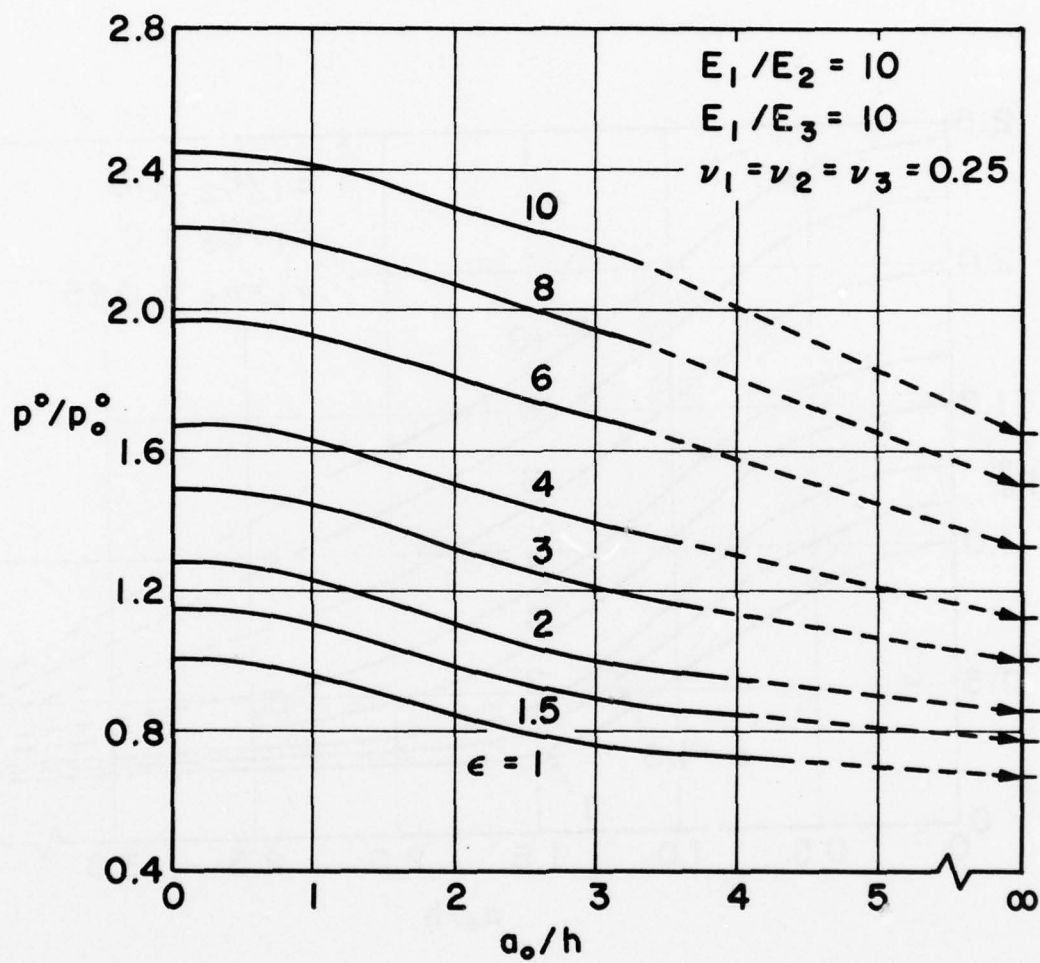


Fig. 5-18 Central Pressure versus Layer Thickness at Fixed Curvature Ratio, Material Combination (iii)

Elementary physical reasoning explains most of the trends shown by these curves. For material combination (i) at a given curvature ratio, a decreasing layer thickness reflects a general stiffening of the system since the substrate is rigid. Thus, at fixed load, the approach decreases (Figure 5-13); the major and minor halfwidths decrease (Figures 5-7 and 5-10) causing the contact area to decrease and the central pressure to increase (Figure 5-16). The opposite trend is shown by material combinations (ii) and (iii). The layer is of higher modulus than the substrate so the system becomes less stiff with decreasing layer thickness. This is consistent with an increasing approach (Figures 5-14 and 5-15), increasing major and minor halfwidths (Figures 5-8, 5-9, 5-11, and 5-12) and, thus, an increasing contact area and a decreasing central pressure (Figures 5-17 and 5-18). The approach, major and minor halfwidths, and central pressure are seen to be less sensitive to layer thickness for material combination (iii) than they are for material combination (ii). Since material combination (iii) contains a low modulus homogeneous solid, a given change in layer thickness makes less of a difference in the overall stiffness of the system than it does for material combination (ii) where the homogeneous solid is rigid. In other words, the relative surface displacement for material combination (iii) is dominated by the low modulus homogeneous solid, while the relative surface displacement for material combination (ii) consists only of the surface displacement of the layered solid.

Figures 5-19, 5-20, and 5-21 show curves of the ellipticity ratio ( $a/b$ ) versus  $a_0/h$  for the three material combinations. These curves are simply obtained as the ratio of values given by the  $a/a_0$  and  $b/a_0$  curves. For a given curvature ratio, material combination (i) shows a steady decrease in  $a/b$  with decreasing layer thickness; the contact zone tends to become more circular with decreasing layer thickness. This reflects the tendency of the low modulus layer material to be displaced in a direction parallel to the minor axis of the rigid elliptical paraboloid that is penetrating the layer. For material combinations (ii) and (iii),  $a/b$  has the same value for an infinitely thick layer ( $a_0/h = 0$ ) as for a vanishing layer ( $a_0/h = \infty$ ) since

AD-A056 232

MECHANICAL TECHNOLOGY INC LATHAM N Y

A NUMERICAL SOLUTION FOR A GENERALIZED ELLIPTICAL CONTACT OF LA--ETC(U)

MAY 78 J A MCCORMICK

N00014-72-C-0083

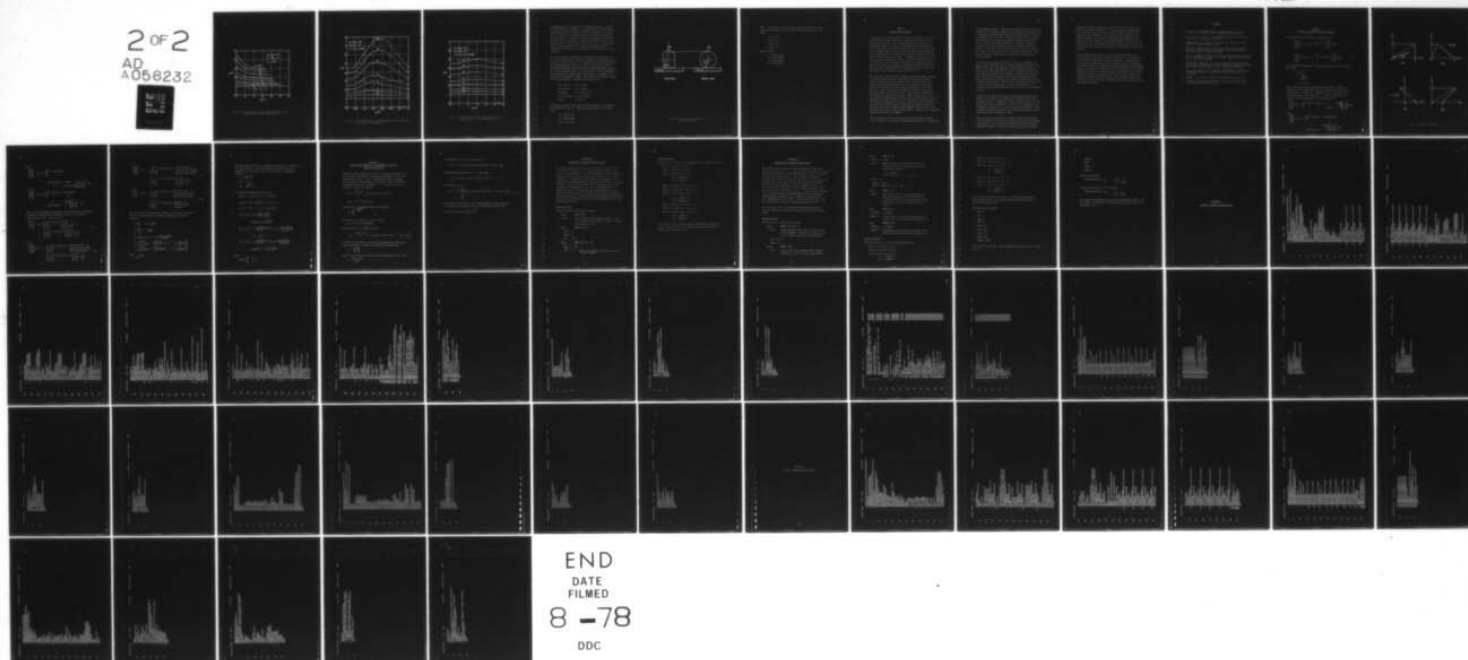
NL

UNCLASSIFIED

MTI-78TR52

2 OF 2

AD  
A056232

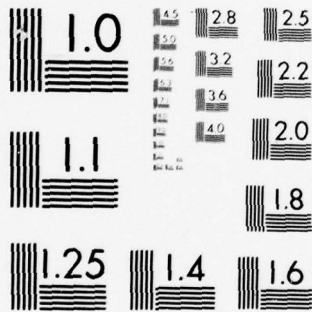


END  
DATE  
FILMED

8 -78

DDC





MICROCOPY RESOLUTION TEST CHART  
NATIONAL BUREAU OF STANDARDS-1963-A

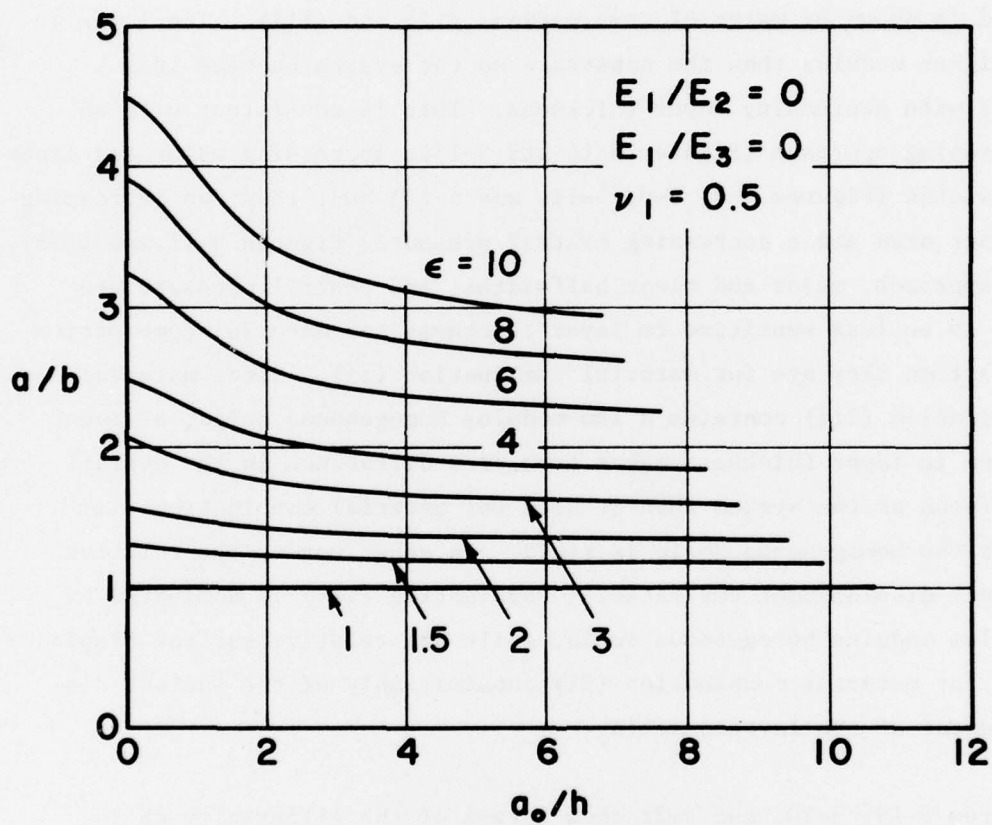


Fig. 5-19 Ellipticity Ratio versus Layer Thickness at Fixed Curvature Ratio, Material Combination (i).

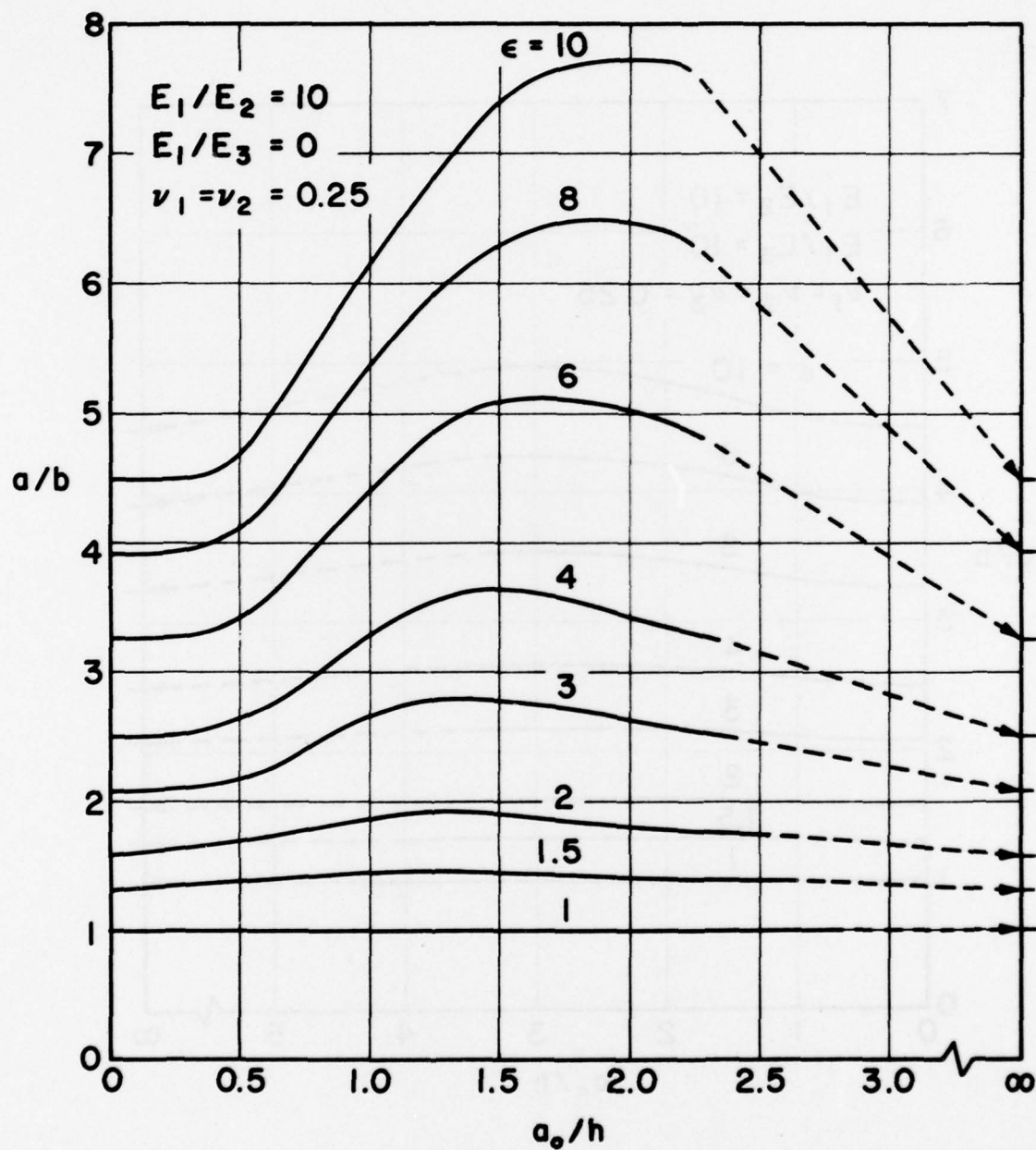


Fig. 5-20 Ellipticity Ratio versus Layer Thickness at Fixed Curvature Ratio, Material Combination (ii).

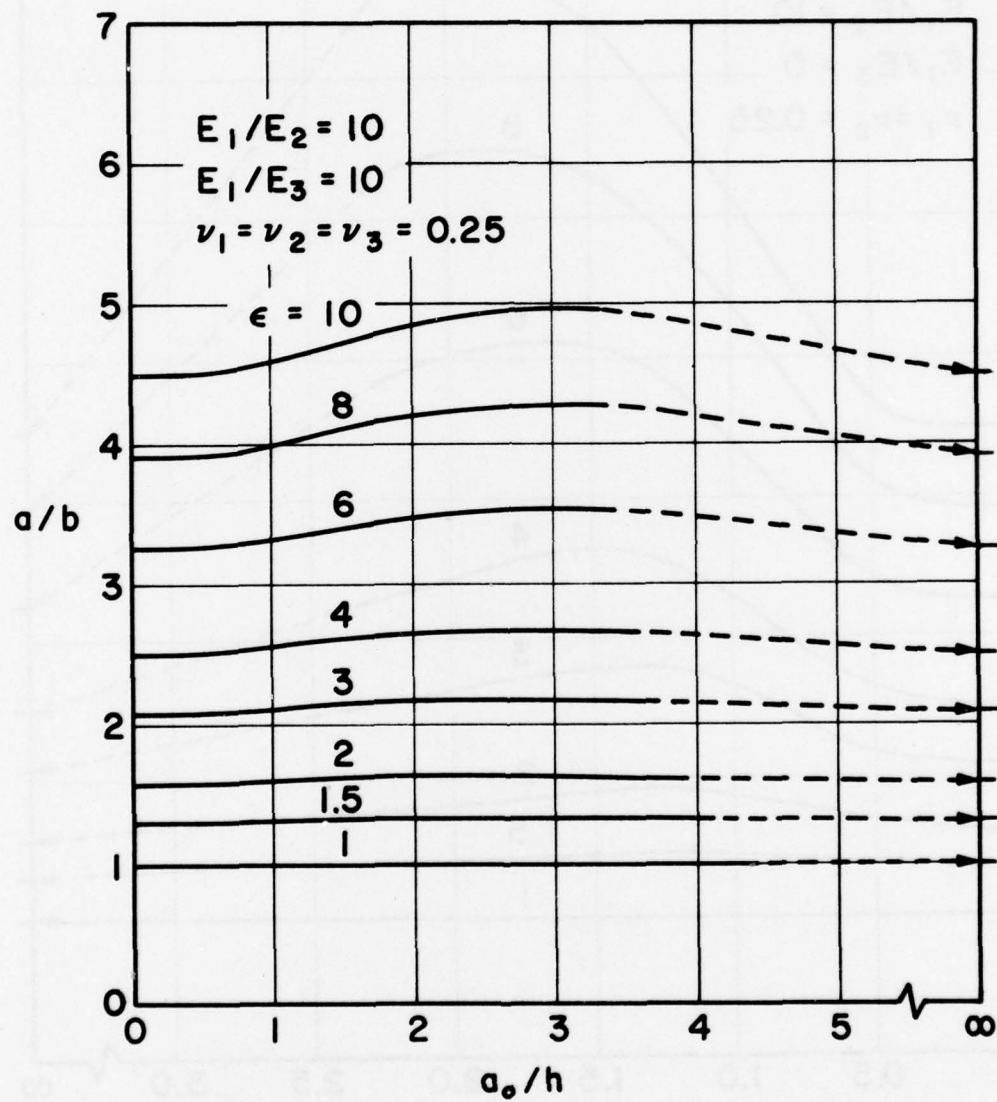


Fig. 5-21 Ellipticity Ratio versus Layer Thickness at Fixed Curvature Ratio, Material Combination (iii).

$a/b$  depends only on curvature ratio in the Hertz solution. Between the two extremes,  $a/b$  increases to a maximum value and then decreases with decreasing layer thickness. Material combination (iii) shows very little rise in  $a/b$  as expected from its relative insensitivity to layer thickness. The rise is prominent for material combination (ii) with  $a/b$  at a particular  $\epsilon$  reaching a maximum value that is less than the value of  $\epsilon$  but at lower  $\epsilon$  very close to it. As the maximum value of  $a/b$  is approached, the contact zone boundary contour is tending to coincide with a curve bounding a cross-section of the rigid paraboloid.

As a simple example to demonstrate the application of these results to an engineering problem, consider the loading of an elastomer surface layer ( $\nu_1 = 0.5$ ) by the edge of a crowned disc as shown in Figure 5-22. The undeformed separation profile near the contact zone will be an elliptical paraboloid of principal radii of curvature  $R_x$  and  $R_y$  where  $R_x$  is the crown radius and  $R_y$  is the disc radius. Let the elastomer have a low enough elastic modulus that the substrate it is bonded to and the disc can be regarded as rigid. Then the data for material combination (i) is applicable. Consider the following case:

Disc Radius:	$R_y = 2$ inches
Crown Radius:	$R_x = 6$ inches
Elastomer:	$E_1 = 1000$ lb/in. <sup>2</sup>
Layer Thickness:	$h = 0.10$ inches
Load:	$W = 20$ lb

One wishes to determine the major and minor halfwidths  $a$ ,  $b$ , approach  $d$ , and central pressure  $p_o^0$ . First, from Equations 3.27, 3.25, and 3.26:

$a_o = 0.407$ inches
$d_o = 0.028$ inches
$p_o^0 = 57.6$ lb/in. <sup>2</sup>



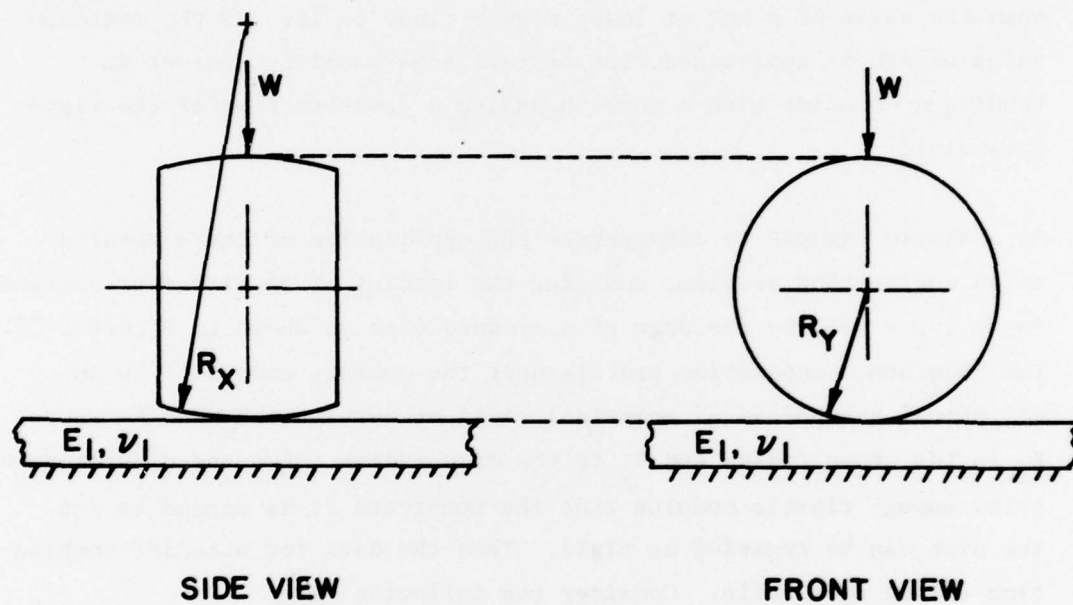


Fig. 5-22 Loading of Surface Layer by  
Edge of Crowned Disc

With  $\epsilon = 3$  and  $a_o/h = 4.07$ ,  $a/a_o$ ,  $b/a_o$ ,  $d/d_o$ , and  $p^o/p_o^o$  can be read directly from Figures 5-7, 5-10, 5-13, and 5-16, respectively. One finds:

$$a/a_o = 0.745$$

$$b/a_o = 0.447$$

$$d/d_o = 0.25$$

$$p^o/p_o^o = 3.9$$

with the result:

$$a = 0.303 \text{ inches}$$

$$b = 0.182 \text{ inches}$$

$$d = 0.007 \text{ inches}$$

$$p^o = 220 \text{ lb/in.}^2$$

PART 6SUMMARY AND CONCLUSIONS

In this study, a numerical method is developed to compute the pressure distribution and normal approach in a generalized elliptical contact between layered solids. The computed quantities are obtained as an approximate numerical solution to an integral equation formulated for the most general case of Hertz's assumptions, that is, the frictionless contact between arbitrary surfaces whose undeformed normal separation can be approximated by the separation between an elliptical paraboloid and the tangent plane at its vertex. The method is applied to the contact between a homogeneous solid and a layered solid consisting of an isotropic surface layer in perfect adhesion to an isotropic substrate. While plane strain and axisymmetric solutions for this case have been reported in the literature [4-8], no solutions have been reported for the general three-dimensional problem dealt with here.

With the kernel function given by a Hankel transform inversion integral, the integral equation must be treated by some approximate method to obtain solutions in a useful numerical form. The method used here combines a discretized representation of the unknown pressure distribution with an essentially exact numerical evaluation of the kernel function. Values of pressure are defined at points on a rectilinear grid representing the contact zone and a linear function approximates the continuous distribution of pressure between adjacent points. By expressing the integral equation at each grid point for this discretized distribution, one arrives at a system of simultaneous linear equations in the grid point pressures with coefficients formed from integrals of the kernel over right triangular regions between adjacent points. The approach and the ratio of the principal radii of curvature of the parabolic separation also appear as unknowns.

The key numerical task in this analysis is the evaluation of a large array of integrals of the kernel function required to form the coefficients

of the unknown pressures. Integration in three variables, the two space variables of the integral equation and the Hankel transform variable  $\omega$ , is performed by Gaussian quadrature with a resultant accuracy of around six decimal places. Once the coefficients are computed, the system of equations for the grid point pressures, approach, and curvature ratio is solved by Gaussian elimination. In physical terms, the solution permits one to determine the major and minor halfwidths, pressures, and approach for a given load, layer thickness, and curvature ratio. The dimensionless load, obtained as the integral of the solution pressure distribution, is equivalent to a dimensionless major halfwidth.

In setting up the contact zone grid for a particular problem, the major to minor halfwidth ratio or ellipticity ratio is defined. The shape of the contact zone boundary contour between the vertices at the major and minor halfwidths must also be defined even though the true shape is an unknown in the problem. In general, the true shape, which is an ellipse in the Hertz solution for homogeneous solids, must be determined iteratively as the shape along which the solution pressure profile vanishes. With a grid of ten uniform divisions along the major and minor halfwidths, a discrete representation of an elliptical contour gave satisfactory results for all cases considered in the study.

Accuracy of the numerical method with the above-mentioned grid was checked at limiting cases by comparison of predicted results with available solutions. Comparisons include the Hertz solution for homogeneous solids [1-3] and numerical results of Chen and Engel [4] for axisymmetric layered solids. The major and minor halfwidths, central pressure, and approach computed by the present method agree to within one percent with the comparison values.

Numerical results generated over a range of ellipticity ratios and major halfwidth to layer thickness ratios are shown for three material combinations as curves that give the dimensionless major and minor halfwidths, approach, and central pressure as a function of layer



thickness at fixed curvature ratio. The load appears in scale factors for the dimensionless variables. At a given load and curvature ratio, the ellipticity ratio of the contact zone is shown to decrease with decreasing layer thickness for a low modulus layer bonded to a high modulus substrate and increase with decreasing layer thickness for a high modulus layer bonded to a low modulus substrate. Pressure profile shapes that differ substantially from the ellipsoid of the Hertz solution appear in the case of a high modulus layer bonded to a low modulus substrate.

The same method can be used to compute the subsurface stresses in a layered halfspace under an arbitrary surface loading. The computation of subsurface stresses under a loading consisting of a computed contact pressure distribution would be of value as a means of determining safe operating loads for surface-coated bearing elements in concentrated contact. In addition, the method can easily be applied to other contact configurations such as the contact between two layered solids, layered solids with interface conditions that involve slip and friction, and solids that contain more than one layer. The inversion integral for the kernel function would have a different form in each case; everything else would be the same.



#### REFERENCES

1. Hertz, H., "Miscellaneous Papers," translated by D.E. Jones and G.A. Schott, pp. 146-162, 163-183, MacMillan, New York, 1896.
2. Love, A.E.H., "A Treatise on the Mathematical Theory of Elasticity," Fourth Edition, Cambridge, London, 1934.
3. Timoshenko, S., and Goodier, J.N., "Theory of Elasticity," Second Edition, McGraw-Hill, New York, 1951.
4. Chen, W.T., and Engel, P.A., "Impact and Contact Stress Analysis in Multilayer Media," International Journal of Solids and Structures, Vol 8, No. 11, Nov. 1972, pp. 1257-1281.
5. Tu, Y., "A Numerical Solution for an Axially Symmetric Contact Problem," Journal of Applied Mechanics, Vol. 35, Trans. ASME, Vol. 89, Series E, No. 2, June 1967, pp. 283-286.
6. Gupta, P.K., and Walowit, J.A., "Contact Stresses between an Elastic Cylinder and a Layered Elastic Solid," Journal of Lubrication Technology, Trans. ASME, Vol. 96, Series F, No. 2, April 1974, pp. 250-257.
7. Wu, J.J., and Ling, F.F., "A Method for Micro-Hardness Analysis of an Elastoplastic Material," Developments in Mechanics, Vol. 6, 1971, pp. 359-372.
8. Sneddon, I.N., "Fourier Transforms," McGraw-Hill, New York, 1951.
9. "Handbook of Mathematical Functions," edited by M. Abramowitz and I.A. Stegun, Dover, New York, 1970.

APPENDIX I  
ANALYTICAL EVALUATION OF BASIC INTEGRALS

The integral functions defined by Equation 4.2.17:

$$\begin{Bmatrix} H_o \\ I_o \\ J_o \end{Bmatrix} (s, t) = \int_0^t \int_0^s (u^2 + v^2)^{-1/2} \begin{Bmatrix} 1 \\ u \\ v \end{Bmatrix} dudv \quad (I.1)$$

$$\begin{Bmatrix} H_o^* \\ I_o^* \\ J_o^* \end{Bmatrix} (s, t, \pm \rho) = \int_s^t \int_{s \mp \rho v}^{s + \rho v} (u^2 + v^2)^{-1/2} \begin{Bmatrix} 1 \\ u \\ v \end{Bmatrix} dudv \quad (I.2)$$

are evaluated by carrying out the double integration in polar coordinates  $(r, \theta)$  with:

$$u = r \cos \theta$$

$$v = r \sin \theta$$

$$r = \sqrt{u^2 + v^2}$$

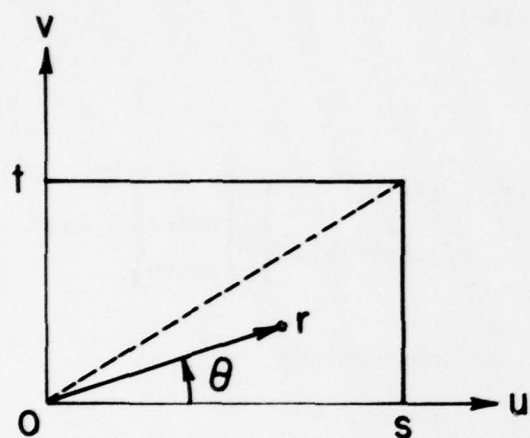
$$\theta = \tan^{-1}(v/u)$$

and the differential element  $dudv$  replaced with  $rdrd\theta$ . Figure I-1 shows the types of regions which must be considered with (a) applying to Equation I.1, (b) and (c) to Equation I.2 for a slope of  $-\rho$ , and (d) to Equation I.2 for a slope of  $+\rho$ . In polar coordinates, the integrals over these regions take the following form:

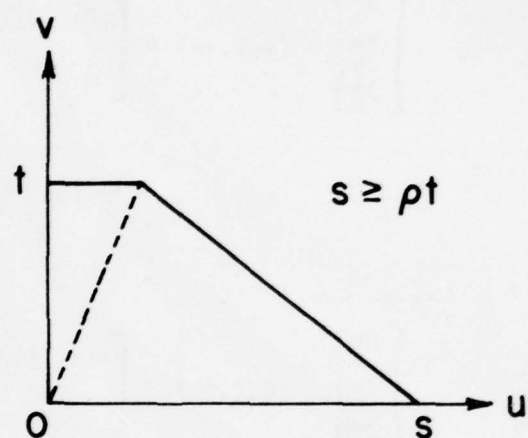
$$\begin{Bmatrix} H_o \\ I_o \\ J_o \end{Bmatrix} (s, t) = \left[ \int_0^{\tan^{-1}(t/s)} \int_0^{s/\cos \theta} + \int_{\tan^{-1}(t/s)}^{\pi/2} \int_0^{t/\sin \theta} \right] \begin{Bmatrix} 1 \\ r \cos \theta \\ r \sin \theta \end{Bmatrix} dr d\theta$$

$s \geq \rho t$

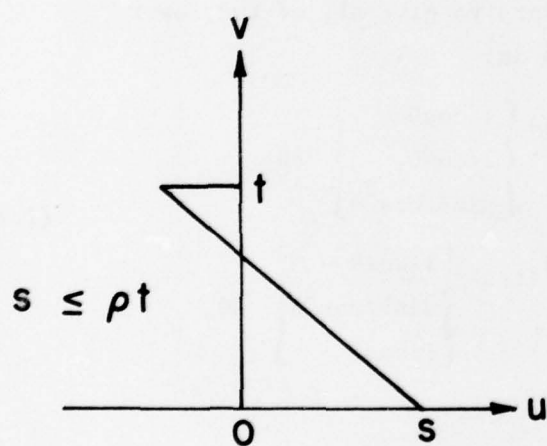
$$\begin{Bmatrix} H_o^* \\ I_o^* \\ J_o^* \end{Bmatrix} (s, t, -\rho) = \left[ \int_0^{\tan^{-1}[t/(s-\rho t)]} \int_0^{s/(\cos \theta + \rho \sin \theta)} + \int_{\tan^{-1}[t/(s-\rho t)]}^{\pi/2} \int_0^{t/\sin \theta} \right] \begin{Bmatrix} 1 \\ r \cos \theta \\ r \sin \theta \end{Bmatrix} dr d\theta$$



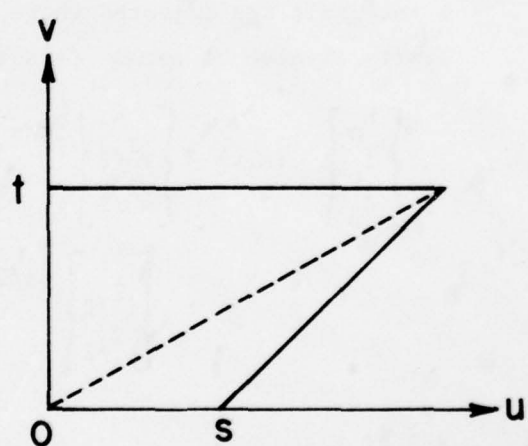
(a)



(b)



(c)



(d)

Fig. I-1 Regions of Integration

$$s \leq \rho t$$

$$\begin{Bmatrix} H_o^* \\ I_o^* \\ J_o^* \end{Bmatrix} (s, t, -\rho) = \begin{bmatrix} \pi/2 & s/(\cos\theta + \rho \sin\theta) \\ \int & \int \\ o & o \end{bmatrix} - \begin{bmatrix} \pi - \tan^{-1}[t/(\rho t - s)] & t/\sin\theta \\ \int & \int \\ \pi/2 & s/(\cos\theta + \rho \sin\theta) \end{bmatrix} \begin{Bmatrix} 1 \\ r \cos\theta \\ r \sin\theta \end{Bmatrix} dr d\theta$$

$$\begin{Bmatrix} H_o^* \\ I_o^* \\ J_o^* \end{Bmatrix} (s, t, +\rho) = \begin{bmatrix} \tan^{-1}[t/(s + \rho t)] & s/(\cos\theta - \rho \sin\theta) \\ \int & \int \\ o & o \end{bmatrix} + \begin{bmatrix} \pi/2 & t/\sin\theta \\ \int & \int \\ \tan^{-1}[t/(s + \rho t)] & o \end{bmatrix} \begin{Bmatrix} 1 \\ r \cos\theta \\ r \sin\theta \end{Bmatrix} dr d\theta$$

Next, the straightforward  $r$  integration is carried out and the remaining  $\theta$  integrals are adjusted where necessary to give all of the lower limits a value of zero. This results in:

$$\begin{Bmatrix} H_o^* \\ I_o^* \\ J_o^* \end{Bmatrix} (s, t) = \begin{Bmatrix} s \\ s^2/2 \\ s^2/2 \end{Bmatrix} \begin{bmatrix} \tan^{-1}(t/s) \\ \int \\ o \end{bmatrix} \begin{Bmatrix} 1/\cos\theta \\ 1/\cos\theta \\ \sin\theta/\cos^2\theta \end{Bmatrix} d\theta + \begin{Bmatrix} t \\ t^2/2 \\ t^2/2 \end{Bmatrix} \begin{bmatrix} \pi/2 - \tan^{-1}(t/s) \\ \int \\ o \end{bmatrix} \begin{Bmatrix} 1/\cos\theta \\ \sin\theta/\cos^2\theta \\ 1/\cos\theta \end{Bmatrix} d\theta \quad (I.3)$$

$$s \geq \rho t$$

$$\begin{Bmatrix} H_o^* \\ I_o^* \\ J_o^* \end{Bmatrix} (s, t, -\rho) = \begin{Bmatrix} s \\ s^2/2 \\ s^2/2 \end{Bmatrix} \begin{bmatrix} \tan^{-1}[t/(s - \rho t)] \\ \int \\ o \end{bmatrix} \begin{Bmatrix} 1/(\cos\theta + \rho \sin\theta) \\ \cos\theta/(\cos\theta + \rho \sin\theta)^2 \\ \sin\theta/(\cos\theta + \rho \sin\theta)^2 \end{Bmatrix} d\theta + \begin{Bmatrix} t \\ t^2/2 \\ t^2/2 \end{Bmatrix} \begin{bmatrix} \pi/2 - \tan^{-1}[t/(s - \rho t)] \\ \int \\ o \end{bmatrix} \begin{Bmatrix} 1/\cos\theta \\ \sin\theta/\cos^2\theta \\ 1/\cos\theta \end{Bmatrix} d\theta \quad (I.4)$$

$$s \leq \rho t$$

$$\begin{aligned} \begin{Bmatrix} H_o^* \\ I_o^* \\ J_o^* \end{Bmatrix} (s, t, -\rho) &= \begin{Bmatrix} s \\ s^2/2 \\ s^2/2 \end{Bmatrix} \int_0^{\pi - \tan^{-1}[t/(\rho t - s)]} \begin{Bmatrix} 1/(\cos\theta + \rho \sin\theta) \\ \cos\theta/(\cos\theta + \rho \sin\theta)^2 \\ \sin\theta/(\cos\theta + \rho \sin\theta)^2 \end{Bmatrix} d\theta \\ &- \begin{Bmatrix} t \\ t^2/2 \\ t^2/2 \end{Bmatrix} \int_0^{\pi/2 - \tan^{-1}[t/(\rho t - s)]} \begin{Bmatrix} 1/\cos\theta \\ -\sin\theta/\cos^2\theta \\ 1/\cos\theta \end{Bmatrix} d\theta \end{aligned} \quad (I.5)$$

$$\begin{aligned} \begin{Bmatrix} H_o^* \\ I_o^* \\ J_o^* \end{Bmatrix} (s, t, +\rho) &= \begin{Bmatrix} s \\ s^2/2 \\ s^2/2 \end{Bmatrix} \int_0^{\tan^{-1}[t/(s + \rho t)]} \begin{Bmatrix} 1/(\cos\theta - \rho \sin\theta) \\ \cos\theta/(\cos\theta - \rho \sin\theta)^2 \\ \sin\theta/(\cos\theta - \rho \sin\theta)^2 \end{Bmatrix} d\theta \\ &+ \begin{Bmatrix} t \\ t^2/2 \\ t^2/2 \end{Bmatrix} \int_0^{\pi/2 - \tan^{-1}[t/(s + \rho t)]} \begin{Bmatrix} 1/\cos\theta \\ \sin\theta/\cos^2\theta \\ 1/\cos\theta \end{Bmatrix} d\theta \end{aligned} \quad (I.6)$$

The above expressions contain the integrals of five basic functions of  $\theta$ , which can be evaluated by elementary techniques to yield the following:

$$\begin{aligned} \int_0^\phi \frac{d\theta}{\cos\theta} &= \log \frac{1 + \sin\phi}{\cos\phi} \\ \int_0^\phi \frac{\sin\theta d\theta}{\cos^2\theta} &= \frac{1 - \cos\phi}{\cos\phi} \\ \int_0^\phi \frac{d\theta}{\cos\theta + \rho \sin\theta} &= \frac{1}{\sigma} \log \frac{(\sigma + \rho)(\sigma \sin\phi + 1)}{\sigma \cos\phi + \rho} \\ \int_0^\phi \frac{\cos\theta d\theta}{(\cos\theta + \rho \sin\theta)^2} &= \frac{1}{\sigma^2} \left[ \frac{\sigma + \rho}{\cos\phi + \rho \sin\phi} + \rho + \int_0^\phi \frac{d\theta}{\cos\theta + \rho \sin\theta} \right] \\ \int_0^\phi \frac{\sin\theta d\theta}{(\cos\theta + \rho \sin\theta)^2} &= \frac{1}{\sigma^2} \left[ \frac{1}{\cos\phi + \rho \sin\phi} - 1 + \rho \int_0^\phi \frac{d\theta}{\cos\theta + \rho \sin\theta} \right] \end{aligned}$$

where

$$\sigma \equiv \sqrt{1 + \rho^2}$$



When the appropriate limits of integration in Equations I.3 through I.6 are substituted for  $\phi$  in these integrals, the final closed form expressions for Equations I.1 and I.2 are obtained. Defining the quantities:

$$R^{\circ} = \sqrt{s^2 + t^2}$$

$$s^{\pm} = s \pm \rho t$$

$$R^{\pm} = \sqrt{s^{\pm 2} + t^2}$$

the resulting expressions take the form:

$$H_0(s, t) = s \log \frac{R^{\circ} + t}{s} + t \log \frac{R^{\circ} + s}{t}$$

$$I_0(s, t) = \frac{1}{2} s^2 \log \frac{R^{\circ} + t}{s} + \frac{1}{2} t(R^{\circ} - t)$$

$$J_0(s, t) = \frac{1}{2} s(R^{\circ} - s) + \frac{1}{2} t^2 \log \frac{R^{\circ} + s}{t}$$

$$H_0^*(s, t, \pm \rho) = \frac{s}{\sigma} \log \frac{(\sigma \mp \rho)(\sigma t + R^{\pm})}{\sigma s^{\pm} \mp \rho R^{\pm}}$$

$$+ \text{Sgn}(s^{\pm}) t \log \frac{R^{\pm} + |s^{\pm}|}{t}$$

$$I_0^*(s, t, \pm \rho) = \frac{1}{2} \left( \frac{s}{\sigma} \right)^2 \left[ \frac{\pm \rho (R^{\pm} - s)}{s} + \frac{1}{\sigma} \log \frac{(\sigma \mp \rho)(\sigma t + R^{\pm})}{\sigma s^{\pm} \mp \rho R^{\pm}} \right]$$

$$+ \frac{1}{2} t (R^{\pm} - t)$$

$$J_0^*(s, t, \pm \rho) = \frac{1}{2} \left( \frac{s}{\sigma} \right)^2 \left[ \frac{R^{\pm} - s}{s} \mp \frac{\rho}{\sigma} \log \frac{(\sigma \mp \rho)(\sigma t + R^{\pm})}{\sigma s^{\pm} \mp \rho R^{\pm}} \right]$$

$$+ \text{Sgn}(s^{\pm}) \frac{1}{2} t^2 \log \frac{R^{\pm} + |s^{\pm}|}{t}$$

where

$$\text{Sgn}(x) \equiv \begin{cases} 1 & x \geq 0 \\ -1 & x < 0 \end{cases}$$

APPENDIX II  
SURFACE DISPLACEMENT DUE TO AXISYMMETRIC ELLIPSOIDAL  
PRESSURE DISTRIBUTION

Equation 2.12 with Equation 2.10 gives the surface displacement  $u_o(\bar{\rho})$  of a layered halfspace due to an arbitrary axisymmetric pressure distribution  $p(\bar{\rho})$  where  $\bar{\rho} = r/h$  is a dimensionless radial coordinate. Let the pressure be distributed over a region of radius  $a$  and define the dimensionless radial coordinate  $\lambda = r/a$ . Written in terms of  $\lambda$ , Equations 2.12 and 2.10 appear as:

$$u_o(\lambda) = \frac{2h(1-\nu_1^2)}{E_1} \int_0^\infty [g_2(\omega) - g_4(\omega)] P(\omega) J_0(\alpha\lambda\omega) d\omega$$

$$P(\omega) = \alpha^2 \int_0^\infty \lambda p(\lambda) J_0(\alpha\lambda\omega) d\lambda$$

Now consider the ellipsoidal pressure distribution:

$$p(\lambda) = \begin{cases} p^o \sqrt{1-\lambda^2} & \lambda \leq 1 \\ 0 & \lambda \geq 1 \end{cases}$$

for which  $P(\omega)$  can be shown to take the form:

$$P(\omega) = \alpha^2 p^o \frac{\sin\alpha\omega - \alpha\omega\cos\alpha\omega}{(\alpha\omega)^3}$$

permitting  $u_o(\lambda)$  to be determined from:

$$u_o(\lambda) = \frac{2ap^o(1-\nu_1^2)}{E_1} \alpha \int_0^\infty [g_2(\omega) - g_4(\omega)] J_0(\alpha\lambda\omega) (\sin\alpha\omega - \alpha\omega\cos\alpha\omega) \frac{d\omega}{(\alpha\omega)^3}$$

To write this expression in terms of the dimensionless pressure  $\phi$  defined in Equation 3.9, define the dimensionless displacement:

$$\tilde{u}_o = u_o \left( \frac{2R_x}{a^2} \right)$$

which is the scaling used implicitly in deriving Equation 3.10. With

$$\phi^o = \frac{2R_x(1-\nu_1^2)p^o}{\pi E_1 a}$$

from Equation 3.9,  $u_o(\lambda)$  can be written as:

$$u_o(\lambda) = 2\pi\phi^o\alpha \int_0^\infty [g_2(\omega) - g_4(\omega)] J_o(\alpha\lambda\omega) (\sin\alpha\omega - \alpha\omega\cos\alpha\omega) \frac{d\omega}{(\alpha\omega)^3}$$

By limiting this expression to  $\lambda \leq 1$ , the result

$$\alpha \int_0^\infty J_o(\alpha\lambda\omega) (\sin\alpha\omega - \alpha\omega\cos\alpha\omega) \frac{d\omega}{(\alpha\omega)^3} = \frac{\pi}{8} (2 - \lambda^2), \quad \lambda \leq 1$$

may be used to obtain

$$u_o(\lambda) = \frac{\pi^2\phi^o}{4} \left[ \frac{8\alpha}{\pi} \int_0^\infty [g_2(\omega) - g_4(\omega) - 1] J_o(\alpha\lambda\omega) (\sin\alpha\omega - \alpha\omega\cos\alpha\omega) \frac{d\omega}{(\alpha\omega)^3} + 2 - \lambda^2 \right], \lambda \leq 1 \quad (II.1)$$

As discussed in Section 2.2., the improper integral in this expression may be given a finite upper limit  $\omega_o$  for numerical evaluation with

an associated error of order  $\omega_o^2 e^{-2\omega_o}$ .

### APPENDIX III

#### DESCRIPTION OF COMPUTER PROGRAM "HIJPRG"

This program computes and writes into a direct access file the arrays of integral functions  $H_1$ ,  $I_1$ ,  $J_1$ ,  $H_1^*$ ,  $I_1^*$ , and  $J_1^*$  according to the analysis given in Section 4.2.2. The program uses the CDC checkpoint/restart facility to permit the execution of longer runs in a series of job steps. The parameter TCHECK, defined in statement No. 10 of HIJPRG, sets the maximum number of central processor seconds for a single job step. In this version, TCHECK = 480. The system clock reading is compared with TCHECK at various points throughout HIJPRG. If TCHECK is exceeded, a checkpoint dump is taken and execution stops. Execution continues from that point when the restart job is submitted. The user should consult the CDC FORTRAN and NOS Operating System Manuals for specific instructions on direct access file handling and the checkpoint/restart facility.

#### Input Description

Punched card input is submitted as follows:

Card 1            FØRMAT (I10)

ICASE =            Integer identification number for direct access  
file containing output data. For ICASE = 0, output  
is not written on file.

Card 2            FØRMAT (5F10.2)

PØIS1 =  $v_1$

PØIS2 =  $v_2$

E1E2 =  $E_1/E_2$

Card 3            FØRMAT (2F10.2, I10)

AH    =  $\alpha = a/h$

RHØ   =  $\rho = a/b$

NDIV =  $n - 1$       (NDIV cannot exceed 10 in present versions of  
HIJPRG and PSØLV)

Output Description

Printer output is given for the computed arrays of integral functions:

$$XH(I,J) = H_1[(I-1)\Delta\xi, (J-1)\Delta\eta]$$

$$XI(I,J) = I_1[(I-1)\Delta\xi, (J-1)\Delta\eta]$$

$$XJ(I,J) = J_1[(I-1)\Delta\xi, (J-1)\Delta\eta]$$

$$I=1, \dots, 2(\text{NDIV}) + 1$$

$$J=1, \dots, 2(\text{NDIV}) + 1$$

$$XHM(I,J) = H_1^*[(I-1)\Delta\xi, (J-1)\Delta\eta, -\rho]$$

$$XIM(I,J) = I_1^*[(I-1)\Delta\xi, (J-1)\Delta\eta, -\rho]$$

$$XJM(I,J) = J_1^*[(I-1)\Delta\xi, (J-1)\Delta\eta, -\rho]$$

$$I=1, \dots, 4(\text{NDIV}) + 1$$

$$J=1, \dots, 2(\text{NDIV}) + 1$$

$$XHP(I,J) = H_1^*[(I-1)\Delta\xi, (J-1)\Delta\eta, +\rho]$$

$$XIP(I,J) = I_1^*[(I-1)\Delta\xi, (J-1)\Delta\eta, +\rho]$$

$$XJP(I,J) = J_1^*[(I-1)\Delta\xi, (J-1)\Delta\eta, +\rho]$$

$$I=1, \dots, 2(\text{NDIV}) + 1$$

$$J=1, \dots, \text{NDIV} + 1$$

In the output listing for each array, "I" designates the number of a line or group of lines. The quantities appear sequentially in "J" in each line or group of lines.



#### APPENDIX IV

##### DESCRIPTION OF COMPUTER PROGRAM "PSOLV"

This program reads the direct access file created by HIJPRG that contains the arrays of  $H_1$ ,  $I_1$ ,  $J_1$ ,  $H_1^*$ ,  $I_1^*$ ,  $J_1^*$  and completes the computations described in Part 4. First, with read-in values of  $E_1/E_3$  and  $\nu_3$ , it computes the arrays of  $H$ ,  $I$ ,  $J$ ,  $H^*$ ,  $I^*$ , and  $J^*$  according to Equations 4.2.15 and 4.2.19 from the arrays of  $H_1$ ,  $I_1$ ,  $J_1$ ,  $H_1^*$ ,  $I_1^*$ , and  $J_1^*$  given by the file. Then, with a read-in contact zone boundary description, the computations contained in Equations 4.2.13, 4.2.6, 4.2.7, 4.2.5, and 4.7 and Table 4-1 are performed to generate the matrix of influence coefficients  $C_{I,J;i,j}$ . In the notation of Equation 4.14, the matrix inversion subroutine MATIN is used to compute the contact pressure distribution  $\phi_{i,j}$ , approach  $\Gamma$ , curvature ratio  $\epsilon$ , and, through Equation 4.17, load  $W$ . The quantities  $a_0/h$ ,  $a/a_0$ ,  $b/a_0$ ,  $d/d_0$ , and  $p/p^0$  are computed from Equations 3.28 through 3.32.

The user should consult the CDC NOS Operating System Manuals for specific instructions on handling the direct access file created by HIJPRG.

##### Input Description

Punched card input is submitted as follows:

Card 1                    FØRMAT (I10, 2F10.3)

JCASE =            Integer identification number for direct access  
file from HIJPRG. This must be the same as the  
value of ICASE specified in executing HIJPRG.

E1E3 =  $E_1/E_3$

PØIS3 =  $\nu_3$

Card 2                    FØRMAT (I10)

ITER =            Integer identification number used to identify  
particular selection of contact zone boundary.

Card 3            FØRMAT (16I5)

(NBDY(I), I=1, NDIV)

NBDY(I) =    Number of grid point along minor halfwidth at  
               which contact zone terminates for Ith division  
               along major halfwidth.

$$m(1) = NBDY(1)$$

$$m(I) = NBDY(I-1) \quad I=2, \dots, NDIV + 1$$

Restrictions:

$$NBDY(1) = NDIV + 1$$

$$NBDY(I) \leq NBDY(I-1) \quad , \quad I=2, \dots, NDIV$$
Card 4            FØRMAT (I10)

NPZERO =    Total number of grid points along boundary at  
               which zero pressure is to be prescribed (not  
               including points at ends of major and minor half-  
               widths where pressure is automatically set to  
               zero).

Card 5            FØRMAT (20I4)

(MZERO(I), I=1, NPZERO)

MZERO(I) =    Vertical grid line (position along major half-  
                   width) locating Ith zero pressure boundary point.

Card 6            FØRMAT (20I4)

(NZERO(I), I=1, NPZERO)

NZERO(I) =    Horizontal grid line (position along minor half-  
                   width) locating Ith zero pressure boundary point.

Output Description

Printer output is given for the following quantities:

$$XH(I,J) = H[(I-1)\Delta\xi, (J-1)\Delta\eta]$$

$$XI(I,J) = I[(I-1)\Delta\xi, (J-1)\Delta\eta]$$

$$XJ(I,J) = J[(I-1)\Delta\xi, (J-1)\Delta\eta]$$

$$I=1, \dots, 2(NDIV) + 1$$

$$J=1, \dots, 2(NDIV) + 1$$

$$XHM(I,J) = H*[(I-1)\Delta\xi, (J-1)\Delta\eta, -\rho]$$

$$XIM(I,J) = I*[(I-1)\Delta\xi, (J-1)\Delta\eta, -\rho]$$

$$XJM(I,J) = J*[(I-1)\Delta\xi, (J-1)\Delta\eta, -\rho]$$

$$I=1,\dots,4(NDIV) + 1$$

$$J=1,\dots,2(NDIV) + 1$$

$$XHP(I,J) = H*[(I-1)\Delta\xi, (J-1)\Delta\eta, +\rho]$$

$$XIP(I,J) = I*[(I-1)\Delta\xi, (J-1)\Delta\eta, +\rho]$$

$$XJP(I,J) = J*[(I-1)\Delta\xi, (J-1)\Delta\eta, +\rho]$$

$$I=1,\dots,2(NDIV) + 1$$

$$J=1,\dots,NDIV + 1$$

In the output listing for each array, "I" designates the number of a line or group of lines. The quantities appear sequentially in "J" in each line or group of lines.

Computed Contact Parameters:

$$RXRY = \epsilon$$

$$GAM = \Gamma$$

$$PHIO = \phi^0$$

$$WBAR = \bar{W}$$

$$ACHH = a_o/h$$

$$AACH = a/a_o$$

$$BACH = b/a_o$$

$$DDCH = d/d_o$$

$$POPOCH = p^0/p_o^0$$

Hertz solution for infinite layer thickness with same values of  $\rho$ ,  $E_1/E_3$ , and  $\nu_3$ :

$$\text{RXRYH} = \varepsilon$$

$$\text{GAMH} = \Gamma$$

$$\text{PHIOH} = \phi^0$$

$$\text{WBARH} = \bar{W}$$

Pressure Distribution:

$$\text{PHI}(\text{XI}(\text{M}), \text{ETA}(\text{N})) = \phi_{\text{M},\text{N}} \quad \begin{array}{l} \text{M}=1, \dots, n \\ \text{N}=1, \dots, m(\text{M}) \end{array}$$

Pressure Distribution for Hertz Solution:

$$\text{PHIH}(\text{XI}(\text{M}), \text{ETA}(\text{N})) = \phi_{\text{M},\text{N}} \quad \begin{array}{l} \text{M}=1, \dots, n \\ \text{N}=1, \dots, m(\text{M}) \end{array}$$

The pressure distributions are listed as two-dimensional arrays. The line number is designated by M and the values on each line are given sequentially in N.

APPENDIX V

LISTING OF COMPUTER PROGRAM "PSOLV"



```

1  PROGRAM PSOLV(INPUT,OUTPUT,FIL,TAPES=INPUT,TAPE6=OUTPUT,
2  1 TAPE7=FILE)
3  DIMENSION NRDY(10),NMAX(11),PHIHT7(121),CMAT(121,121),CVEC(121,2),
4  1 WC(121),NZERO(16),NZERO(16)
5  COMMON/BLKINF/AHDXI,AHDETA,RHOI,TUPI
6  COMMON/BLKCF/DXI,DETA,RHO
7  COMMON/BLKABG/XH(31,31),XI(31,31),XJ(31,31)
8  COMMON/BLKABGS/XHP(31,16),XIP(31,16),XJP(31,16),XHM(61,31),
9  1 XIM(61,31),XJM(61,31)
10 COMMON/BLKPRI/NH,NMU,NMV,NPU,NPV,AH,RHO2,NDIV
11 COMMON/BLKPPX/POIS1,POIS2,POIS3,POIS4,EIE2,EIE3,ICASE
12 COMMON/BLKWAT/CMAT,CVEC,TCHECK,NCK
13 COMMON/BLKT/SIG,SSQ
14 CALL SECOND(CPSEC)
15 WRITE(6,810)CPSEC
16 TCHECK=480.
17 NCK=0
18 READ(5,820)JCASE,EIE3,POIS3
19 NF=7
20 WRITE(6,3004)JCASE
21 READ(NF,3000)ICASE,NREC
22 IF(ICASE.NE.JCASE)GO TO 3
23 IF(NREC.NE.1)GO TO 4
24 READ(NF,3000)ICASE,NREC,EIE2,POIS1,POIS2
25 READ(NF,3001)ICASE,NREC,NDIV,AH,RHO
26 BETA=EIE3*(1.-POIS3**2)/(1.-POIS1**2)
27 CALL HTZCON(RHO,BETA,RXRYH,GAMH,PHI0H,WBARH)
28 DXI=1./FLOAT(NDIV)
29 DETA=DXI/RHO
30 AHDXI=AH*DXI
31 AHDETA=AH*DETA
32 RHO1=RHO
33 RH02=RHO
34 TUPI=8.*ATAN(1.)
35 NH=2*NDIV+1
36 NMU=4*NDIV+1
37 NMV=NH
38 NPU=NH
39 NPV=NDIV+1
40 READ(NF,3000)ICASE,NREC
41 DO 300 I=1,NH
42 DO 300 J=1,NH,6
43 JLAST=MIN0(J0+5,NH)
44 300 READ(NF,3000)ICASE,NREC,(XH(I,J),J=J0,JLAST)
45 READ(NF,3000)ICASE,NREC
46 DO 302 I=1,NH
47 DO 302 J=1,NH,6
48 JLAST=MIN0(J0+5,NH)
49 302 READ(NF,3000)ICASE,NREC,(XI(I,J),J=J0,JLAST)
50 READ(NF,3000)ICASE,NREC
51 DO 304 I=1,NH
52 DO 304 J=1,NH,6
53 JLAST=MIN0(J0+5,NH)
54 304 READ(NF,3000)ICASE,NREC,(XJ(I,J),J=J0,JLAST)
55 READ(NF,3000)ICASE,NREC
56 DO 306 I=1,NPU
57 DO 306 J0=1,NPV,6

```

```

60      JLAST=MIN0(J0*5,NPV)
306 READ (NF,3000) ICASE,NREC,(XHP(I,J),J=J0,JLAST)
      READ (NF,3000) ICASE,NREC
      DO 308 I=1,NPU
      DO 308 J0=1,NPV*6
      JLAST=MIN0(J0*5,NPV)
308 READ (NF,3000) ICASE,NREC,(XIP(I,J),J=J0,JLAST)
      READ (NF,3000) ICASE,NREC
      DO 310 I=1,NPU
      DO 310 J0=1,NPV*6
      JLAST=MIN0(J0*5,NPV)
310 READ (NF,3000) ICASE,NREC,(XJP(I,J),J=J0,JLAST)
      READ (NF,3000) ICASE,NREC
      DO 312 I=1,NMU
      DO 312 J0=1,NMV*6
      JLAST=MIN0(J0*5,NMV)
312 READ (NF,3000) ICASE,NREC,(XHM(I,J),J=J0,JLAST)
      READ (NF,3000) ICASE,NREC
      DO 314 I=1,NMU
      DO 314 J0=1,NMV*6
      JLAST=MIN0(J0*5,NMV)
314 READ (NF,3000) ICASE,NREC,(XIM(I,J),J=J0,JLAST)
      READ (NF,3000) ICASE,NREC
      DO 316 I=1,NMU
      DO 316 J0=1,NMV*6
      JLAST=MIN0(J0*5,NMV)
316 READ (NF,3000) ICASE,NREC,(XJM(I,J),J=J0,JLAST)
      AHSQ=AH*AH
      RETAI=BETA*1.
      SIG=SQRT(1.-RHO*RHO)
      SSQ=SIG*SIG
      T10=ALOG(SIG*RHO)
      T20=SIG-1.
      TAU3=ALOG((SIG*RHO)*(SIG+1.)/RHO)/SIG
      TAU4=(RHO-1.)*TAU3/SSQ
      TAU5=(1./RHO-1.)*RHO*TAU3/SSQ
      RNEG=-RHO
      DO 8 J=2,NH
      DO 8 I=2,NH
      CALL HIJ0(I,J,XH0,XI0,XJ0)
      XH(I,J)=XH(I,J)/AH*RETAI*XH0
      XI(I,J)=XI(I,J)/AHSQ*RETAI*XI0
      XJ(I,J)=XJ(I,J)/AHSQ*RETAI*XJ0
      A XJ(I,J)=XJ(I,J)/AHSQ*RETAI*XJ0
      DO 9 J=2,NHV
      V=DETA*FLOAT(J-1)
      CV1=RHO*V
      CV2=CV1*CV1/2.
      XHM(J,J)=XHM(J,J)/AH*RETAI*CV1*TAU3
      XIM(J,J)=XIM(J,J)/AHSQ*RETAI*CV2*TAU4
      XJM(J,J)=XJM(J,J)/AHSQ*RETAI*CV2*TAU5
      J1=J*1
      DO 9 I=1,NMU
      U=DXI*FLOAT(I-1)
      CALL T12345(U,V,RNEG,T1,T2,T3,T4,T5)
      USQ2=U*U/2.
      VSQ2=V*V/2.
      XHM0=U*T3*V*T1

```

```

115      XIM0=USQ2*T4+VSQ2*T2
      XJM0=USQ2*T5+VSQ2*T1
      XHM(I,J)=XHM(I,J)/AH*BETAL*XHM0
      XIM(I,J)=XIM(I,J)/AHSQ*BETAL*XIM0
9      XJM(I,J)=XJM(I,J)/AHSQ*BETAL*XJM0
      JDIV=NDIV+1
      DO 10 J=2,JDIV
      V=DETA*FLOAT(J-I)
      VSQ2=V*V/2.
      XHM(I,J)=XHM(I,J)/AH*BETAL*V*T10
      XIM(I,J)=XIM(I,J)/AHSQ*BETAL*VSQ2*T20
10      XJM(I,J)=XJM(I,J)/AHSQ*BETAL*VSQ2*T10
      NMV1=NMV-1
      DO 11 I=2,NMV1
      U=DXI*FLOAT(I-1)
      JLO=I+1
      JHI=MIN0(NMV,I+NDIV)
      DO 11 J=JLO,JHI
      V=DETA*FLOAT(J-I)
      CALL T12345(U,V,RHO,T1,T2,T3,T4,T5)
      USQ2=U*U/2.
      VSQ2=V*V/2.
      XHM0=U*T3+V*T1
      XIM0=USQ2*T4+VSQ2*T2
      XJM0=USQ2*T5+VSQ2*T1
      XHM(I,J)=XHM(I,J)/AH*BETAL*XHM0
      XIM(I,J)=XIM(I,J)/AHSQ*BETAL*XIM0
11      XJM(I,J)=XJM(I,J)/AHSQ*BETAL*XJM0
      DO 12 J=2,NPV
      XHP(I,J)=XHM(I,J)
      XIP(I,J)=XIM(I,J)
      XJP(I,J)=XJM(I,J)
      N=J-1
      V=DETA*FLOAT(N)
      ILAST=NPU-N
      DO 12 I=2,ILAST
      U=DXI*FLOAT(I-1)
      CALL T12345(U,V,RHO,T1,T2,T3,T4,T5)
      VSQ2=V*V/2.
      USQ2=U*U/2.
      XHP0=U*T3+V*T1
      XIP0=USQ2*T4+VSQ2*T2
      XJP0=USQ2*T5+VSQ2*T1
      XHP(I,J)=XHP(I,J)/AH*BETAL*XHP0
      XIP(I,J)=XIP(I,J)/AHSQ*BETAL*XIP0
12      XJP(I,J)=XJP(I,J)/AHSQ*BETAL*XJP0
      IPR=3
      CALL PRIOUT(IPR)
      READ(5,820)ITER
      READ(5,2050)(NBDY(I),I=1,NDIV)
      WRITE(6,2052)ICASE
      WRITE(6,3070)
      WRITE(6,3080)POIS1,POIS2,POIS3
      WRITE(6,3090)
      WRITE(6,3080)E1E2,E1F3
      WRITE(6,4000)
      WRITE(6,4010)AH,RHO,NDIV

```

PROGRAM PSOLV 74/74 OPT=i PAGE 4

FTN 4.6.452 78/02/13. 16.25.48

```

175      WRITE(6,2054)ITER
        WRITE(6,2060)
        WRITE(6,2070) (NBODY(I), I=1,NDIV)
        READ(5,820)NPZERO
        IF (NPZERO.EQ.0) GO TO 318
        READ(5,2051) (MZERO(I), I=1, NPZERO)
        READ(5,2051) (NZERO(I), I=1, NPZERO)
        WRITE(6,3040)
        WRITE(6,3050) (MZERO(I), I=1, NPZERO)
        WRITE(6,3060) (NZERO(I), I=1, NPZERO)
318      RHOSQ=PHO*RHO
        NMAX(I)=NBODY(I)
        NDIM=NDIV+1
        DO 19 I=2,NDIM
19      NMAX(I)=NBODY(I-1)
        IROW=0
        DO 20 M=1,NDIM
        NMAX1=NMAX(M)
        XISO=(DXI*FLOAT(M-I))*2
        DO 20 N=1,NMAX1
        IROW=IROW+1
        ETASQ=(DETA*FLOAT(N-1))*2
        CVEC(IROW,I)=-XISO
        ELLIPS=1.-XISO-RHOSQ*ETASQ
        PHINTZ(IROW)=0.
        IF (ELLIPS.GT.0.) PHINTZ(IROW)=PHIOH*SQRT(ELLIPS)
        VC(I)=1.
        CHAT(IROW,I)=CFI(M,N,I,1)
        DO 21 J=2,NDIV
        VC(J)=3.
21      CHAT(IROW,J)=CFI(M,N,I,J)*CF3(M,N,I,J)
        VC(NDIM)=2.
        CHAT(IROW,NDIM)=-1.
        JCOL=NDIM
        DO 22 I=2,NDIV
        JCOL=JCOL+1
        VC(JCOL)=3.
        CHAT(IROW,JCOL)=CFI(M,N,I,1)*CF2(M,N,I,1)
        NMAX=NMAX(I+1)
        NMAX1=NMAX(I)
        JLIM=NMAX1-1
        IF (JLIM.LT.2) GO TO 32
        DO 23 J=2,JLIM
        JCOL=JCOL+1
        VC(JCOL)=6.
23      CHAT(IROW,JCOL)=CFI(M,N,I,J)*CF2(M,N,I,J)*CF3(M,N,I,J)*
1      CF4(M,N,I,J)
32      JCOL=JCOL+1
        IF (NMAX1-NMAX) 24,24,25
24      CHAT(IROW,JCOL)=CF3(M,N,I,MAXL)*CF4(M,N,I,MAXL)
        VC(JCOL)=3.
        GO TO 22
25      CHAT(IROW,JCOL)=CF2(M,N,I,MAXR)*CF3(M,N,I,MAXR)*CF4(M,N,I,MAXR)
        VC(JCOL)=5.
        NMAX1=NMAX+1
        IF (NMAX1-NMAX) 27,27,26
26      NMAX1=NMAX-1

```

```

230      DO 29 J=MAXI,MAXI
          JCOL=JCOL+1
          WC(JCOL)=3.
235      28 CHAT(IROW,JCOL)=CF2(M,N,I,J)+CF4(M,N,I,J)
          27 JCOL=JCOL+1
          WC(JCOL)=1.
          CHAT(IROW,JCOL)=CF4(M,N,I,MAXI)
          22 CONTINUE
          JCOL=JCOL+1
          WC(JCOL)=2.
          CHAT(IROW,JCOL)=ETASQ
          JCOLB=JCOL
          MAX=NMAX(NDIM)
          IF (MAX-2) 30,30,29
          29 MAXI=MAX-1
          DO 31 J=2,MAXI
              JCOL=JCOL+1
              WC(JCOL)=3.
          31 CHAT(IROW,JCOL)=CF2(M,N,NDIM,J)+CF4(M,N,NDIM,J)
          30 JCOL=JCOL+1
              WC(JCOL)=1.
          CHAT(IROW,JCOL)=CF4(M,N,NDIM,MAX)
          20 CONTINUE
          NPTS=IROW
          IF (NPZERO.EQ.0) GO TO 46
          DO 48 IPT=1,NPZERO
              M0=MZERO(IPT)-1
              N0=NZERO(IPT)
              IROW=0
          50 DO 50 M=1,M0
              IROW=IROW+NMAX(M)
              IROW=IROW+N0
          52 DO 52 JCOL=1,NPTS
              CHAT(IROW,JCOL)=0.
              CHAT(IROW,IROW)=1.
          48 CVEC(IROW,1)=0.
          46 CALL MATIN(NPTS,1,DETERM,1D)
              GAM=CVFC(NDIM,1)
              RXRY=CVFC(JCOLR,1)
              CVEC(NDIM,1)=0.
              CVEC(JCOLB,1)=0.
              WBAR=0.
          34 DO 34 JCOL=1,NPTS
              WBAR=WBAR+WC(JCOL)*CVEC(JCOL,1)
              WBAR=WBAR+DAI*DETA*2./3.
              PHI0=CVFC(1,1)
              PI=4.*ATAN(1.)
              AACH=2./3.*PI*RETA1*WBAR**2./3.
              RACH=AACH/RHO
              DDCH=GAM/2.*AACH**2.
              POP0CH=PI*PI/4.*RETA1*AACH*PHI0
              ACHH=AH/AACH
              WRITE(6,20R0)
              WRITE(6,20R2)
              WRITE(6,20R0)RXRY,GAM,PHI0,WBAR
              WRITE(6,2072)
              WRITE(6,2074)
285

```



```

290      WRITE(6,2090)ACHH,AACH,BACH,DDCH,PDP0CH
        WRITE(6,2084)
        WRITE(6,2086)
        WRITE(6,2090)RXRYH,GAMH,PHIOH,WBARH
        WRITE(6,2100)
        WRITE(6,2101)
        JSTOP=0
        DO 42 I=1,NDIM
          JSTART=JSTOP+1
          JSTOP=JSTOP+NMAX(I)
          WRITE(6,1010) (CVEC(J,1),J=JSTART,JSTOP)
          WRITE(6,1020)
          WRITE(6,2110)
          WRITE(6,2111)
          JSTOP=0
          DO 44 I=1,NDIM
            JSTART=JSTOP+1
            JSTOP=JSTOP+NMAX(I)
            WRITE(6,1010) (PHINTZ(J),J=JSTART,JSTOP)
            WRITE(6,1020)
            CALL SECOND(CPSEC)
            WRITE(6,810)CPSEC
            STOP
            3 WRITE(6,3010)ICASE
            WRITE(6,3030)
            STOP
            4 WRITE(6,3020)NREC
            WRITE(6,3030)
            STOP
            810 FORMAT(1H0,7HCPSEC =,F10.2)
            820 FORMAT(1H0,2F10.3)
            1010 FORMAT(1H,11F11.6)
            1020 FORMAT(//)
            2050 FORMAT(16I5)
            2051 FORMAT(20I4)
            2052 FORMAT(1H1,/,9H CASE NO.,I6)
            2054 FORMAT(///,23H BOUNDARY ITERATION NO.,I6)
            2060 FORMAT(///,5X,7HNRDY(I))
            2070 FORMAT(1H,16I8)
            2072 FORMAT(///,44H PARAMETERS SCALED ON CIRCULAR HERTZ CONTACT)
            2074 FORMAT(1H0,11X,4HACHH,11X,4HACH,11X,4HBACH,11X,4HDDCH,9X,6HPDP0CH
            1)
            2080 FORMAT(///,28H COMPUTED CONTACT PARAMETERS)
            2082 FORMAT(1H0,11X,4HXRXY,12X,3HGAM,11X,4HPHIO,11X,4HWBAR)
            2084 FORMAT(///,51H CONTACT PARAMETERS FOR HERTZ PROBLEM WITH SAME RHO
            1)
            2086 FORMAT(1H0,10X,5HXRXYH,11X,4HGAMH,10X,5HPHIOH,10X,5HWBARH)
            2090 FORMAT(1H,5F15.5)
            2100 FORMAT(1H1,///,32H COMPUTED NORMALIZED PRESSURE I,
            1 4HPHI(XI(M), ETA(N)) M=ROW NO. XI=(M-1)/NDIV)
            2101 FORMAT(1H,51X,29HN=COL NO. ETA=(N-1)/NDIV/RHO,///)
            2110 FORMAT(1H1,///,42H NORMALIZED PRESSURES FOR HERTZ PROBLEM I,
            1 4HSPHIH(XI(M), FTA(N)) M=ROW NO. XI=(M-1)/NDIV)
            2111 FORMAT(1H,62X,29HN=COL NO. ETA=(N-1)/NDIV/RHO,///)
            3000 FORMAT(214,1P6E19.10)
            3001 FORMAT(314,2F12.8)
            3004 FORMAT(1H1,5X,RHCASE NO.,I5)

```

```

3010 FORMAT(///,5X,27HDATA FILE CONTAINS CASE NO.,I5)
3020 FORMAT(///,5X,30HDATA FILE BEGINS AT RECORD NO.,I5)
3030 FORMAT(//,5X,12HNO EXECUTION)
3040 FORMAT(//,1H0.43HCOORDINATES OF ZFROED BOUNDARY PRESSURES : ,
1 33HXI=(N-1)/NDIV, ETA=(N-1)/NDIV/RHO)
3050 FORMAT(2H0M,3X,30I4)
3060 FORMAT(2H N,3X,30I4)
3070 FORMAT(///,1H ,7X,5HP01S1,7X,5HP01S2,7X,5HP01S3)
3080 FORMAT(1H ,3F12.2)
3090 FORMAT(///,1H ,8X,4HE1E2,8X,4HE1E3)
4000 FORMAT(///,1H ,10X,2HAM,9X,3HRHO,8X,4HNDIV)
4010 FORMAT(1H ,2F12.2,1I2)
      END

```

345

350

355

PAGE 1

78/02/13. 16.25.48

FTN 4.6452

74/74 OPT=1

SURROUTINE HTZCON

```

1  SURROUTINE HTZCON(RHO,RETA,RXRY,GAM,PHI0,WBAR)
    PI=4.*ATAN(1.)
    RHOSQ=RHO*RHO
    X=1.-1./RHOSQ
    XKF=CELINT1(X)
    XEF=CELINT2(X)
    IF (RHO.EQ.1.)GO TO 1
    RXRY=(RHOSQ*XEF-XKF)/(XKF-XEF)
    GO TO 2
    1 RXRY=1.
    2 GAM=(1.-RXRY)*XKF/XEF/RHOSQ
    PHI0=(1.-RXRY)/(1.-RETA)/XEF/RHO/PI
    WBAR=PHI0*2./3./RHO*PI
    RETURN
    END

```

10

15

PAGE 1

78/02/13. 16.25.48

FTN 4.6.452

FUNCTION CELINTI 74/74 OPT=1

```
1  FUNCTION CELINTI(X)
    IF (X.EQ.1.) GO TO 1
    XI=1.-X
    PA=1.38629436112*X1*(.0966344259*X1*(.03590092383*X1*
5  1 (.03742563713*X1*.01451196212)))
    PB=.5*X1*(.12498593597*X1*(.06880748576*X1*(.03328355346*X1*
    1 .00441787012)))
    CELINTI=PA-PB*ALOG(X1)
    RETURN
10  CELINTI=1.E40
    RETURN
    END
```

PAGE 1

78/02/13. 16.25.48

FTN 4.6.452

FUNCTION CELINT2 74/74 OPT=1

```

1  FUNCTION CELINT2(X)
   IF(X.EQ.1.160 TO 1
   X1=1.-X
   PA=1.-X1*(.44325141463+X1*(.06260601220+X1*(.04757303546+X1*
5  .01736506451)))
   PB=X1*(.24998368310+X1*(.09200180037+X1*(.04069697526+X1*
1  .00526449639)))
   CELINT2=PA-PB*ALOG(X1)
   RETURN
10  CELINT2=1.
   RETURN
   END

```



```

1      SUBROUTINE MATIN (N1,M1,DETERM,ID)
2      MATRIX INVERSION WITH ACCOMPANYING SOLUTION OF LINEAR EQUATIONS
3      NOVEMBER 1992 S GOOD DAVID TAYLOR MODEL BASIN AM MATI
4      COMMON/BLKMAT/A,R,TCHECK,NCK
5
6      C
7      C
8      C
9      C
10     C
11     C
12     C
13     C
14     C
15     C
16     C
17     C
18     C
19     C
20     C
21     C
22     C
23     C
24     C
25     C
26     C
27     C
28     C
29     C
30     C
31     C
32     C
33     C
34     C
35     C
36     C
37     C
38     C
39     C
40     C
41     C
42     C
43     C
44     C
45     C
46     C
47     C
48     C
49     C
50     C
51     C
52     C
53     C
54     C
55     C
56     C
57     C
58     C
59     C
60     C
61     C
62     C
63     C
64     C
65     C
66     C
67     C
68     C
69     C
70     C
71     C
72     C
73     C
74     C
75     C
76     C
77     C
78     C
79     C
80     C
81     C
82     C
83     C
84     C
85     C
86     C
87     C
88     C
89     C
90     C
91     C
92     C
93     C
94     C
95     C
96     C
97     C
98     C
99     C
100    C
101    C
102    C
103    C
104    C
105    C
106    C
107    C
108    C
109    C
110    C
111    C
112    C
113    C
114    C
115    C
116    C
117    C
118    C
119    C
120    C
121    C
122    C
123    C
124    C
125    C
126    C
127    C
128    C
129    C
130    C
131    C
132    C
133    C
134    C
135    C
136    C
137    C
138    C
139    C
140    C
141    C
142    C
143    C
144    C
145    C
146    C
147    C
148    C
149    C
150    C
151    C
152    C
153    C
154    C
155    C
156    C
157    C
158    C
159    C
160    C
161    C
162    C
163    C
164    C
165    C
166    C
167    C
168    C
169    C
170    C
171    C
172    C
173    C
174    C
175    C
176    C
177    C
178    C
179    C
180    C
181    C
182    C
183    C
184    C
185    C
186    C
187    C
188    C
189    C
190    C
191    C
192    C
193    C
194    C
195    C
196    C
197    C
198    C
199    C
200    C
201    C
202    C
203    C
204    C
205    C
206    C
207    C
208    C
209    C
210    C
211    C
212    C
213    C
214    C
215    C
216    C
217    C
218    C
219    C
220    C
221    C
222    C
223    C
224    C
225    C
226    C
227    C
228    C
229    C
230    C
231    C
232    C
233    C
234    C
235    C
236    C
237    C
238    C
239    C
240    C
241    C
242    C
243    C
244    C
245    C
246    C
247    C
248    C
249    C
250    C
251    C
252    C
253    C
254    C
255    C
256    C
257    C
258    C
259    C
260    C
261    C
262    C
263    C
264    C
265    C
266    C
267    C
268    C
269    C
270    C
271    C
272    C
273    C
274    C
275    C
276    C
277    C
278    C
279    C
280    C
281    C
282    C
283    C
284    C
285    C
286    C
287    C
288    C
289    C
290    C
291    C
292    C
293    C
294    C
295    C
296    C
297    C
298    C
299    C
300    C
301    C
302    C
303    C
304    C
305    C
306    C
307    C
308    C
309    C
310    C
311    C
312    C
313    C
314    C
315    C
316    C
317    C
318    C
319    C
320    C
321    C
322    C
323    C
324    C
325    C
326    C
327    C
328    C
329    C
330    C
331    C
332    C
333    C
334    C
335    C
336    C
337    C
338    C
339    C
340    C
341    C
342    C
343    C
344    C
345    C
346    C
347    C
348    C
349    C
350    C
351    C
352    C
353    C
354    C
355    C
356    C
357    C
358    C
359    C
360    C
361    C
362    C
363    C
364    C
365    C
366    C
367    C
368    C
369    C
370    C
371    C
372    C
373    C
374    C
375    C
376    C
377    C
378    C
379    C
380    C
381    C
382    C
383    C
384    C
385    C
386    C
387    C
388    C
389    C
390    C
391    C
392    C
393    C
394    C
395    C
396    C
397    C
398    C
399    C
400    C
401    C
402    C
403    C
404    C
405    C
406    C
407    C
408    C
409    C
410    C
411    C
412    C
413    C
414    C
415    C
416    C
417    C
418    C
419    C
420    C
421    C
422    C
423    C
424    C
425    C
426    C
427    C
428    C
429    C
430    C
431    C
432    C
433    C
434    C
435    C
436    C
437    C
438    C
439    C
440    C
441    C
442    C
443    C
444    C
445    C
446    C
447    C
448    C
449    C
450    C
451    C
452    C
453    C
454    C
455    C
456    C
457    C
458    C
459    C
460    C
461    C
462    C
463    C
464    C
465    C
466    C
467    C
468    C
469    C
470    C
471    C
472    C
473    C
474    C
475    C
476    C
477    C
478    C
479    C
480    C
481    C
482    C
483    C
484    C
485    C
486    C
487    C
488    C
489    C
490    C
491    C
492    C
493    C
494    C
495    C
496    C
497    C
498    C
499    C
500    C
501    C
502    C
503    C
504    C
505    C
506    C
507    C
508    C
509    C
510    C
511    C
512    C
513    C
514    C
515    C
516    C
517    C
518    C
519    C
520    C
521    C
522    C
523    C
524    C
525    C
526    C
527    C
528    C
529    C
530    C
531    C
532    C
533    C
534    C
535    C
536    C
537    C
538    C
539    C
540    C
541    C
542    C
543    C
544    C
545    C
546    C
547    C
548    C
549    C
550    C
551    C
552    C
553    C
554    C
555    C
556    C
557    C
558    C
559    C
560    C
561    C
562    C
563    C
564    C
565    C
566    C
567    C
568    C
569    C
570    C
571    C
572    C
573    C
574    C
575    C
576    C
577    C
578    C
579    C
580    C
581    C
582    C
583    C
584    C
585    C
586    C
587    C
588    C
589    C
590    C
591    C
592    C
593    C
594    C
595    C
596    C
597    C
598    C
599    C
600    C
601    C
602    C
603    C
604    C
605    C
606    C
607    C
608    C
609    C
610    C
611    C
612    C
613    C
614    C
615    C
616    C
617    C
618    C
619    C
620    C
621    C
622    C
623    C
624    C
625    C
626    C
627    C
628    C
629    C
630    C
631    C
632    C
633    C
634    C
635    C
636    C
637    C
638    C
639    C
640    C
641    C
642    C
643    C
644    C
645    C
646    C
647    C
648    C
649    C
650    C
651    C
652    C
653    C
654    C
655    C
656    C
657    C
658    C
659    C
660    C
661    C
662    C
663    C
664    C
665    C
666    C
667    C
668    C
669    C
670    C
671    C
672    C
673    C
674    C
675    C
676    C
677    C
678    C
679    C
680    C
681    C
682    C
683    C
684    C
685    C
686    C
687    C
688    C
689    C
690    C
691    C
692    C
693    C
694    C
695    C
696    C
697    C
698    C
699    C
700    C
701    C
702    C
703    C
704    C
705    C
706    C
707    C
708    C
709    C
710    C
711    C
712    C
713    C
714    C
715    C
716    C
717    C
718    C
719    C
720    C
721    C
722    C
723    C
724    C
725    C
726    C
727    C
728    C
729    C
730    C
731    C
732    C
733    C
734    C
735    C
736    C
737    C
738    C
739    C
740    C
741    C
742    C
743    C
744    C
745    C
746    C
747    C
748    C
749    C
750    C
751    C
752    C
753    C
754    C
755    C
756    C
757    C
758    C
759    C
760    C
761    C
762    C
763    C
764    C
765    C
766    C
767    C
768    C
769    C
770    C
771    C
772    C
773    C
774    C
775    C
776    C
777    C
778    C
779    C
780    C
781    C
782    C
783    C
784    C
785    C
786    C
787    C
788    C
789    C
790    C
791    C
792    C
793    C
794    C
795    C
796    C
797    C
798    C
799    C
800    C
801    C
802    C
803    C
804    C
805    C
806    C
807    C
808    C
809    C
810    C
811    C
812    C
813    C
814    C
815    C
816    C
817    C
818    C
819    C
820    C
821    C
822    C
823    C
824    C
825    C
826    C
827    C
828    C
829    C
830    C
831    C
832    C
833    C
834    C
835    C
836    C
837    C
838    C
839    C
840    C
841    C
842    C
843    C
844    C
845    C
846    C
847    C
848    C
849    C
850    C
851    C
852    C
853    C
854    C
855    C
856    C
857    C
858    C
859    C
860    C
861    C
862    C
863    C
864    C
865    C
866    C
867    C
868    C
869    C
870    C
871    C
872    C
873    C
874    C
875    C
876    C
877    C
878    C
879    C
880    C
881    C
882    C
883    C
884    C
885    C
886    C
887    C
888    C
889    C
890    C
891    C
892    C
893    C
894    C
895    C
896    C
897    C
898    C
899    C
900    C
901    C
902    C
903    C
904    C
905    C
906    C
907    C
908    C
909    C
910    C
911    C
912    C
913    C
914    C
915    C
916    C
917    C
918    C
919    C
920    C
921    C
922    C
923    C
924    C
925    C
926    C
927    C
928    C
929    C
930    C
931    C
932    C
933    C
934    C
935    C
936    C
937    C
938    C
939    C
940    C
941    C
942    C
943    C
944    C
945    C
946    C
947    C
948    C
949    C
950    C
951    C
952    C
953    C
954    C
955    C
956    C
957    C
958    C
959    C
960    C
961    C
962    C
963    C
964    C
965    C
966    C
967    C
968    C
969    C
970    C
971    C
972    C
973    C
974    C
975    C
976    C
977    C
978    C
979    C
980    C
981    C
982    C
983    C
984    C
985    C
986    C
987    C
988    C
989    C
990    C
991    C
992    C
993    C
994    C
995    C
996    C
997    C
998    C
999    C
1000   C

```

```

60      430 DO 450 L=1,N
        450 A(I,I)=A(I,I,L)-A(JCOLUM,L)*T
        455 IF(M) 550, 550, 460
        460 DO 500 L=1,M
        500 R(I,L)=R(I,L)-R(JCOLUM,L)*T
        550 CONTINUE
        600 DO 710 I=1,N
        610 L=N+1-I
        620 IF (INDEX(I,1)-INDEX(L,2)) 630, 710, 630
        630 JROW=INDEX(L,1)
        640 JCOLUM=INDEX(L,2)
        650 DO 705 K=1,N
        660 SWAP=A(K,JROW)
        670 A(K,JROW)=A(K,JCOLUM)
        700 A(K,JCOLUM)=SWAP
        705 CONTINUE
        710 CONTINUE
        DO 730 K = 1,N
        720 IF (INDEX(K,3) -1) 715,720,715
        720 CONTINUE
        730 CONTINUE
        ID =1
        740 RETURN
        715 ID =2
        GO TO 740
        END

75      MAT10069
        MAT10070
        MAT10071
        MAT10072
        MAT10073
        MAT10074
        MAT10078
        MAT10079
        MAT10080
        MAT10081
        MAT10082
        MAT10083
        MAT10084
        MAT10085
        MAT10086
        MAT10087
        MAT10088
        MAT10089
        MAT10090
        MAT10093
        MAT10094
        MAT10095
        MAT10096
        MAT10091
        MAT10092
        MAT10098

```

```

1  SURROUTINE PRIOUT(IPRINT)
COMMON/BLKARG/XH(31,31),XI(31,31),XJ(31,31)
COMMON/BLKARG/XHP(31,16),XIP(31,16),XJP(31,16),XHM(61,31),
5  XIM(61,31),XJM(61,31)
COMMON/RLKPRI/NH,NHU,NMV,NPU,NPV,AH,RHO,NDIV
COMMON/RLKPX/POIS1,POIS2,POIS3,ELE2,ELE3,ICASE
WRITE(6,1030)
WRITE(6,1040)ICASE
WRITE(6,2000)
10 WRITE(6,2010)POIS1,POIS2,POIS3
WRITE(6,2020)
WRITE(6,2010)ELE2,ELE3
WRITE(6,2030)
WRITE(6,2040)AH,RHO,NDIV
WRITE(6,1001)
DO 100 I=1,NH
15 WRITE(6,1010)(XH(I,J),J=1,NH)
DO 100 I=1,NH
WRITE(6,1020)
DO 102 I=1,NH
20 WRITE(6,1010)(XI(I,J),J=1,NH)
WRITE(6,1002)
DO 104 I=1,NH
25 WRITE(6,1020)
DO 104 I=1,NH
WRITE(6,1003)
DO 112 I=1,NHU
30 WRITE(6,1010)(XHM(I,J),J=1,NHV)
WRITE(6,1020)
DO 114 I=1,NMU
35 WRITE(6,1008)
DO 114 I=1,NMU
WRITE(6,1010)(XIM(I,J),J=1,NMV)
WRITE(6,1020)
DO 116 I=1,NMU
40 WRITE(6,1010)(XJM(I,J),J=1,NPV)
WRITE(6,1020)
IF(IPRINT,F0.2)GO TO 10
WRITE(6,1004)
DO 106 I=1,NPU
45 WRITE(6,1010)(XHP(I,J),J=1,NPV)
WRITE(6,1020)
DO 108 I=1,NPU
WRITE(6,1005)
DO 108 I=1,NPU
50 WRITE(6,1010)(XIP(I,J),J=1,NPV)
WRITE(6,1020)
DO 110 I=1,NPU
WRITE(6,1006)
DO 110 I=1,NPU
WRITE(6,1010)(XJP(I,J),J=1,NPV)
WRITE(6,1020)
10 CALL SECOND(CPSEC)
WRITE(6,810)CPSEC
RETURN
810 FORMAT(1H0,7HCPSEC =,F10.2)
920 FORMAT(1H1,////,5X,RHCASE NO.,16)
55

```

PAGE 2

78/02/13. 16.25.48

FTN 4.6.452

SURROUTINE PRINT 74/74 OPT=1

```

1001 FORMAT(1H) , ///, 5X, 7HXH(I,J) , ///
1002 FORMAT(1H) , ///, 5X, 7HXI(I,J) , ///
1003 FORMAT(1H) , ///, 5X, 7HXJ(I,J) , ///
1004 FORMAT(1H) , ///, 5X, 8HXHP(I,J) , ///
1005 FORMAT(1H) , ///, 5X, 8HXIP(I,J) , ///
1006 FORMAT(1H) , ///, 5X, 8HXJP(I,J) , ///
1007 FORMAT(1H) , ///, 5X, 8HXHM(I,J) , ///
1008 FORMAT(1H) , ///, 5X, 8HXIM(I,J) , ///
1009 FORMAT(1H) , ///, 5X, 8HXJM(I,J) , ///
1010 FORMAT(1H , 10F12.7)
1020 FORMAT(/)
1030 FORMAT(1H) , ///, 29H COMPLETE INFLUENCE FUNCTIONS)
1040 FORMAT(///, 5X, AHCASE NO., I6)
2000 FORMAT(//, 1H , 7X, 5HPOTS1, 7X, 5HPOTS2, 7X, 5HPOTS3)
2010 FORMAT(1H , 3F12.2)
2020 FORMAT(//, 1H , 4X, 4HF1F2, 4X, 4HE1E3)
2030 FORMAT(//, 1H , 10X, 2HAH, 9X, 3HRHO, 4X, 4HNDIV)
2040 FORMAT(1H , 2F12.2, 112)
      END

```

PAGE 1

78/02/13. 16.25.48

FTN 4.6+452

74/74 OPT=1

FUNCTION CFI

```

1:  FUNCTION CFI(M,N,I,J)
      COMMON/BLKCF/DXI,DETA,RHO
      XI=DXI*FLOAT(I)
      ETA=DETA*FLOAT(J-1)
      CALL ARGIM(N,I,J,AA,RR,GG)
      CALL ARGSTAR(M,N,I,J,ASTAR,BSTAR,GSTAR)
      ALPHL=(AA*ASTAR)/DXI
      RETL=(RR*BSTAR)/DXI
      GAML=(GG*GSTAR)/DXI
      CFI=XI*ALPHL-RETL*RHO*(ETA*ALPHL-GAML)
      RETURN
      END

```

5

10



PAGE 1

78/02/13. 16.25.48

FTN 4.6.452

74/74 OPT=1

FUNCTION CF2

```

1  FUNCTION CF2(M,N,I,J)
COMMON/BLKCF/DXI,DETA,PHO
XI=DXI*FLOAT(I-2)
DETA=DETA*FLOAT(IJ)
5  CALL ARG(M,N,I-1,J,AAL,RRL,XXX)
CALL ARGSTAR(M,N,I-1,J,ASTAR,RSTAR,GSTAR)
CALL ARG(M,N,I,J,AAU,XXX,GGU)
ALPHL=(AAL*ASTAR)/DXI
RETL=(RRL*ASTAR)/DXI
10  ALPHU=-(AAU*ASTAR)/DXI
GAMU=-(GGU*GSTAR)/DXI
CF2=-XI*ALPHL*RETL*RH0*(DETA*ALPHU-GAMU)
RETURN
END

```

PAGE 1

78/02/13. 16.25.48

FTN 4.6\*452

FUNCTION CF3 74/74 OPT=1

```

1  FUNCTION CF3(M,N,I,J)
COMMON/BLKCF/DXI,DETA,RHO
XI=DXI*FLOAT(I)
5  ETA=DETA*FLOAT(J-2)
CALL ARG(M,N,I,J-1,AAL,XXX,GGL)
CALL ARGSTAR(M,N,I,J-1,ASTAR,BSTAR,GSTAR)
CALL ARG(M,N,I,J-1,AAU,RRU,XXX)
ALPHU=- (AAU*ASTAR)/DXI
10  RETU=- (RRU*BSTAR)/DXI
ALPHL= (AAL*ASTAR)/DXI
GAML= (GGL*GSTAR)/DXI
CF3=XI*ALPHU-BETU-RHO*(ETA*ALPHL-GAML)
RETURN
END

```

PAGE 1

78/02/13. 16.25.48

FTN 4.6.452

74/74 OPT=1

FUNCTION CF4

```

1  FUNCTION CF4(M,N,I,J)
COMMON/RLKCF/DXI,DETA,RHO
XI=DXI*FLOAT(I-2)
5  ETA=DETA*FLOAT(J-1)
CALL ARG(M,N,I,J-1,AA,RR,GG)
CALL ARGSTAR(M,N,I-1,J-1,ASTAR,RSTAR,GSTAR)
ALPHU=- (AA*ASTAR)/DXI
RETI=- (RR*RSTAR)/DXI
10 GAMU=- (GG*GSTAR)/DXI
CF4=-XI*ALPHU+RETI-RHO*(ETA*ALPHU-GAMU)
RETURN
END

```

PAGE 1

78/02/13. 16.25.48

FTN 4.6.452

74/74 OPT=1

SURROUTINE ARG

```

1  SURROUTINE ARG(M,N,I,J,AA,RR,GG)
COMMON/RLKCF/DXI,DETA,RHO
COMMON/RLKARG/XH(31,31),XI(31,31),XJ(31,31)
DIMENSION IGX(R),IGY(R),ZJ(R),ZJ(8)
MMI=M-I
MPI=M+I
NMJ=N-J
NPJ=N+J
IGX(1)=MMI
IGX(2)=MMI
IGX(3)=MPI-2
IGX(4)=MPI-2
IGX(5)=MMI
IGX(6)=MMI
IGX(7)=MPI-2
IGX(8)=MPI-2
IGY(1)=NMJ-1
IGY(2)=NMJ
IGY(3)=NMJ-1
IGY(4)=NMJ
IGY(5)=NPJ-1
IGY(6)=NPJ-2
IGY(7)=NPJ-1
IGY(8)=NPJ-2
DO 1 K=1,8
NX=IGX(K)
NY=IGY(K)
ISGX=ISIGN(1,NX)
ISGY=ISIGN(1,NY)
NXA=NX*ISGX
NYA=NY*ISGY
NXI=NXA+1
NYI=NYA+1
ZH(K)=XH(NXI,NYI)*ISGX*ISGY
ZI(K)=XI(NXI,NYI)*ISGY
1  ZJ(K)=XJ(NXI,NYI)*ISGX
H1=ZH(1)
H2=ZH(2)
H3=ZH(3)
H4=ZH(4)
H5=ZH(5)
H6=ZH(6)
H7=ZH(7)
H8=ZH(8)
AA=-H1+H2+H3+H4+H5+H6+H7+H8
XIMH=DXI*FLOAT(M-1)*(-H1+H2+H3+H4+H5+H6+H7+H8)
ETNH=DETA*FLOAT(N-1)*(-H1+H2+H3+H4+H5+H6+H7+H8)
RR=XIMH+ZI(1)-ZI(2)+ZI(3)-ZI(4)+ZI(5)+ZI(6)-ZI(7)+ZI(8)
GG=ETNH+ZJ(1)-ZJ(2)+ZJ(3)+ZJ(4)+ZJ(5)-ZJ(6)+ZJ(7)+ZJ(8)
RETURN
END

```

PAGE 1

78/02/13. 16.25.48

FTN 4.6.452

SURROUTINE ARGSTAR 74/74 OPT=1

```

1  SURROUTINE ARGSTAR(M,N,I,J,ASTAR,RSTAR,GSTAR)
   COMMON/RLKCF/DXI,DETA,RHO
   COMMON/RLKABGS/XHP(31,16),XIP(31,16),XJP(31,16),XHM(61,31),
5  XIM(61,31),XJM(61,31)
   DIMENSION IGK0(8),IGMU(8),IGY(8),ZIS(8),ZJS(8),ZHS(8)
   MMJ=M-I
   MPI=M+I
   NMJ=N-J
   NPJ=N+J
10  IGK0(1)=MMJ+NMJ-1
   IGK0(2)=MMJ+NMJ-1
   IGK0(3)=MPI+NMJ-1
   IGK0(4)=MPI+NMJ-1
   IGK0(5)=MMJ+NPJ-1
   IGK0(6)=MMJ+NPJ-1
   IGK0(7)=MPI+NPJ-1
   IGK0(8)=MPI+NPJ-1
   IGMU(1)=-1
   IGMU(2)=-1
   IGMU(3)=1
   IGMU(4)=1
   IGMU(5)=1
   IGMU(6)=1
   IGMU(7)=-1
   IGMU(8)=-1
   IGY(1)=NMJ-1
   IGY(2)=NMJ-1
   IGY(3)=NMJ-1
   IGY(4)=NMJ-1
   IGY(5)=NPJ-1
   IGY(6)=NPJ-2
   IGY(7)=NPJ-1
   IGY(8)=NPJ-2
   DO 1 K=1,8
   KO=IGK0(K)
   NY=IGY(K)
   ISGK0=ISIGN(1,KO)
   IF (KO.EQ.0) ISGK0=1
   ISGY=ISIGN(1,NY)
   KOA=KO*ISGK0
   NYA=NY*ISGY
   MU=IGMU(K)*ISGK0*ISGY
   KOI=KOA+1
   NYI=NYA+1
   IF (MU)/2,2,3
2  ZHS(K)=XHM(KOI,NYI)*ISGK0*ISGY
   ZIS(K)=XIM(KOI,NYI)*ISGY
   ZJS(K)=XJM(KOI,NYI)*ISGK0
   GO TO 1
3  ZHS(K)=XHP(KOI,NYI)*ISGK0*ISGY
   ZIS(K)=XIP(KOI,NYI)*ISGY
   ZJS(K)=XJP(KOI,NYI)*ISGK0
1  CONTINUE
   HSI=ZHS(1)
   HSP=ZHS(2)
   HSI=ZHS(3)
   HSI=ZHS(4)
55

```



MS5=ZHS(5)  
 MS6=ZHS(6)  
 MS7=ZHS(7)  
 MS8=ZHS(8)

ASTAR=MS1-MS2-MS3-MS4-MS5-MS6-MS7-MS8

XIMHS=DXI\*FLOAT(M-1)\*(MS1-MS2-MS3-MS4-MS5-MS6-MS7-MS8)

FTNHS=DETA\*FLOAT(N-1)\*(MS1-MS2-MS3-MS4-MS5-MS6-MS7-MS8)

RSTAR=XIMHS-715(1)\*715(2)-715(3)\*715(4)+715(5)-715(6)+715(7)-

1 715(8)

GSTAR=FTNHS-715(1)\*715(2)+715(3)-715(4)-715(5)+715(6)+715(7)-

1 715(8)

RETURN

END

60

65

70

PAGE 1

78/02/13. 16.25.48

FTN 4.6.452

74/74 OPT=1

SUBROUTINE HIJ0

```

1      SUBROUTINE HIJ0(I,J,XH0,XI0,XJ0)
COMMON/HLKCF/DXI,DETA,XXX
5      U=DXI*FLOAT(I-1)
      V=DETA*FLOAT(J-1)
      USQ=U*U
      VSQ=V*V
      R=SQRT(USQ+VSQ)
      XLOG1=ALOG((R+V)/U)
      XLOG2=ALOG((R+U)/V)
      XH0=U*XLOG1+V*XLOG2
      XI0=USQ/2.*XLOG1+V/2.*(R-V)
      XJ0=U/2.*(R-U)+VSQ/2.*XLOG2
      RETURN
      END

```

1

5

10

SUBROUTINE T12345 74/74 OPT=1

```

1  SUBROUTINE T12345(U,V,XMU,T1,T2,T3,T4,T5)
COMMON/BLKT/SIG,SSQ
UV=U+XMU*V
R0=SQRT(UV*UV*V)
T1=ALOG((R0+ABS(UV))/V)
T2=(R0-V)/V
TOP=(SIG-XMU)*(SIG*V+R0)
ROT=SIG*UV-XMU*R0
T3=ALOG(TOP/ROT)/SIG
R01=(R0-U)/U
T4=(XMU*R0U+T3)/SSQ
T5=(R0U-XMU*T3)/SSQ
RETURN
END

```

10

APPENDIX VI

LISTING OF COMPUTER PROGRAM "HIJPRG"

```

1  PROGRAM HIJPRG(INPUT,OUTPUT,FILL,TAPES=INPUT,TAPES=OUTPUT,
2  1  TAPE7=FILL)
3  COMMON/BLKINF/AHDX1,AHDETA,RH01,TUPI
4  COMMON/BLKPROP/XN1,XN2,TUNU1,TUNU2,GAM
5  COMMON/BLKABG/XI(31,31),XI(31,31),XJ(31,31)
6  COMMON/BLKABGS/XHP(31,16),XIP(31,16),XJP(31,16),XHM(61,31),
7  XIM(61,31),XJM(61,31)
8  COMMON/BLKPRI/NH,NMU,NMV,NPU,NPV,AH,RHO,NDIV
9  COMMON/BLKPK/POIS1,POIS2,EIE2,ICASE
10 DATA NCK,TCHECK/0.480./
11 CALL SECOND(CPSEC)
12 WRITE(6,810)CPSEC
13 READ(5,800)ICASE
14 READ(5,900)POIS1,POIS2,EIE2
15 READ(5,910)AH,RHO,NDIV
16 TUNU1=2.*POIS1
17 TUNU2=2.*POIS2
18 XN1=1.,TUNU1
19 XN2=1.,TUNU2
20 GAM=EIE2*(1.+POIS2)/(1.+POIS1)
21 DX1=1./FLOAT(NDIV)
22 DETA=DX1/RHO
23 AHDX1=AH*DX1
24 AHDETA=AH*DETA
25 RH01=RHO
26 TUPI=8.*ATAN(1.)
27 NH=2*NDIV+1
28 NMU=4*NDIV+1
29 NMV=NH
30 NPU=NH
31 NPV=NDIV+1
32 DO 1 J=1,NH
33 DO 1 I=1,NH
34 XH(I,J)=0.
35 XI(I,J)=0.
36 XJ(I,J)=0.
37 DO 3 J=1,NMV
38 DO 3 I=1,NMU
39 XHM(I,J)=0.
40 XIM(I,J)=0.
41 XJM(I,J)=0.
42 DO 6 J=1,NPV
43 DO 6 I=1,NPU
44 XHP(I,J)=0.
45 XIP(I,J)=0.
46 XJP(I,J)=0.
47 IPR=1
48 DO 2 J=2,NH
49 N=J-1
50 DO 2 I=2,NH
51 M=I-1
52 CALL DHJ(J,M,N,0,DM,DI,DJ)
53 XH(I,J)=DM*XH(I-1,J)+XH(I,J)-XH(I-1,J-1)
54 XI(I,J)=DI*XI(I-1,J)+XI(I,J)-XI(I-1,J-1)
55 XJ(I,J)=DJ*XJ(I-1,J)+XJ(I,J)-XJ(I-1,J-1)
56 IF (SECOND(CP),LT,TCHECK)GO TO 2
57 CALL PRIOUT(IPR)

```



PAGE 2

78/02/13. 13.47.03

FTN 4.6452

PROGRAM HIJPRG 74/74 OPT=1

```

60      CALL CHEKPTX(NCK)
        IF (SECOND(CP).GE.TCHECK) STOP
        2 CONTINUE
        IPR=2
        DO 4 J=2,NMV
            N=J-1
            CALL DHIJ(N,N,1,DM,DI,DJ)
            XHM(J,J)=DM+XHM(J,J-1)
            XIM(J,J)=DI+XIM(J,J-1)
            XJM(J,J)=DJ+XJM(J,J-1)
            IF (SECOND(CP).LT.TCHECK) GO TO 20
            CALL PRIOUT(IPR)
            CALL CHEKPTX(NCK)
            IF (SECOND(CP).GE.TCHECK) STOP
            20 JI=J+1
            DO 4 I=J1,NMU
                M=I-1
                CALL DHIJ(M,N,1,DM,DI,DJ)
                XHM(I,J)=DM+XHM(I-1,J)+XHM(I,J-1)-XHM(I-1,J-1)
                XIM(I,J)=DI+XIM(I-1,J)+XIM(I,J-1)-XIM(I-1,J-1)
                XJM(I,J)=DJ+XJM(I-1,J)+XJM(I,J-1)-XJM(I-1,J-1)
                IF (SECOND(CP).LT.TCHECK) GO TO 4
                CALL PRIOUT(IPR)
                CALL CHEKPTX(NCK)
                IF (SECOND(CP).GE.TCHECK) STOP
                4 CONTINUE
                CALL DHIJ(0,1,1,DM,DI,DJ)
                XHM(1,2)=DM
                XIM(1,2)=DI
                XJM(1,2)=DJ
                IF (SECOND(CP).LT.TCHECK) GO TO 21
                CALL PRIOUT(IPR)
                CALL CHEKPTX(NCK)
                IF (SECOND(CP).GE.TCHECK) STOP
                21 DO 5 J=3,NMV
                    N=J-1
                    CALL DHIJ(N-1,N,1,DM,DI,DJ)
                    XHM(J-1,J)=DM+XHM(J-1,J-1)
                    XIM(J-1,J)=DI+XIM(J-1,J-1)
                    XJM(J-1,J)=DJ+XJM(J-1,J-1)
                    IF (SECOND(CP).LT.TCHECK) GO TO 22
                    CALL PRIOUT(IPR)
                    CALL CHEKPTX(NCK)
                    IF (SECOND(CP).GE.TCHECK) STOP
                    22 MLAST=M*10(N,NDIV)
                    DO 5 M1=2,MLAST
                        M=N-M1
                        T=M+1
                        CALL DHIJ(M,N,1,DM,DI,DJ)
                        XHM(I,J)=DM+XHM(I,J-1)+XHM(I,1,J)-XHM(I,1,J-1)
                        XIM(I,J)=DI+XIM(I,J-1)+XIM(I,1,J)-XIM(I,1,J-1)
                        XJM(I,J)=DJ+XJM(I,J-1)+XJM(I,1,J)-XJM(I,1,J-1)
                        IF (SECOND(CP).LT.TCHECK) GO TO 5
                        CALL PRIOUT(IPR)
                        CALL CHEKPTX(NCK)
                        IF (SECOND(CP).GE.TCHECK) STOP
                        5 CONTINUE

```

```

115 IPR=3
    DO 7 J=2,NPV
      XMP(1,J)=XHM(1,J)
      XIP(1,J)=XIM(1,J)
      XJP(1,J)=XJM(1,J)
      N=J-1
      ILAST=NPV-N
      DO 7 I=2,ILAST
        M=I-1
        CALL DHIJ(M,N,2,M,DI,DJ)
        XHP(1,J)=XHP(1,J)+XMP(I,J)+XMP(I-1,J-1)
        XIP(1,J)=DI+XIP(1,J)+XIP(I,J)+XIP(I-1,J-1)
        XJP(1,J)=DJ+XJP(1,J)+XJP(I,J)+XJP(I-1,J-1)
        IF (SECOND(CP).LT.TCHECK) GO TO 7
        CALL PRIOUT(IPR)
        CALL CHECKPTA(NCK)
        IF (SECOND(CP).GE.TCHECK) STOP
        7 CONTINUE
        CALL PRIOUT(IPR)
        IF (ICASE.EQ.0) STOP
        NF=7
        NREC=1
        WRITE(NF,3000) ICASE,NREC
        NREC=2
        WRITE(NF,3000) ICASE,NREC,E1E2,POIS1,POIS2
        NREC=3
        WRITE(NF,3001) ICASE,NREC,NDIV,AM,RHO
        NREC=4
        WRITE(NF,3000) ICASE,NREC
        DO 300 I=1,NH
          DO 300 J0=1,NH*6
            NREC=NREC+1
            JLAST=MIN0(J0+5,NH)
            300 WRITE(NF,3000) ICASE,NREC,(XH(I,J),J=J0,JLAST)
            NREC=NREC+1
            WRITE(NF,3000) ICASE,NREC
            DO 302 I=1,NH
              DO 302 J0=1,NH*6
                NREC=NREC+1
                JLAST=MIN0(J0+5,NH)
            302 WRITE(NF,3000) ICASE,NREC,(XI(I,J),J=J0,JLAST)
            NREC=NREC+1
            WRITE(NF,3000) ICASE,NREC
            DO 304 I=1,NH
              DO 304 J0=1,NH*6
                NREC=NREC+1
                JLAST=MIN0(J0+5,NH)
            304 WRITE(NF,3000) ICASE,NREC,(XJ(I,J),J=J0,JLAST)
            NREC=NREC+1
            WRITE(NF,3000) ICASE,NREC
            DO 306 I=1,NPV
              DO 306 J0=1,NPV*6
                NREC=NREC+1
                JLAST=MIN0(J0+5,NPV)
            306 WRITE(NF,3000) ICASE,NREC,(XHP(I,J),J=J0,JLAST)
            NREC=NREC+1
            WRITE(NF,3000) ICASE,NREC

```

PAGE 4

78/02/13. 13.47.03

FTN 4.6.452

PROGRAM HIJPRG 74/74 OPT=1

```

175      DO 308 I=1,NPU
          DO 308 J0=1,NPV,6
              NREC=NREC+1
              JLAST=MIN0(J0*5,NPV)
308      WRITE(NF,3000)ICASE,NREC,(XIP(I,J),J=J0,JLAST)
              NREC=NREC+1
              WRITE(NF,3000)ICASE,NREC
          DO 310 I=1,NPU
              DO 310 J0=1,NPV,6
                  NREC=NREC+1
                  JLAST=MIN0(J0*5,NPV)
310      WRITE(NF,3000)ICASE,NREC,(XJP(I,J),J=J0,JLAST)
              NREC=NREC+1
              WRITE(NF,3000)ICASE,NREC
          DO 312 I=1,NMU
              DO 312 J0=1,NMV,6
                  NREC=NREC+1
                  JLAST=MIN0(J0*5,NMV)
312      WRITE(NF,3000)ICASE,NREC,(XHM(I,J),J=J0,JLAST)
              NREC=NREC+1
              WRITE(NF,3000)ICASE,NREC
          DO 314 I=1,NMU
              DO 314 J0=1,NMV,6
                  NREC=NREC+1
                  JLAST=MIN0(J0*5,NMV)
314      WRITE(NF,3000)ICASE,NREC,(XIM(I,J),J=J0,JLAST)
              NREC=NREC+1
              WRITE(NF,3000)ICASE,NREC
          DO 316 I=1,NMU
              DO 316 J0=1,NMV,6
                  NREC=NREC+1
                  JLAST=MIN0(J0*5,NMV)
316      WRITE(NF,3000)ICASE,NREC,(XJM(I,J),J=J0,JLAST)
              STOP
800      FORMAT(110)
810      FORMAT(1H0,7HCPSEC =,F10.2)
900      FORMAT(5F10.2)
910      FORMAT(2F10.2,110)
3000      FORMAT(214,1P6E19.10)
3001      FORMAT(314,2F12.8)
          END

```

```

1  SUBROUTINE PRIOUT(IPRINT)
   COMMON/BLKABG/XH(31,31),XI(31,31),XJ(31,31),XK(31,31)
   COMMON/BLKABGS/XHP(31,16),XIP(31,16),XJP(31,16),XHM(61,31),
5  1 XIM(61,31),XJM(61,31)
   COMMON/BLKPR1/NH,NMU,NMV,NPU,NPV,AM,RHO,NDIV
   COMMON/BLKPPX/POIS1,POIS2,EIE2,ICASE
   WRITE(6,1030)
   WRITE(6,1040) ICASE
10  WRITE(6,2000)
   WRITE(6,2010) EIE2,POIS1,POIS2
   WRITE(6,2030)
   WRITE(6,2040) AM,RHO,NDIV
   WRITE(6,1001)
   DO 100 I=1,NH
15  WRITE(6,1010) (XH(I,J),J=1,NH)
   WRITE(6,1020)
   DO 102 I=1,NH
20  WRITE(6,1010) (XI(I,J),J=1,NH)
   WRITE(6,1020)
   DO 104 I=1,NH
25  WRITE(6,1010) (XJ(I,J),J=1,NH)
   WRITE(6,1020)
   IF(IPRINT,EQ,1) GO TO 10
   WRITE(6,1007)
   DO 112 I=1,NMU
30  WRITE(6,1010) (XHM(I,J),J=1,NMV)
   WRITE(6,1020)
   DO 114 I=1,NMU
35  WRITE(6,1010) (XIM(I,J),J=1,NMV)
   WRITE(6,1020)
   DO 116 I=1,NMU
40  WRITE(6,1010) (XJM(I,J),J=1,NPV)
   WRITE(6,1020)
   IF(IPRINT,EQ,2) GO TO 10
   WRITE(6,1004)
   DO 106 I=1,NPU
45  WRITE(6,1010) (XHP(I,J),J=1,NPV)
   WRITE(6,1020)
   DO 108 I=1,NPU
50  WRITE(6,1010) (XIP(I,J),J=1,NPV)
   WRITE(6,1020)
   DO 110 I=1,NPU
   WRITE(6,1010) (XJP(I,J),J=1,NPV)
   WRITE(6,1020)
10  CALL SECOND(CPSEC)
   WRITE(6,810) CPSEC
   RETURN
810 FORMAT(1H0,7MCPSEC =,F10.2)
920 FORMAT(1H1,////,5X,8MCASE NO.,I6)
1001 FORMAT(1H1,////,5X,7HAX(I,J),//)
1002 FORMAT(1H1,////,5X,7HXI(I,J),//)

```



PAGE 2

78/02/13. 13.47.03

FTN 4.6\*452

SURROUTINE PRIDUT 74/74 OPT=1

```

60      1003 FORMAT(1H,///,5X,7HXJ(I,J),///)
        1004 FORMAT(1H,///,5X,8HXHP(I,J),///)
        1005 FORMAT(1H,///,5X,8HXIP(I,J),///)
        1006 FORMAT(1H,///,5X,8HXJP(I,J),///)
        1007 FORMAT(1H,///,5X,8HXHM(I,J),///)
        1008 FORMAT(1H,///,5X,8HXIM(I,J),///)
        1009 FORMAT(1H,///,5X,8HXJM(I,J),///)
        1010 FORMAT(1H,10F12.7)
        1020 FORMAT(/)
        1030 FORMAT(1H,///,45H FOURIER INTEGRAL PART OF INFLUENCE FUNCTIONS)
        1040 FORMAT(///,5X,8HCASE NO.,I6)
        2000 FORMAT(///,1H,8X,4HE1E2,7X,5HP0IS1,7X,5HP0IS2)
        2010 FORMAT(1H,3F12.2)
        2030 FORMAT(///,1H,10X,2HAI,9X,3HRHO,8X,4HNDIV)
        2040 FORMAT(1H,2F12.2,112)
        END
70

```



```

1  SUBROUTINE DHIJ(M,N,IFCT,DH,DI,DJ)
COMMON/BLKTNF/AHDXI,AHDETA,RHO,TUPI
COMMON/BLKGAUS/X0(10),WGT(10),NDMTN,NDMAX,SMAX
COMMON/BLKLI IM/VL,VU,UL,UI,RHOL,RHOU
COMMON/BLKPROP/XN1,XN2,TUNU1,TUNU2,GAM
U0=AHDXI*FLOAT(M)
VU=AHDETA*FLOAT(N)
VL=VU-AHDETA
IF (IFCT-1) 3,2
1  UL=U0-AHDXI
UU=U0
RHOL=0.
RHOU=0.
UMAX=UU
GO TO 4
15 2  UL=U0-AHDXI
UU=U0
RHOL=RHO
RHOU=RHO
UMAX=UI+RHO*VU
GO TO 4
20 3  IF (M-N) 7,5,6
5  UL=0.
UU=VU+RHO
RHOL=0.
RHOU=-RHO
UMAX=AHDXI
GO TO 4
25 6  UL=U0-AHDXI
UU=U0
RHOL=-RHO
RHOU=-RHO
UMAX=UI-RHO*VU-AHDXI
GO TO 4
30 7  IF (M-N) 11,9,8,8
8  UL=VL+RHO
UU=0.
RHOL=-RHO
RHOU=0.
UMAX=AHDXI
GO TO 4
35 9  UL=U0
UU=U0-AHDXI
RHOL=-RHO
RHOU=-RHO
UMAX=RHO*VU-UL
4  RMAX=SQRT(UMAX*UMAX+VU*VU)
NDS=IFIX(SMAX*RMAX/TUPI*.5)
IF (NDS.LT.NDMIN) NDS=NDMIN
DELS=SMAX/FLOAT(NDS)
DS2=DELS/2.
DH=0.
DI=0.
DJ=0.
DO 10 IS=1,NDS
DDH=0.
DDI=0.

```

PAGE 2

78/02/14. 10.32.49

FTN 4.6\*452

SUBROUTINE DHIJ 74/74 OPT=1

```

60 DDJ=0.
   SSUM=DELS*FLOAT(2*IS-1)
   DO 11 I=1,10
   S=(SSUM*X0(I)*DELS)/2.
   TUS=2.*S
   E2S=EXP(TUS)
   GAMB=GAM*(3.-2.*TUNU2)
   H1=(1.*GAMB)*E2S
   H2=1.-GAMB*H1
   C11=3.-2.*TUNU1-GAMB*H1
   C12=TUS*H1
   C21=(1.-GAMB)*(3.-2.*TUNU1-TUS)+2.*GAM*(TUNU2-TUNU1)*H1
   C22=2.*(1.*GAM*(TUNU2*XN1+TUNU1*XN2+2.*TUNU1-1.))
   C22=C22-(1.*GAMB)*(2.*TUNU1-1.-TUS)
   C22=1.-GAMB+E2S*C22
   FOF5=(H1*(C21+C22)-H2*(C11+C12))/(C11*C22-C12*C21)-1.
   SFAC=WGT(I)*FOF5
   CALL DUBGAUS(S,XH,XI,XJ)
   DDH=DDH+SFAC*XH
   DDI=DDI+SFAC*XI
11 DDJ=DDJ+SFAC*XJ
   DH=DH+DS2*DDH
   DI=DI+DS2*DDI
10 DJ=DJ+DS2*DDJ
   RETURN
   END

```

75

80

PAGE 1

78/02/13, 13.47.03

FTN 4.6.452

SUBROUTINE DUBGAUS 74/74 OPT=1

```

1  SUBROUTINE DUBGAUS(S,TH,TI,TJ)
COMMON/BLKIM/VL,VU,UL,UU,RHOL,RHOU
DIMENSION X0(5),WGT(5)
5  DATA X0/-.9061798459,-.5384693101,0.,.5384693101,.9061798459/
DATA WGT/.2369268851,.4786286705,.5688888889,.4786286705,
1.2369268851/
NO=5
VSUM=VU*VL
DV=VU-VL
DV2=DV/2.
TH=0.
TI=0.
TJ=0.
DO 1 IV=1,NO
V=(VSUM*X0(IV)*DV)/2.
VSO=V*V
UL=UL+RHOL*V
UU=UU+RHOU*V
USUM=UU*UL
DU=UU-UL
VFAC=WGT(IV)*DU/2.
DTH=0.
DTI=0.
DO 2 IU=1,NO
U=(VSUM*X0(IU)*DU)/2.
ARG=SQRT(UU*VSO)
TERM=WGT(IU)*FCTJO(ARG)
DTH=DTH+TERM
2 DTI=DTI+U*TERM
TH=TH+VFAC*DTH
TI=TI+VFAC*DTI
1 TJ=TJ+VFAC*DTH*V
TH=TH*DV2
TI=TI*DV2
TJ=TJ*DV2
RETURN
END

```

10

15

20

25

30

35

PAGE 1

78/02/13. 13.47.03

FTN 4.6.452

BLOCK DATA BLKDAT. 74/74 OPT=1

1 BLOCK DATA  
COMMON/BLKGAUS/U0(10),WGT(10),NDMIN,NDMAX,SMAX  
DATA U0/,-.9739065285,-.8650633667,-.6794095683,-.4333953941,  
1 -.1488743390,.1488743390,.4333953941,.6794095683,.8650633667,  
5 1 .9739065285/  
DATA WGT/.0666713443,.1494513492,.2190863625,.2692667193,  
1 .2955242247,.2955242247,.2692667193,.2190863625,.1494513492,  
1 .0666713443/  
DATA NDMIN,NDMAX,SMAX/6,30,10./  
END

10

PAGE 1

78/02/13. 13.47.03

FTN 4.6\*452

74/74 OPT=1

FUNCTION FCTJ0

```

1  FUNCTION FCTJ0(X)
   IF (X-3) 4,4,3
3  Y=3./X
   F=-.79788456*Y*(-.77E-6*Y*(-.55274E-2*Y*(-.9512E-4*Y*(.137237E-2*Y*
5   1*(-.72805E-3*.14476E-3*Y))))
   T=X-.78539816*Y*(-.04166397*Y*(-.3954E-4*Y*(.262573E-2*Y*
   1*(-.5*125E-3*Y*(-.29333E-3*.13558E-3*Y))))
   SR=SQRT(X)
   FCTJ0=F*COS(T)/SR
10  RETURN
   4  Y=(X/3)**2
   FCTJ0=1./Y*(-2.2499997*Y*(1.2656208*Y*(-.3163866*Y*(.0444479*Y*
   1*(-.39444E-2*.21E-3*Y))))
   RETURN
15  END

```